Photodissociation Studies of Gas Phase Metal Ion–Molecule Complexes

by

Gregory Alan Grieves

(Under the direction of Michael A. Duncan)

Abstract

A survey of metal ion-molecule complexes produced by pulsed laser vaporization and studied in the gas phase is presented. The technique of laser vaporization is explored for its utility in generating important and interesting complexes. The first systematic application of this method for producing doubly charged metal ion solvation complexes is reported. Certain multiply charged clusters are thermodynamically unstable to charge transfer at long range, yet these were also able to be generated. A consistent criterion to determine which of the unstable complexes could be produced is the proximity of the degeneracy point of the doubly charged state with the charge transfer state, which has important implications for solvation effects in these clusters. Fixed frequency photodissociation can provide important clues to the structure of metal clusters where spectroscopic techniques fail. Application of fixed frequency photodissociation to novel extended structures of lanthanide metal-cyclooctatetraene complexes is demonstrated. Patterns in the dissociation products indicate that these clusters form extended multi-decker "sandwich" type structures with up to three ligand layers. Infrared photodissociation spectroscopy is a powerful tool for studies of model systems of metal ion solvation in the gas phase. Utilizing this technique, nickel ions clustered with carbon dioxide distinctly show signatures of ligand shell layering. The first coordination sphere of nickel with carbon dioxide was demonstrated to exist at four carbon dioxide molecules. Results indicate a solvent-induced intracluster reaction occurs in the clusters producing a multiply charged nickel core while immersed in a carbon dioxide cluster.

Index words: Laser vaporization, Metal clusters, Metal ion solvation, Resonance Enhanced Photodissociation Spectroscopy, REPD, Infrared Photodissociation

Photodissociation Studies of Gas Phase Metal Ion–Molecule Complexes

by

Gregory Alan Grieves

B.Sc., Eastern Michigan University, 1996

A Dissertation Submitted to the Graduate Faculty
of The University of Georgia in Partial Fulfillment
of the
Requirements for the Degree

Doctor of Philosophy

Athens, Georgia

2003

Photodissociation Studies of Gas Phase Metal Ion–Molecule Complexes

by

Gregory Alan Grieves

Approved:

Major Professor: Michael A. Duncan

Committee: Henning H. Meyer
Geoffrey D. Smith

Electronic Version Approved:

Maureen Grasso
Dean of the Graduate School
The University of Georgia
May 2003

Dedication

To my parents for their love and wisdom,

Barbara Lenora Grieves

and

Richard Gordon Grieves

I dedicate this dissertation to mother and father for providing me with the courage and motivation to pursue higher education. I would like to thank my mother for helping me make that first step in to college. I wouldn't have made that step without her, and that was the key to my discovery of chemistry, physics and mathematics that has driven my pursuits to culmination in this degree. She is bold and strong in character and bright and witty and grounded in good common sense. And to my father whose passion for knowledge and lifelong learning set a quintessential example for me at a formative stage. He was a highly creative man in the arts and humanities, in language and history, music, painting and poetry. Science requires one to explore, dissect and examine nature, and yet also to synthesize ideas, adapt and be creative, it is a lofty pursuit, but above all it is a practical matter. It is the very best talents in both of them that provided me with the best possible resources for a life in science.

Acknowledgements

I would first like to acknowledge Prof. Michael A. Duncan for his guidance and inspiration. Mike is supremely talented at being a mentor. He knows exactly how to inspire excitement and enthusiasm even when the immediate outlook appears bleak. He is also an excellent teacher with a unique ability to reach his students and bring the abstract down to the tangible. His skill and acumen in science is also an inspiring quality. How does he make it all look so easy!

I was introduced to the laboratory by a very interesting collection of people including John Buchanan, Michelle France, Dr. Steve Pullins, Dr. Areatha Knight Ketch and Prof. John Reddic. Together they instilled in me the group spirit and sense of the collective process of research. I would also like to individually thank Prof. John Reddic for his friendship and good times during our collaborations, Dr. Areatha Ketch for her wonderful good nature to be around and always fascinating conversation, and Dr. Steve Pullins for his intriguing insight and rather different perspectives.

Several postdocs I've worked with along the way have given me a glimpse of what's on the other side of this degree, as well as informed me of the role a postdoc can play in the laboratory and as a mentor. These include Dr. Andreas Stangassinger, Dr. Jurgen Agreiter, Dr. James Fye, Dr. Gilles Gregoire and Dr. Nicholas Walker. A special thanks to Nick for his friendship and alliance during the many trials of working with App 2 and the beguiling laser system. Nick has also been a source of

new insight on worldly affairs and he exudes a unique empathy for the underprivileged in the world. Also his avid interest in literature has in some small part rubbed off on me.

I have seen many people come and many go in my time here. Among the people I have appreciated the opportunity to work with are Nancy Flynn, Angela Carroll, Todd Jaeger, Jared Jaeger and Richard Walters. Special acknowledgement to Angela for much comfort in times of distress, and also for many "funner" times. Richard has been a good ally and friend in the lab. He has a strong and diligent work style that was interesting to watch and is something I can learn from in the future. We've had many fascinating discussions about a variety of topics and he has always shed new light on many things for me. Storm the front!

Close friends have been a ground and a source of energy for me. Nichole Foster was among the most interesting and delightful people to have known and worked with. I would like to give special thanks to her, for she is a very special individual and she overcame a tremendous amount to come to UGA and to get through UGA. I would also like say thanks to Jessica McKee for being a good bud, and for the fishing trip, roller skating and just all around fun times. Joe Velasquez is and always shall be a good friend and compatriot. Working with him in the lab and through Henning's class, we established a rapoire and a mutual respect. To this day I continue to learn about life and many refined pursuits from him, and I look forward to our adventures to come. Hola vato! To Tim Ayers I am appreciative of his everpresent witty and idiosyncratic nature. He has been a very good friend to me and always knows how to lighten things up when I get too serious. Good luck with your future projects, and I also look forward to future adventures. Fire in the hole!

I would also like to mention the new members of the group, with whom I have not had much opportunity to collaborate with, but they represent the future of the lab. Karen Sinclair, Brian Ticknor and Dinesh Pillai each show a good attitude and

interest in the science done here, I wish them the best in their careers. Also I would like to mention Chris Molek for his friendship and for some good times together. Thanks Chris! And to Jason McLain, one wild individual with a far out view of things, thanks for all the good times and good laughs. Best of luck to Chris and Jason down in the astrochem lab.

Last but not least is a very special acknowledgement to Valerie Sharpton. She is a wonderful friend, companion and love.

Table of Contents

Chapter 1

Introduction

The majority of elements on the periodic table are metals. Although a tremendous amount is known about the chemistry of nonmetals, largely due to their well behaved bonding characteristics, metals span a wide spectrum of physical and chemical properties that defy compact description. Metals also exhibit another interesting attribute in that they may form clusters in size anywhere from two to thousands of atoms. The properties of metal clusters fall into a strange regime between the quantum mechanical atomic scale and the macroscopic metallurgical scale that are not always simply a continuous line from one to the other. The wide expanse of distinct properties of metals gives way to their enormous utility in chemical synthesis and development of new technologies. Metal and metal oxide surfaces and metal clusters supported on surfaces act as catalysts[7] that accelerate the rates of production of important materials such as polymers, petroleum products and pharmaceuticals, as well as to moderate exhaust emissions from cars and industrial smoke stacks. Detailed knowledge of these processes could produce catalysts with high specificity and allow precise control of the reactions to be optimized while minimizing useless byproduct and waste. Metal clusters and nanoparticles also exhibit unique electrical, optical and magnetic properties that can be exploited to develop new technologies like nanoscopic quantum computers,[8] photonic processors,[9] optical data storage and chemical sensors for detecting things such as bioterrorism agents like anthrax and small pox.[10] In addition to their fascinating chemistry, metals are universally present and play a significant role in every physical environment in the universe. Metals are present in the corona of the sun,[1] interstellar nebulae,[2] the atmospheres of planetary satellites,[3] in meteorites[4] which then shed them into our own atmosphere when they burn up on entry. The salts of the oceans are replete with metal ions, they are essential in biological systems[5] as electrolytes and as active sites in proteins and enzymes,[6] and they control signal conduction in the neurons in our brains.[6] Quite literally, the very way we think depends on metal ions. Metal ion-molecule complexes

represent model systems by which properties of larger systems may be extrapolated and are tractable to theory as well as experiment. Studies in the gas phase allow the system to be isolated from the complicating interactions of the bulk such as ligand exchange with solvent or the dielectric qualities of the embedding medium, as well as the necessity of counter-ions. The focus of this dissertation is the study of the gas phase production and photophysics of metal ion-molecule clusters.

A wealth of information has been garnered from the study of singly charged metal ion-molecule complexes utilizing a number of experimental and theoretical methods.[11] A number of important molecular parameters for metal ion-molecule dimers have been measured including bond dissociation energies,[40] energies required to produce the ion,[12] electronic spectra and in some cases geometries.[12] Although there is considerable interest in singly charged complexes for fundamental understanding of ion interactions, most elements occur naturally in solution or in crystals in higher charge states.[13] Solvation of such species has a profound effect on the rate, course and outcome of chemical reactions in bulk.[14] A number of important systems have been studied that model fundamental solvation interactions such as metal-water complexes ($M^{2+}(H_2O)_n$, M = Mg,[16,20] Ca,[15] Sr,[15] Ba,[15] Be,[14] V,[14] Mn,[15] Fe,[15] Co,[15,17] Ni,[15] Zn,[15] Cu,[18] Cd[19] and others. However, multiply charged metal ions with other ligands also illuminate how fundamental intermolecular forces operate. Ligands with dipole (NH_3,[16a,22] CH_3CN,[16a] DMSO,[16a,20] etc.) or quadrupole moments (CO_2,[23] etc.), or degrees of polarizability (Ar,[24,23] C_2H_4,[21] C_6H_6,[22] etc.) can affect the coordination, geometry and overall stability of multiply charged clusters. Only relatively recent advances[25] have allowed for the efficient production of multiply charged cluster ions. This is because the relative energetics of the ionization potentials in these clusters make many of them unstable to charge transfer at small cluster sizes.[26] Stabilizing the higher charged state is a defining feature of solvation, and many studies have attempted to find the minimum cluster size necessary to

allow the higher charged metal ions to exist.[14,16,17] This factor of minimum size was assumed to preclude the use of laser vaporization for their production. Presented in this work is the first systematic study of multiply charged metal ion complexes produce by laser vaporization.

The basic understanding of metal bonding interactions was greatly expanded with the discovery of ferrocene, $Fe(C_5H_5)_2$, subsequently leading to the 1974 Nobel Prize in chemistry by Fischer and Wilkinson.[27] The remarkable stability of this complex is attributed to favorable orbital overlap of the metal d orbitals with the ligand as well as an electron count that satisfies both the 18 electron rule on the metal and the Hückel number of electrons on the cyclic ligand. This discovery helped form a bridge between the fields of inorganic and organic chemistry and a floodgate of activity was spawned.[30] Later, a whole series of "sandwich" compounds was discovered, including dibenzene chromium,[28] $Cr(C_6H_6)_2$, and many others that utilize a host of substitutional variants on the ring molecule and nearly every transition metal.[29] Metal benzene complexes have been studied in the gas phase with a wide variety of techniques. Kaya and coworkers reported[31] an interesting pattern in mass spectrometry studies whereby it appeared that certain transition metal-benzene complexes formed extended arrays of stacking. Magic numbers appeared with the stoichiometry of $M_n(C_6H_6)_{n+1}$ indicating alternating layers of metals between benzene in a so-called "multi-decker sandwich" array. Cyclic hydrocarbon complexes with the f-block lanthanide and actinide metals were also investigated by conventional organometallic synthesis. 1,3,5,7-Cyclooctatetraene (COT) is an 8-membered ring that is nonplanar but would become planar and aromatic if given two additional electrons. The first actinide complex found was uranocene, $U(C_8H_8)_2$ by Streitwieser and Müller-Westerhoff[32] in 1968. Since uranium favors a +4 oxidation, the electron counting matches well with a pair of COT ligands and the bonding is covalent. Lanthanide metals with COT proved to be more of a challenge however, since most lan-

thanides strictly prefer the +3 oxidation state, even at the cost of not achieving aromaticity on the COT ligand. Thus complexes of the form $Ln^{+3}(COT^{-1.5})_2$ attach by ionic bonding not involving f-orbital overlap. Divalent lanthanide metals form half-sandwich complexes where solvent molecules cap the metal from further stacking. These properties of lanthanide metals inhibited studies of sandwich complexes and $Ce_2(C_8H_8)_3$ is the only complex that has been isolated that exhibits multi-decker sandwich formation without counterions or additional ligands. Gas phase study, however, eliminates the interference from solvent molecules. Kaya and coworkers[33] have studied lanthanide metal COT complexes by mass spectrometry, photoionization spectroscopy and photoelectron spectroscopy and indeed observed clusters of the form $M_n(C_8H_8)_{n+1}$ with spectra consistent with multi-decker sandwiches. In this dissertation the study of lanthanide metals with COT is undertaken in order to provide confirmation of these structures and to probe for possible isomeric structures using fixed frequency photodissociation.

Much of what is known about the detailed structure of metal ion-ligand complexes comes from electronic spectroscopy in mass spectrometers.[34–66] This is due to the availability of tunable pulsed dye lasers coupled with the high sensitivity of ion detectors. Studies of M^+-L complexes, where L = rare gas atoms (Ne, Ar, Kr, Xe) or small molecule (N_2, CH_4, H_2O, CO_2, NH_3 etc.) form the foundation for modelling solvation systems. Transition metal ion complexes have been studied by resonance enhanced photodissociation spectroscopy (REPD).[45–47,52–66] These systems often have electronic transitions in the visible region of the spectrum, however they are often very complex due to the large number of unpaired d electrons. REPD studies of complexes with alkaline earth metal ions, most notably Mg^+ and Ca^+, have proven highly fruitful.[55,57–61,65,66] These ions have intense atomic $^2P \leftarrow {}^2S$ transitions analogous to the sodium 'D' line. Because the interactions of small molecules with these metals are weak, the spectra occur near the metal atomic transitions, with shifts,

electronic multiplets and rovibronic structure arising from the details of the bonding in the ground and excited electronic state. Low resolution spectroscopy has yielded vibrationally resolved spectra for a number of complexes including Mg^+D_2,[48] Mg^+RG (RG = Ar, Kr, Xe),[52] Mg^+CO_2,[53] Mg^+N_2,[54] Mg^+H_2O,[55] $Mg^+C_2H_4$,[56] Ca^+RG,[57] Ca^+CO_2,[58] Ca^+N_2,[59] Ca^+H_2O,[60] $Ca^+C_2H_2$[61] and others. Structures of complexes have been determined by high resolution REPD spectroscopy for such systems as Ba^+Ar,[50] Mg^+Ar,[65] Mg^+Ne,[65] Ca^+N_2[59] and $Ca^+C_2H_2$.[61] However, a problem often arises due to the necessity of having theoretical support in the assignment of spectra. Theory often has problems calculating excited states, and therefore it is often hard to obtain assignments of spectra. Electronic excitation also can lead to photoinduced reactions that broaden the spectra and remove interpretable structure due to shortened lifetime of the excited state. Predissociation is also a major problem for multiligand complexes. Because of these issues almost no vibrationally resolved spectra have been obtained for multi-ligand species.[66] It is therefore of interest to focus studies on the ground electronic state. Predissociation and photoinduced reactions are less likely to occur and it becomes possible to obtain the spectra for multiligand species. Obtaining information about size selected multiligand clusters opens the door to understanding ion solvation incrementally from small clusters to large ones approaching the bulk. To accomplish this, tunable infrared light sources must be available in the frequency range of the molecular ligand. Recent experiments utilizing the Free Electron Laser for Infrared eXperiments at the FOM Institute in the Netherlands have acquired vibrational spectra for metal ion-benzene complexes[67] $M^+(C_6H_6)_n$, M = Al , V, Ti, Fe, Co with as many as three ligands. These spectra have confirmed that the structures of the gas phase clusters have metals situated over the sixfold ring of the benzene and that the multi-ligand complexes are indeed sandwich structures. The recent availability of high peak power, easily tunable, tabletop IR light sources has allowed us to bring IR-REPD to our own laboratory for the

study of metal ion complexes. Initial studies focussed on M^+CO_2 complexes because CO_2 has a strong IR active vibration in the region covered by the laser. Spectra were obtained for clusters of $M^+(CO_2)_n$ for M = Fe, Mg,[68] Al and n=1 to up to a dozen or more ligands. The vibrational spectra obtained yielded information about the structure and formation of inner coordination spheres and multiple solvation layers. More recently, studies of $Ni^+(C_2H_2)_n$ clusters[69] have demonstrated that the metal ion can act as a medium supporting ring cyclization reactions to produce cyclobutadiene. This work presents new data on the $Ni^+(CO_2)_n$ system that adds to the mounting body of data on first row transition metal interactions with carbon dioxide. Nickel has been predicted[70] to be the most strongly bound of any first row transition metal to CO_2. This exceptional affinity of nickel for CO_2 makes this system particularly interesting when considering the possibility of intracluster chemistry.

Thus, the study of metal ion-ligand complexes is rich with interesting chemical physics, and has important applications in a wide variety of interdisciplinary fields. The tools utilized in this dissertation for the study of these types of complexes are a laser vaporization/molecular beam cluster source coupled to a reflectron time-of-flight mass spectrometer for mass analysis and photodissociation studies.

1.1 References

[1] E. Anders and N. Grevesse, *Geochimica et Cosmochimica Acta*, **53(1)**, 197-214 (1989).

[2] Y.G. Samis, M.J. Barlow, X.-W. Liu, I. J. Danziger and P. J. Storey, *Monthly Notices of the Royal Astronomical Society*, **338(3)**, 687-710(2003).

[3] (a) T. E. Madey, R.E. Johnson and T.M. Orlando, *Surf. Sci.*, **500(1-3)**, 838-858 (2002). J.R. Lyons, *Science*, **67**, 648 (1995); (b) H.A. Weaver, M.F. A'Hearn, C. Arpigny, D.C. Boice, P.D. Feldman, et al., *Science*, **267**, 1282 (1995); (c) P.D,

Feldman, H.A. Weaver, D.C. Boice and S.A. Stern, *Icarus*, **121**, 442 (1996). K.S. Noll, M.A. McGrath, L.M. Tafton, S.K. Atreya and J.J. Caldwell, *et al. Science*, **267**, 1307 (1996).

[4] (a) W.J. McNeil, *A model of the Atmospheric Metal Deposition by Cosmic Dust Particles*, Rep. U.S. Air Force Phillips Lab., Dir. Geophys., Hanscomb AFB, 1993.; (b) J.M.C. Plane, *Intl. Rev. Phys. Chem.*, **10**, 55 (1991).

[5] R.A. Kumpf and D.A. Dougherty, *Science*, **261**, 1708 (1993).

[6] M.K. Campbell, *Biochemistry*, 2nd ed. (Saunders, Philadelphia, 1995).

[7] M.C. Wu, C.A. Estrada and D.W. Goodman, *Phys. Rev. Lett.*, **67**, 2910 (1991).

[8] G. Burkard, D. Loss, *Acta Physica Polonica, A*, **100(2)**, 109-127 (2001).

[9] S. Takeuchi, *Springer Series in Chemical Physics*, **70** (Chemistry of Nanomolecular Systems), 183-193 (2003).

[10] (a) B. Schneider, *SPIE OEMagazine*, April 2002.; (b) B. Schneider and E. Dickinson, *Biosensors Bioelectron.*, **15**, 597 (2000).

[11] (a) M.A. Duncan, *Ann. Rev. Phys. Chem.*, **48**, 69 (1997); (b) V.E. Bondybey, M.K. Beyer, *Intl. Rev. Phys. Chem.*, **21**, 277 (2002); (c) (c) P.D. Kleiber, *Adv. Metal Semicond. Clusters 5* 267 (2001); (d) M. Velegrakis, *Adv. Metal Semicond. Clusters 5*, 227 (2001); (e) D.S. Yang, *Adv. Metal Semicond. Clusters 5* 187 (2001); (f) J.M. Lisy, *Cluster Ions*, **217** (1993). Editors: C. Ng, T. Baer, I. Powis, Wiley, Chichester, UK.; (g) K. Eller and H. Schwarz, *Chem. Rev.*, **91**, 1121 (1991); (h) M.T. Rodgers and P.B. Armentrout, *Mass Spectrom. Rev.*, **19**, 215 (2000); (i) P. Kebarle, *Ann. Rev. Phys. Chem.*, **28**, 445 (1977).

[12] J.K Agreiter, A.M. Knight and M.A. Duncan, *Chem. Phys. Lett.*, **313**, 162 (1999).

[13] A.J. Stace, *J. Phys. Chem. A*, **106**, 7993 (2002)

[14] V.E. Bondybey and M.K. Beyer, *Int. Rev. Phys. Chem.*, **21(2)**, 277 (2002).

[15] (a) A.T. Blades, P. Jayaweera, M.G. Ikonomou and P. Kebarle, *J. Chem. Phys.*, **92(10)** 5900 (1990); (b) J.S. Klassen, Y. Ho, A.T. Blades, P. Kebarle, *Adv. Gas Phase Ion Chem.*, **3**, 255(1998); (c) M. Peschke, A.T. Blades and P. Kebarle, *Intl. J. Mass Spectrom.*, **185/186/187**, 685 (1999).

[16] (a) N.R. Walker, M.P. Dobson, R.R. Wright, P.E. Barran, J.N. Murrell and A.J. Stace, *J. Am. Chem. Soc.*, **122**, 11138 (2000); (b) J.M. Martinez, R.R. Pappalardo and E.S. Marcos, *J. Am. Chem. Soc.*, **121**, 3175 (1999); (c) G.D. Markham, J.P. Glusker and C.W. Bock, *J. Phys. Chem. B*, **106**, 5118 (2002); (d) S. Petrie, *J. Phys. Chem. A*, **106**, 7034 (2002); (e) S. Petrie and L. Radom, *Intl. J. Mass Spectrom.*, **192**, 173 (1999); (f) M. Pavlov, P.M. Siegbahn, M. Sandström, Sandström, *J. Phys. Chem. A*, **102**, 219 (1998); (g) E. Glendening, D. Feller, *J. Phys. Chem.*, **100**, 4790 (1996); (f) C. W. Bauschlicher, Jr., M. Sodupe, H. Partridge, *J. Chem. Phys.*, (g) H. Watanabe, S. Iwata, K. Hashimoto, F. Misaizu, K. Fuke, *J. Am. Chem. Soc.*, **117**, 755 (1995); (h) H. Watanabe, S. S. Iwata, K. Hashimoto, F. Misaizu, K. Fuke, *J. Am. Chem. Soc.*, **117**, 755 (1995); (i) M. Peschke, A.T. Blades, P. Kebarle, *J. Phys. Chem. A*, **102**, 9978 (1998); (j) P.E. Barran, N.R. Walker, A.J. Stace, *J. Chem. Phys.*, **112**, 6173 (2000); (k) C.C. Pye, W.W. Rudolph, *J. Phys. Chem. A*, **102**, 9933 (1998); (l) S.E. Rodriguez-Cruz, R.A. Jockusch, E.R. Williams, *J. Am. Chem. Soc.*, **121**, 1986 (1999).

[17] (a) A.A. Shvartsburg, K.W.M. Siu, *J. Am. Chem. Soc.*, **123**, 10071 (2001); (b) C. Lüder, E. Georgiou, M. Velegrakis, *Intl. J. Mass Spectrom. Ion Proc.*, **153**, 129 (1996).

[18] P.E. Barran, N.R. Walker and A.J. Stace, *J. Chem. Phys.*, **112**, 6173 (2000).

[19] Z.L. Cheng, K.W.M. Siu, R. Guevremont and S.S. Berman, *Org. Mass Spectrom.*, **27**, 281 (1992).

[20] A.A. Shvartsburg, *J. Am. Chem. Soc.*, **124**, 12343 (2002).

[21] N.R. Walker, S. Firth and A.J. Stace, *Chem. Phys. Lett.*, **292**, 125 (1998).

[22] N.R. Walker, R.R. Wright and A.J. Stace, *J. Am. Chem. Soc.*, **121**, 4837 (1999).

[23] N.R. Walker, G.A. Grieves, J.B. Jaeger, R.S. Walters and M.A. Duncan, *Intl. J. Mass Spectrom.*, *in press.*

[24] M. Velegrakis and Ch. Luder, *Chem. Phys. Lett.*, **223**, 139 (1994).

[25] (a) A.J. Stace, *Adv. Metal Semicond. Clusters 5*, 121 (2001); (b) A.J. Stace, *J. Phys. Chem. A*, **106**, 7993 (2002); (c) A.T. Blades, P. Jayaweera, M.G. Ikonomou and P. Kebarle,*J. Chem. Phys.*, **92**, 5900 (1990); (d) J.S. Klassen, Y. Ho, A.T. Blades and P. Kebarle, *Adv. Gas Phase Ion Ion Chem. 3*, 255 (1998); (e) L.A. Posey, *Adv. Metal Semicond. Clusters 5*, 145 (2001); (f) T.G. Spence, T.D. Burns and L.A. Posey, *J. Phys. Chem. A.*, **101**, 139 (1997).

[26] D. Schröder, H. Schwarz, *J. Phys. Chem. A*, **103**, 7385 (1999).

[27] (a) T.J. Kealy and P.L Paulson, *Nature*, **168**, 1039 (1951); (b) Fischer, *Angew. Chem.*, **67**, 475 (1955).

[28] A. Haaland, *Acta Chem. Scand.*, **19**, 41 (1965).

[29] F.A. Cotton and G. Wilkinson "Advanced Inorganic Chemistry." 3rd Ed., Wiley-Interscience, New York, 1972.

[30] G. Wilkinson, *J. Organometal. Chem.*, **100**, 273 (1975).

[31] (a) K. Hoshino, T. Kurikawa, H. Takeda, A. Nakajima and K. Kaya, *J. Phys. Chem.*, **99(10)**, 3053 (1995); (b) T. Kurikawa, H. Takeda, A. Nakajima and K. Kaya , *Zeitschrift fuer Physik D: Atoms, Molecules and Clusters*, **40(1-4)**, 65-69 (1997).

[32] A. Streitwieser and U. Müller-Westerhoff, *J. Am. Chem. Soc.*, **90**, 7364 (1968).

[33] (a) T. Kurikawa, Y. Negishi, F. Hayakawa, S. Nagao, K. Miyajima, A. Nakajima and K. Kaya, *J. Am. Chem. Soc.*, **120** 11766 (1998); (b) K. Miyajima, T. Kurikawa, M. Hashimoto, A. Nakajima and K. Kaya, *Chem. Phys. Lett.*, **306**, 256 (1999).

[34] P. Kebarle, *Ann. Rev. Phys. Chem.*, **28**, 445 (1977).

[35] (a) A. W. Castleman, P.M. Holland, D.M. Lindsay and K.I. Peterson, *J. Am. Chem. Soc.*, **100**, 6039 (1978); (b) A.W. Castleman, *Chem. Phys. Lett.*, **53**, 560 (1978); (c) P.W. Holland and A.W. Castleman, *J. Chem. Phys.*, **76**, 4195 (1982); (d) K.L. Glein, B.C. Guo, R.G. Keesee and A.W. Castleman, *J. Phys. Chem.*, **93**, 6805 (1989); (e) B.C. Guo, J.W. Purnell and A.W. Castleman, *Chem. Phys. Lett.*, **168**, 155 (1990); (f) B.C. Guo and A W. Castleman, *Chem. Phys. Lett.*, **181**, 16 (1991).

[36] T.F. Magnera, D.E. David and J. Michl, *J. Am. Chem. Soc.*, **111**, 4100 (1989).

[37] P.I. Marinelli and P.R Squires, *J. Am. Chem. Soc.*, **111**, 4101 (1989).

[38] F. Bouchard, J.W. Hepburn and T.B. McMahon, *J. Am. Chem. Soc.*, **111**, 8934 (1989).

[39] M.S. El-Shall, K.E. Shriver, R.L. Whetten and M.J. Mautner, *J. Phys. Chem.*, **93**, 7969 (1989).

[40] (a)RH. Schultz and P.B. Armentrout, *J. Phys. Chem.*, **97**, 596 (1993); (b) Y.M.Chen and P.B. Armentrout, *Chem. Phys. Lett.*, **210**, 123 (1993); (c) N.F. Dalleska, B.L. Tjelta and P.B. Armentrout, *J. Phys. Chem.*, **98**, 4191 (1994); (d)N.F. Dalleska, K. Homma, L.S. Sunderlin and P.B. Armentrout, *J. Am. Chem. Soc.*, **116,** 3519 (1994).

[41] (a) C. Heinemann, J. Schwarz and H. Schwarz, *J. Phys. Chem.*, **100**, 6088 (1996); (b) R.C. Dunbar, S.J. Klippenstein, J. Hrusak, D. Stockigt and H. Schwarz, *J. Am. Chem. Soc.*, **118**, 5277 (1996).

[42] (a) R.L. Hettich and B.S. Freiser, *J. Am. Chem. Soc.*, **109**, 3543 (1987); (b) B.S. Freiser, *Chemtracts-Anal. and Phys. Chem.*, **1**, 65 (1989); (c) L.M. Lech, *Ph.D. Thesis*, Purdue University, 1988.; (d) R.L. Hettich, T.C. Jackson, E.M. Stanko and B.S. Freiser, *J. Am. Chem. Soc.*, **108**, 5086(1986); (e) L. Operti, E.C. Tews and B.S. Freiser, *J. Am. Chem. Soc.*, **110**, 3847 (1988); (f) L. Operti, E.C. Tews, T.J. MacMahon and B.S. Freiser, *J. Am. Chem. Soc.*, **111**, 9152 (1989); (g) Y.A. Ranasinghe and B.S. Freiser, *Chem. Phys. Lett.*, **200**, 135 (1992); (h) S. Afzaal and B.S. Freiser, *Chem. Phys. Lett.*, **218**, 254 (1994).

[43] (a) W.L. Liu and J.M. Lisy, *J. Chem. Phys.*, **89**,605 (1988); (b) T.S. Selegue, N. Moe, I.A Draves and J.M. Lisy, *J. Chem. Phys.*, **96**, 7268 (1992); (c) T.J. Selegue and J.M. Lisy, *J. Phys. Chem.*, **96**, 4143 (1992); (d) T.J. Selegue and J. M. Lisy, *J. Am. Chem. Soc.*, **116**, 4874 (1994); (e) C.J. Weinheirner and J.M. Lisy, *J. Chem. Phys.*, **105**, 2938 (1996).

[44] (a) P.R Kemper and M.T. Bowers, *J. Phys. Chem.*, **95**, 5134 (1991); (b) P.R Kemper, M.T. Hsu and M.T. Bowers, *J. Phys. Chem.*, **95**, 10,600 (1991); (c) G. von Helden, P.R Kemper, M.T. Hsu and M.T. Bowers, *J. Chem. Phys.*, **96**,

6591 (1992); (d) P.R Kemper, J. Bushnell, G. von Helden and M.T. Bowers, *J. Phys. Chem.*, **97**, 52 (1993).

[45] (a) K.F. Willey, P.Y. Cheng, T.G. Taylor, M.B. Bishop and M.A. Duncan, *J. Phys. Chem.* 94, 1544 (1990); (b) K.F. Willey, P.Y. Cheng, M.B. Bishop and M.A. Duncan, *J. Am. Chem. Soc.*, **113**, 4721 (1991); (c) K.F. Willey, C.S. Yeh, D.L. Robbins and M.A. Duncan, *J. Phys. Chem.*, **96**, 9106 (1992).

[46] (a) M.H. Shen and I.M. Farrar, *J. Phys. Chem.* **93**, 4386 (1989); (b) M.H. Shen and J.M. Farrar, *J. Chem. Phys.*, **94**, 3322 (1991); (c) C.A. Schmuttenmaer, J. Qian, S.G. Donnelly, M.J. DeLucia, D.F. Varley, *et al*, J. Phys. Chem. **97**, 3077 (1993); (d) S.G. Donnelly and J.M. Farrar, *J. Chem. Phys.*, **98**, 5450 (1993); (e) J.M. Farrar, *Cluster Ions*, edited by C.Y. Ng, T. Baer and I. Powis (John Wiley and Sons, New York), p. 243, (1993); (f) J. Qian, AJ. Midey, S.G. Donnelly, J.I. Lee and J.M. Farrar, Chem. Phys. Lett. **244**, 414 (1995).

[47] (a)D.E. Lessen and P.J. Brucat, *J. Chem. Phys.*, **90**, 6296 (1989); (b)D.E. Lessen and P.J. Brucat, *J. Chem. Phys.*, **91**, 4522 (1989); (c) D.E. Lessen, R.L. Asher and P.J. Brucat, *J. Chem. Phys.*, **93**, 6102 (1990); (d)D.E. Lessen, R.L. Asher and P.J. Brucat, *J. Chem. Phys.*, **95**, 414 (1991); (e)D.E. Lessen, R.L. Asher and P.J. Brucat, *Advances in Metal and Semiconductor Clusters*, edited by M.A. Duncan (JAI, Greenwich, CT, 1995), Vol. I; (f) R L. Asher, D. Bellert, T. Buthelezi and P.J. Brucat, *Chem. Phys. Lett.*, **227**, 623 (1994) (g) R L. Asher, D. Bellert, T. Buthelezi, G. Weerasekera and P. J. Brucat, *Chem. Phys. Lett.*, 228, 390 (1994); (h) R L. Asher, D. Bellert, T. Buthelezi and P. J. Brucat, *Chem. Phys. Lett.*, **228**, 599 (1994); (i) R L. Asher, D. Bellert, T. Buthelezi and P. J. Brucat, *Chem. Phys. Lett.*, **227**, 277 (1994); (j) R L. Asher, D. Bellert, T. Buthelezi, D. Lessen and P. J. Brucat, *Chem. Phys. Lett.*, **234**,

119 (1995); (k) T. Buthelezi, D. Bellert, V. Lewis and P.J. Brucat, *Chem. Phys. Lett.*, **242**, 627 (1995).

[48] (a)L. N. Ding, M. A. Young, P. D. Kleiber, W. C. Stwalley and A. M. Lyyra, *J. Phys. Chem.*, **97**, 2181 (1993); (b) L.N. Ding, P.D. Kleiber, Y.C. Cheng, M.A. Young and S.V. O'Neil, *J. Chem. Phys.*, **102**, 5235 (1995).

[49] (a) F. Misaizu, M. Sanekata, K. Tsukamoto, K. Fuke and S. Iwata, *J. Phys. Chem.*, **96**, 8259 (1992); (b) K. Fuke, M. Misaizu, M. Sanekata, K. Tsukamoto and S. Iwata, *Supplement to Z. Phys. D*, **26**, S 180 (1993); (c) F. Misaizu, M. Sanekata and K. Fuke, *J. Chem. Phys.* **100**, 1161 (1994); (d) M. Sanekata, F. Misaizu, K. Fuke, S. Iwata and K. Hashimoto, *J. Am. Chem. Soc.*, **117**, 747 (1995); (e) H. Watanabe, S. Iwata, K. Hashimoto, F. Misaizu and K. Fuke, *J. Am. Chem. Soc.*, **117**, 755 (1995); (f) M. Sanekata, F. Misaizu and K. Fuke, *J. Chem. Phys.*, **104**, 9768 (1996).

[50] S.I. Panov, J.M. Williamson and T.A. Miller, *J. Chem. Phys.*, **102,** 7359 (1995).

[51] (a) C.W. Bauschlicher, H. Partridge and S.H. Langhoff, *Chem. Phys. Lett.*, **165**, 272 (1990); (b) C. W. Bauschlicher and H. Partridge, *J. Phys. Chem.*, **95**, 3946 (1991); (c) C. W. Bauschlicher and H. Partridge, *J. Phys. Chem.*, **95**, 9694 (1991); (d) C. W. Bauschlicher and H. Partridge, *Chem. Phys. Lett.*, **181**, 129 (1991); (e) M. Sodupe, C. W. Bauschlicher and H. Partridge, *Chem. Phys. Lett.*, **192**, 185 (1992); (f) M. Sodupe, C. W. Bauschlicher, S.R. Langhoff, H. Partridge, *J. Phys. Chem.*, **96**, 2118 (1992); (g) C.W. Bauschlicher, M. Sodupe and H. Partridge, *J. Chem. Phys.*, **96**, 4453 (1992); (h) H. Partridge, C.W. Bauschlicher and S.R. Langhoff, *J. Phys. Chem.*, **96**, 5350 (1992); (i) M. Sodupe, C.W. Bauschlicher and H. Partridge, *Chem. Phys. Lett.*, **195**, 494 (1992); (j) C. W. Bauschlicher, *Chem. Phys. Lett.*, **201**, 11 (1993); (k) M. Sodupe and

C. W. Bauschlicher, *Chem. Phys Lett.*, **203**, 215 (1993); (l) C.W. Bauschlicher and M. Sodupe, *Chem. Phys. Lett.*, **214**, 489 (1993); (m) H. Partridge and C.W. Bauschlicher, *J. Phys. Chem.*, **98**, 2301 (1994); (n) P. Maitre and C. W. Bauschlicher, *Chem. Phys. Lett.*, **225**, 467 (1994); (o) C.W. Bauschlicher, H. Partridge and S.R. Langhoff, *Advances in Metal and Semiconductor Clusters,* edited by M.A. Duncan (JAI, Greenwich, CT, 1994), Vol. II; (p) M. Sodupe and C.W. Bauschlicher, *Chem. Phys.*, **185**, 163 (1994); (q) C.W. Bauschlicher and H. Partridge, *Chem. Phys. Lett.*, **239,241** (1995).

[52] (a) J.S. Pilgrim, C.S. Yeh and M.A. Duncan, *Chem. Phys. Lett.*, **210**, 322 (1993); (b) J.S. Pilgrim, C.S. Yeh, K.R. Berry and M.A. Duncan, *J. Chem. Phys.*, **100**, 7945 (1994); (c) C.S. Yeh, K.F. Willey, D.L. Robbins and M.A. Duncan, *Intl. J. Mass Spectrom. Ion Proc.*, **131**, 307 (1994); (d) C.S. Yeh, J.S. Pilgrim, K.F. Willey, D.L. Robbins and M.A. Duncan, *Intl. Rev. Phys. Chem.*, **13**, 231 (1994).

[53] (a) K.F. Willey, C.S. Yeh, D.L. Robbins and M.A. Duncan, *Chem. Phys. Lett.*, **192**, 179 (1992); (b) C.S. Yeh, K.F. Willey, D.L. Robbins, J.S. Pilgrim and M.A. Duncan, *J. Chem. Phys.*, **98**, 1867 (1993); (c) C.S. Yeh, K.F. Willey, D.L. Robbins and M.A.Duncan, *J. Phys. Chem.*, **96**, 7833 (1992).

[54] D.L. Robbins, L.R. Brock, J.S. Pilgrim and M.A. Duncan, *J. Chem. Phys.*, **102**, 1481 (1995).

[55] (a) C.S. Yeh, K.F. Willey, D.L. Robbins, J.S. Pilgrim and M.A. Duncan, *Chem. Phys. Lett.*, **196**, 233 (1992); (b) K.F. Willey, C.S. Yeh, D.L. Robbins, J.S. Pilgrim and M.A. Duncan, *J. Chem. Phys.*, **97**, 8886 (1992).

[56] J. Chen, T.H. Wong, Y.C. Cheng, K. Montgomery and P.D. Kleiber, *J. Chem. Phys.*, **108**, 2285 (1998).

[57] S.H. Pullins, C.T. Scurlock, J.E. Reddic and M.A. Duncan, *J. Chem. Phys.*, **104**, 7518 (1996).

[58] C.T. Scurlock, S.H. Pullins and M.A. Duncan, *J. Chem. Phys.*, **105**, 3579 (1996).

[59] S.H. Pullins, J.E. Reddic, M.R France and M.A. Duncan, *J. Chem. Phys.*, **108**, 2725 (1998).

[60] C.T. Scurlock, S.H. Pullins and M.A. Duncan, *J. Chem. Phys.*, **104**, 4591 (1996).

[61] M.R. France, S.H. Pullins and M.A. Duncan, *J. Chem. Phys.*, **108**, 7049 (1998).

[62] C. Luder, D. Prekas, A. Vourliotaki and M. Velegrakis, *Chem. Phys. Lett.*, **267**, 49 (1997).

[63] C. Luder and M. Velegrakis, *J. Chem. Phys.*, **105**, 2167 (1996).

[64] D. Prekas, B. Feng and M. Velegrakis, *J. Chem. Phys.*, **108**, 2712 (1998).

[65] C.T. Scurlock, J.S. Pilgrim and M.A. Duncan, *J. Chem. Phys.*, **103**, 3293 (1995).; Erratum *J. Chem. Phys.*, **105**, 7876 (1996).

[66] J. Velasquez, K.N. Kirschner, J.E. Reddic and M.A. Duncan, *Chem. Phys. Lett.*, **343(5,6)** 613 (2001).

[67] (a) D. van Heijnsbergen, T.D. Jaeger, G. von Helden, G. Meijer and M.A. Duncan *Chem. Phys. Lett.*, **364(3,4)** 345 (2002); (b)D. van Heijnsbergen, G. von Helden, G. Meijer, P. Maitre and M.A. Duncan, *J. Am. Chem. Soc.*, **124(8)**, 1562-1563 (2002).

[68] G. Gregoire, N.R. Brinkmann, D. van Heijnsbergen, H.F. Schaefer and M.A. Duncan *J. Phys. Chem. A*, **107(2)** 218 (2003).

[69] R.S. Walters, T.D. Jaeger and M.A. Duncan, *J. Phys. Chem. A*, **106(44)**, 10482 (2002).

[70] M. Sodupe, V. Branchadell, M. Rosi and C.W. Bauschlicher, *J. Phys. Chem. A*, **101**, 7854 (1997).

Chapter 2

Experimental

The study of weakly bound metal ion-ligand complexes requires both the ability to produce the complexes of interest, and to keep them intact long enough to probe them. Due to the weak nature of the bonding in many of these clusters, contact with ambient molecules such as those in solution or in air at room temperature would readily disrupt or destroy them. Likewise, clusters that have been thermalized to room temperature will exhibit broad and complex spectral features making interpretation difficult. Since the clusters of interest also possess an electrostatic charge they would be further perturbed by interaction with their surroundings and would require the presence of a counter ion if in solution. Thus it is necessary to study these metal ion-ligand complexes *in vacuo* in a molecular beam[1] to keep them cold and stable long enough to study. The problem of introducing metal into the gas phase and bringing it into contact with the ligand of interest to generate the clusters is solved by use of the laser vaporization/pulsed nozzle cluster source.[2]

2.1 The Molecular Beam Apparatus

The molecular beam machine instrument used in these experiments is shown in Figure 2.1 and is built around a pair of differentially pumped vacuum chambers. The first of the chambers contains a laser vaporization/pulsed nozzle supersonic jet cluster source. This chamber is pumped with a VHS-10 (Varian Inc.) diffusion pump capable of 5300 l/s pumping speed. The metal atoms are cooled in a pulse of buffer gas seeded with the ligand of interest, clusters condense in the expansion and then are skimmed into a molecular beam through a skimmer cone separating the two chambers. The second chamber is held at a constant pressure $\sim 10^{-7}$ torr by a Varian VHS-6 diffusion pump. The clusters produced may either already be ions from the vaporization laser plasma or they may be photoionized in the second chamber. The second chamber is equipped with a homemade Reflectron Time-of-

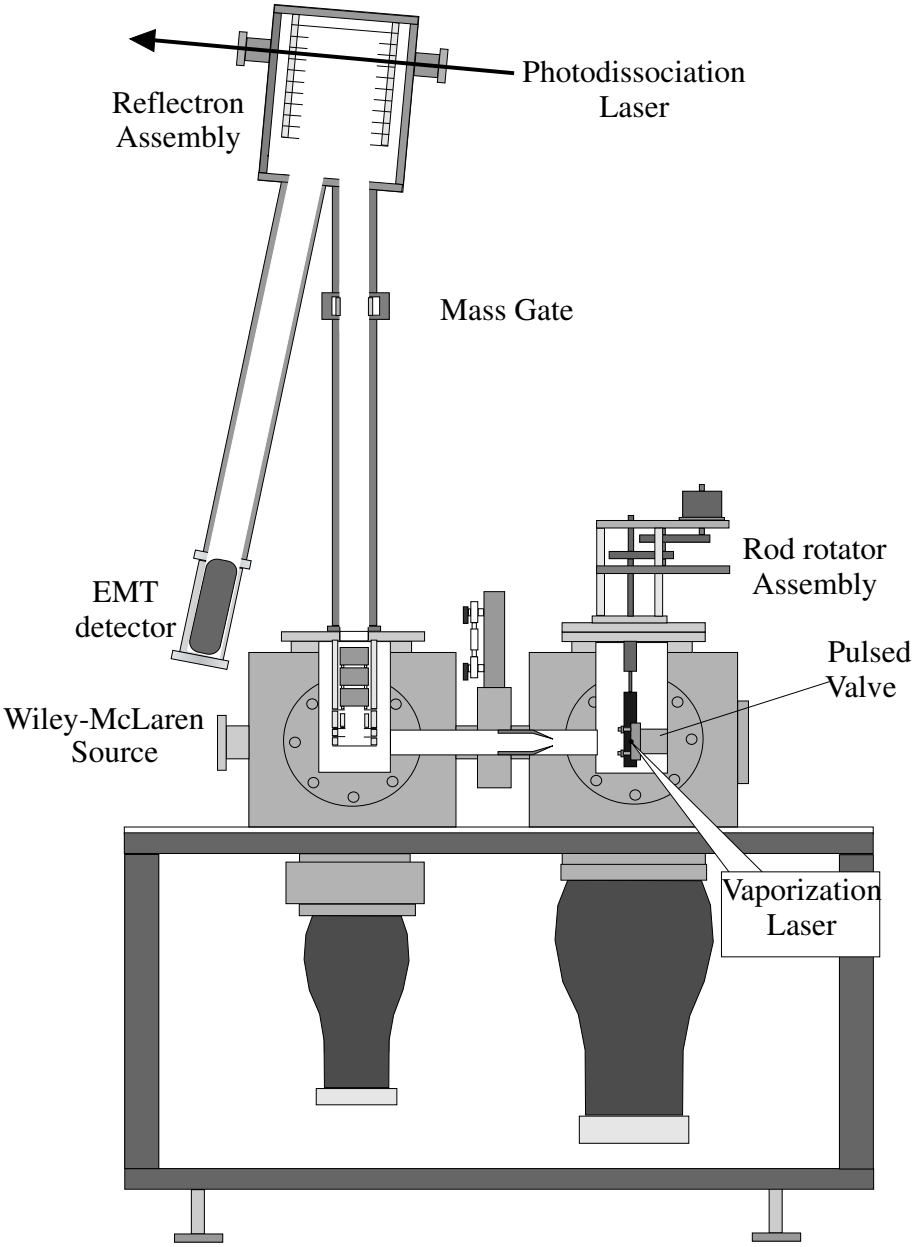

Figure 2.1:
The two-chamber, differentially pumped molecular beam apparatus used for the study of metal containing cluster ions.

Flight (RTOF) mass spectrometer of the Wiley-McLaren type[5] with modified reflectron for photodissociation.[6]

2.2 Pulsed Laser Vaporization

Laser vaporization coupled with pulsed nozzle supersonic expansion has been found to be a highly effective technique for producing clusters with metal atoms.[2,3] It can produce clusters with any metal, metal alloys and many semimetals and nonmetals that can be formed into an appropriately shaped target. In the experiments described herein the vaporization laser is a high power pulsed Nd:YAG (Spectra Physics GCR-11, DCR-11, INDI 30) operating either in second or third harmonic (532 or 355 nm respectively). The pulse is 5-10 ns duration at 10 Hz repetition, 10-50 mJ in energy and focussed to approximately a 1 mm spot on the rod. Timing and synchronization in the experiment are controlled by digital delay generators (SRS DG535). The metal of interest is installed in the apparatus in the form of a $\frac{1}{2}$ in. or $\frac{1}{4}$ in. diameter rod that is both rotated and translated to continually expose fresh surface. The rod holder is a rectangular block that surrounds or partially surrounds the sample rod and has a channel aligned with a fast gas pulse nozzle orifice and an aperture for the vaporization laser to intersect this channel. The rod holder has been described previously[7] and two variations are shown in Figure 2.2. The high intensity radiation focussed onto the rod can be directly absorbed by the metal, causing localized heating that desorbs or ablates the metal, or alternatively can cause electrical breakdown of the beam gas which then etches the metal surface. The resulting plume of plasma can achieve temperatures of several thousand Kelvin. The plasma as a whole is electrically neutral, but contains cations, anions and a balance of hot electrons as well as uncharged species.

An inert carrier gas is pulsed through a 0.5 mm orifice directly over the point of vaporization. The gas pulse nozzle (Parker - General Valve Series 9) must be capable of a fast rise-time to achieve maximum effectiveness. The gas pulse duration typically found to be effective is between 150-250 μs and is held short to limit loading of the vacuum system. The pulse of gas entrains the metal vapor and rapidly quenches the plasma down to nozzle temperature $\sim$300 K in a region of high collision density. The vapor-containing pulse is then allowed to expand into the first vacuum chamber. The expansion occurs quickly to prevent any further energy exchanging collisions with the environment. Thus the expansion is approximately adiabatic.[1]

The ligands of interest can be introduced into the expansion in several ways. Ligands that exist in the gas phase can be seeded directly into the expansion gas in proportionate mixture. Often, the expansion gas itself is the pure ligand. In some cases the seed molecule exists as a liquid at room temperature and has a vapor pressure sufficient to place directly in the gas line leading to the nozzle. Some examples of these are water, methanol, iron pentacarbonyl, and cyclooctatetraene (COT).

For studies involving the heavy polyaromatic hydrocarbons (PAH) or Buckminsterfullerene (C_{60}), the ligand is applied to the metal rod in a thin film using a vapor deposition apparatus, shown in Figure 2.3. In this apparatus the sample rod is prepared prior to installation in the beam machine. The rod is set atop a rotating stage before a tantalum oven cell containing a small amount of the PAH desired. The system is then covered by a glass bell jar and evacuated. The oven cell is then resistively heated until the PAH coats the rod. The sample is stable under air and can be transported to the cluster instrument for study. These highly stable ligands can survive the laser plasma and desorb along with the metal into the gas phase.

Depending on the type of clusters desired, the source can be configured in either of two ways. The coldest expansions are needed to produce clusters such as neutral van der Waals and metal ion-electrostatic complexes and are achieved using a “cut-away”

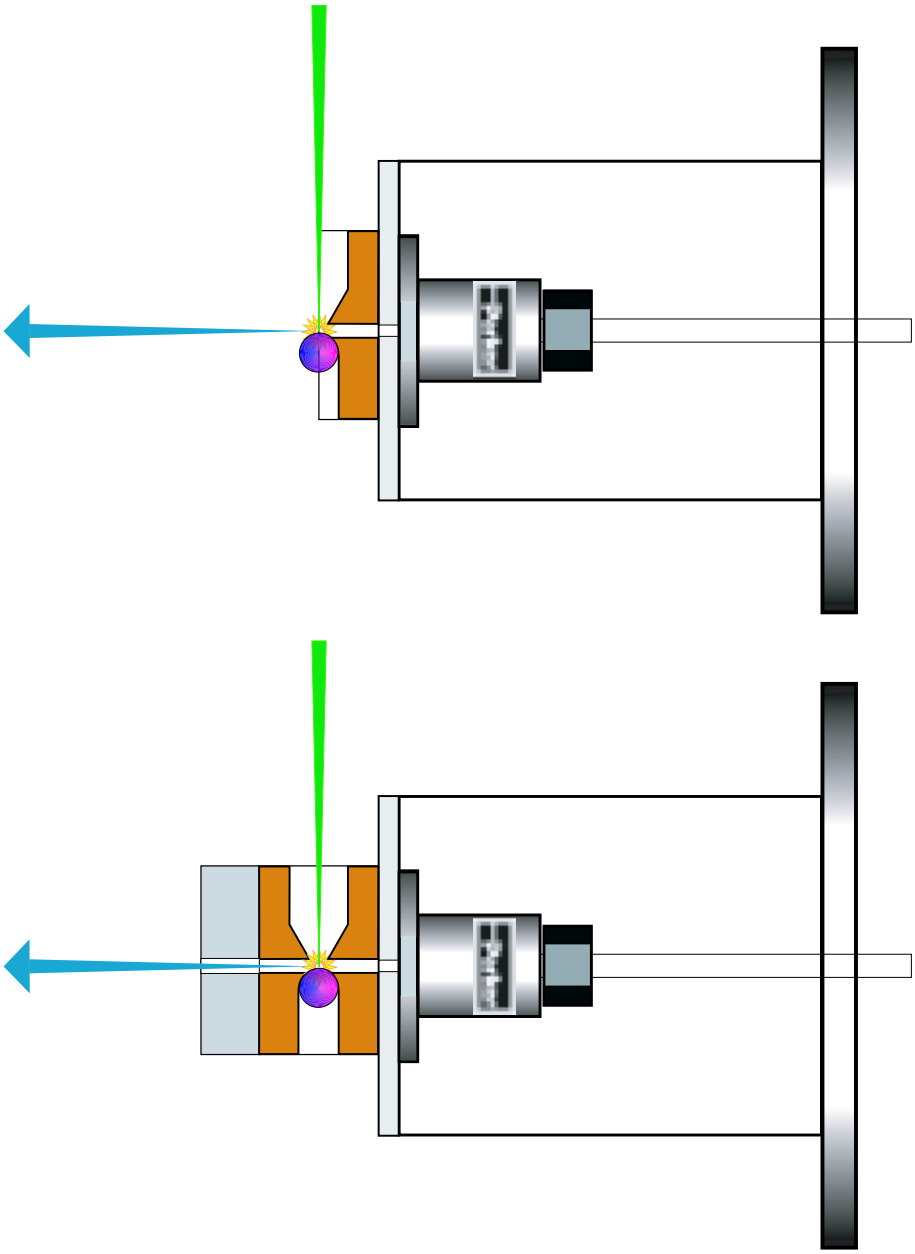

Figure 2.2:
(a) (Above) Diagram of the laser vaporization cluster source of the "cutaway" design used for producing weakly bound metal clusters at very low temperatures.; (b) (Below) The extended channel source configuration used for growth of larger, stronger bound clusters.

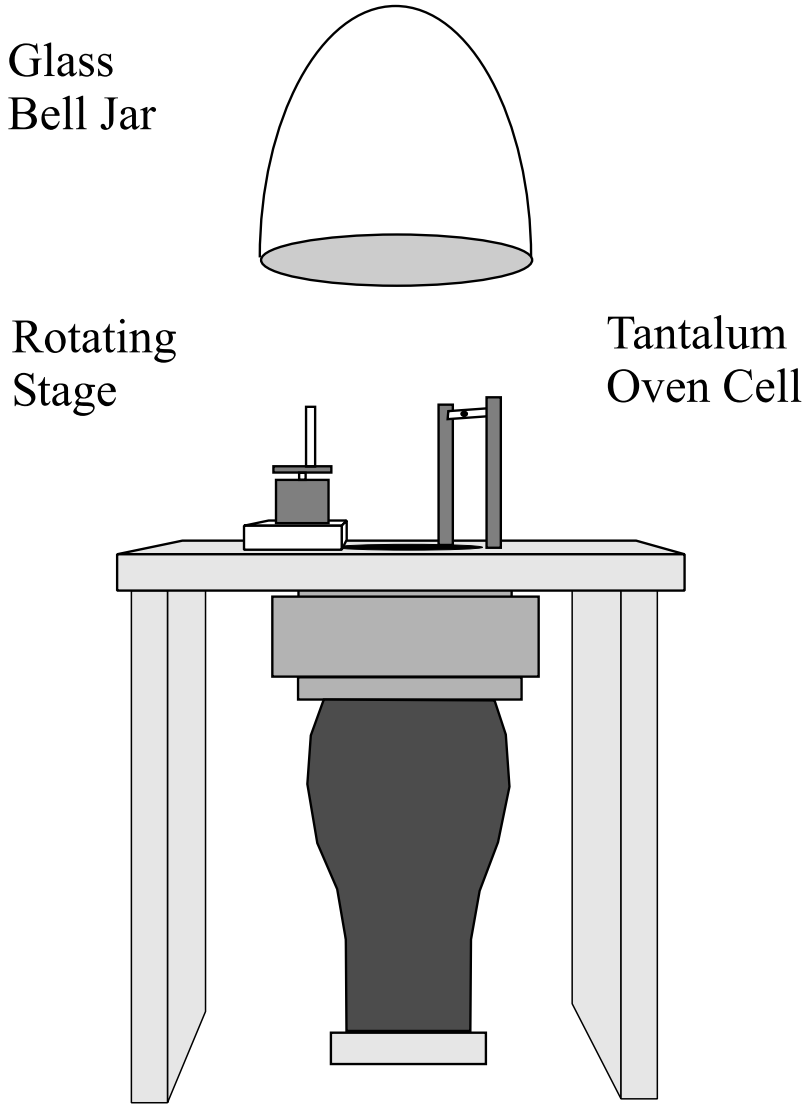

Figure 2.3:
Diagram of the rig used to deposit thin films of polyaromatic hydrocarbon sample onto the metal rods before study in the molecular beam machine.

design[9] shown in Figure 2.2a. The cut-away allows the gas pulse to expand immediately after the point of vaporization. In some cases it may actually be desirable to spoil the cooling ability of the expansion. In order to grow large, strongly bound clusters it is necessary to have more metal-metal collisions and to allow the atoms to sample the largest range of configuration space possible. Annealing the cluster in this way gives the system a better chance to find the global minimum potential energy. This may require making and breaking bonds in one or more intermediate structures along the way. Cooling too rapidly freezes the structure in its kinetically most probable state, whereas allowing the cluster to thermalize to room temperature for a sustained period leaves enough energy for the system to find its thermodynamically favored state. To achieve this a growth channel of variable length is added to the rod holder[7] as shown in Figure 2.2b. A photograph of the cluster source with full rod holder is shown in Figure 2.4. Additionally, the channel introduces turbulence in the flow and creates further opportunity for successful encounters of the clusters with more building materials. One other variation on this is the "waiting room" design in which the gas flow passes through a length of increased bore diameter before being constricted again. With each added channel extension there is improved chance of clustering to larger sizes but also increased likelihood that the clusters will condense out on the inner surface of the channel and never be observed.

2.3 Cluster Separation and Detection

The expanding gas pulse passes through a 3 mm orifice skimmer cone (Beam Dynamics, Inc. Minneapolis, MN) located approximately 10 inches away which selects out the center portion of the expansion with a small angular distribution. This produces a collimated beam of gas containing the metal clusters in the second differentially pumped chamber where analysis will take place. The pressure in this

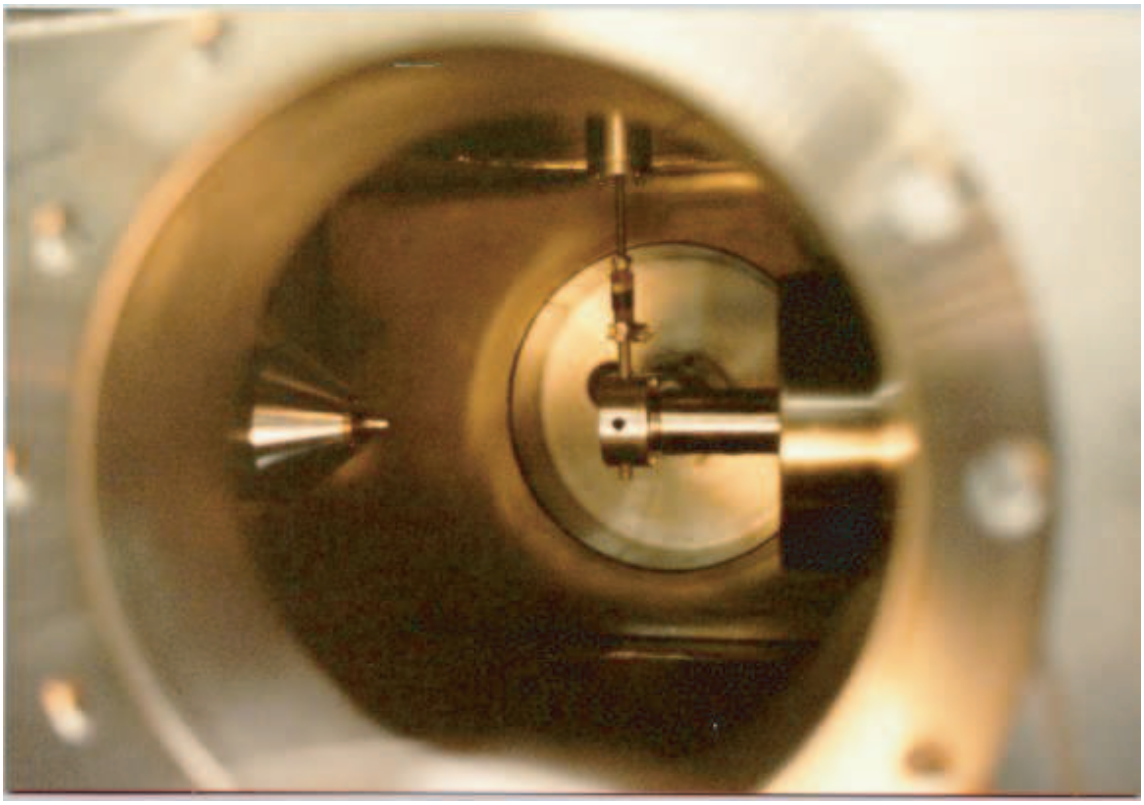

Figure 2.4:
Photograph of the cluster source in the vacuum chamber. The metal sample rod is seen extending above the rod holder. The vaporization laser enters from the opposite side. Also visible is the skimmer cone that separates this chamber from the mass spectrometer.

second chamber is held at a better vacuum ($\sim 10^{-7}$ torr) than the source chamber by a smaller diffusion pump since there is much less gas entering this chamber. The total distance from source to the extraction plates is 60 cm. The requirement for the pressure in the mass spectrometer chamber is that the ion packets may travel the length of the flight tube (about 3 meters) without collisions with the background gas. The mean free path of nitrogen at 10^{-8} torr is about 7 meters.

The ions are accelerated down the first flight tube by a two-stage Wiley-McLaren type source consisting of a repeller plate, draw-out-grid and a ground plate.[5] The Wiley-McLaren design was chosen to compensate the resolution for the finite spatial volume the clusters occupy in the molecular beam. The molecular beam is about the same diameter as the skimmer cone orifice at the point of extraction. The flight tube is situated perpendicular to the molecular beam to eliminate any initial velocity in the direction of extraction which also benefits the resolution. A horizontal deflection plate is used after the source to compensate for the initial transverse velocity from the motion of the clusters in the beam. There is also an einzel lens which acts to focus the ion packets onto the detector, analogous to an optical lens.

The ions separate in time according to their mass-to-charge ratio by the energy relation $E = qV = (1/2)m_0v^2 = (1/2)m_0(\frac{d}{t-t_0})^2$, where q is the charge of the ion, V the voltage on the repeller plate, m is the mass, d the length of the flight tube, and t the time. Assignment of the mass spectrum is performed by first assigning a known ion, recognized by its isotope pattern or other identifiable features of the spectrum. The rest of the masses in the spectrum can be assigned relative to this known by the relation $m_i/t_i^2 = m_0/t_0^2$. The mass assignment can be further refined once more peaks can be identified.

Time of flight mass spectrometry requires that the clusters have an electrostatic charge. Clusters that are ionized directly in the vaporization plasma will enter the mass spectrometer if the plates are held at ground potential before they arrive.

These ions are then extracted with a high voltage pulse on the TOF plates at an optimally chosen time. Clusters that are uncharged in the beam must be ionized to be detected. If one desires to probe neutral clusters, they can be ionized at a fixed wavelength, usually 193 nm from an ArF excimer laser (Lambda Physik Compex 102, Lumonics Pulsemaster 842), and the mass spectrometer plates can be left at constant voltage.

As the ions approach the reflectron assembly they pass by a field plate used as a "mass gate". When mass selection is desired the field plate is held at a constant potential of 250 V to reject all ions preceding the one of interest. The voltage is then synchronously triggered to pulse to ground for a controlled duration while the ion packet desired is allowed through. The voltage is then switched back on to continue to reject later ions.

The reflectron assembly at the end of the first flight tube consists of a set of ten plates. The plates have a potential gradient applied to them to slow the ion packets down, and then redirect them down the second fight tube. The voltage on the reflectron is chosen so that the turn-around point falls directly between the pair of window ports mounted on either side of the assembly. In our application, the turn-around point allows us to intersect the clusters with a high power pulsed laser to initiate photodissociation.[6] Photodissociation can be accomplished with the fixed frequency harmonics of a Nd:YAG laser, with tunable UV-visible light from a dye laser, or with tunable infrared from an OPO. Since the clusters are effectively at rest when probed, any spectroscopy performed will be essentially free of any Doppler shift or broadening.

The ions end their life at the electron multiplier tube detector (Hamamatsu R595). The detector amplifies the ion signal by a factor of 10^7. The signal then gains an extra factor of 10 amplification by an Ortec 9301 fast preamplifier. The signal is then collected by a Digital Sampling Oscilloscope (DSO) (LeCroy 9310, LT347

Waverunner) with a sampling rate of 100-500 MHz. The data is transferred to a PC via the GPIB (IEEE 488.2) protocol using a National Instruments interface card (NI PCI-GPIB) and custom data acquisition software written in Microsoft Visual Basic 6 (sp5) utilizing the LeCroy ActiveDSO ActiveX control. This software also simultaneously controls the scanning of the tunable lasers.

2.4 Pulsed Tunable Infrared Light Source

Resonance enhanced infrared photodissociation spectroscopy is performed with the use of a newly developed tunable infrared optical parametric oscillator (OPO) (LaserVision, Bellevue, WA). The OPO is a nonlinear optical device capable of generating two photons of longer wavelength from a pump photon in a process called downconversion. OPO technology has existed for many years,[10,11] however no high power, easily tunable pulsed infrared sources in the mid-IR region where vibrational spectroscopy occurs have existed until now. The high peak power necessary to achieve multiphoton photodissociation was not available until this system was developed. Infrared light is produced in a two stage process. The first stage is the oscillator composed of two KTP crystals situated between a fixed diffraction grating with tilting mirror and the output coupler. The oscillator crystals are pumped with vertically polarized 532 nm generated in the system from 1064 nm delivered by a frequency stabilized Nd:YAG laser (Continuum Powerlite 9010). The crystals then generate two wavelengths called the signal and idler, and their wavelengths are controlled by angle tuning both the crystals and the grating mirror. The signal wavelength is continuously tunable from 710 to 845 nm while at the same time the idler tunes from 1350 to 2000 nm such that the sum of the energy of these two photons equals the energy of the pump photon at 532 nm. The idler then is passed on to the amplifier stage which consists of four KTA crystals that are pumped by

the Nd:YAG fundamental at 1064 nm. In this stage, the idler and the pump undergo difference frequency mixing to produce the desired output in the range of 2000 to 5000 nm. The pulse energy varies with wavelength but falls between 1 to 10 mJ per pulse at 10 Hz. The resolution is 0.2 cm^{-1}, dictated by the linewidth of the pump. The nonlinear optical conversion process is highly sensitive to the peak power of the pump beam and the resolution of the output is limited by the linewidth of the pump. Therefore it is required that the pump be injection seeded. Injection seeding uses a CW IR laser diode that actively couples to the cavity on a shot-to-shot basis. This stimulates emission in a narrower frequency range than would otherwise spontaneously occur in an ordinary Q-switched laser. The CW laser also reduces the time it takes for the cavity to build up enough radiation density to lase, and thereby shortens the pulse duration. Shorter pulse duration translates into higher peak power. Additionally, injection seeding helps to eliminate spatial and temporal fluctuations in the output beam which can produce spatial "hot spots" and spurious power spikes. These intense transients could easily exceed the damage threshold of the delicate nonlinear crystals. Thus, injection seeding allows the system to run at powers just below the damage threshold without uncontrolled spikes pushing it over the edge. The pump system needed adds significantly to the cost and complexity of the experiment but the benefits are invaluable.

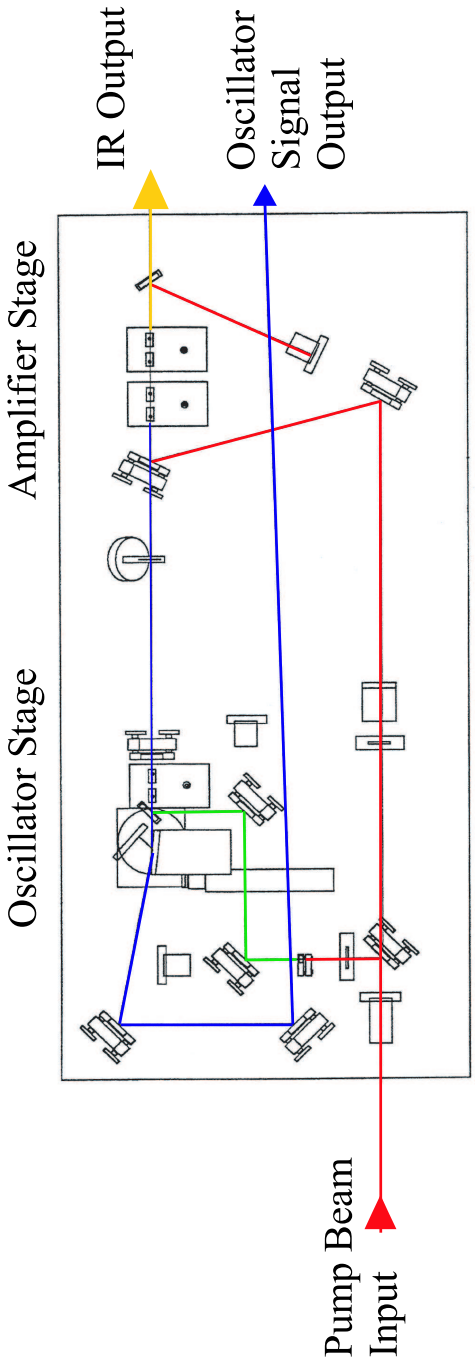

Figure 2.5:
Schematic diagram of the LaserVision Infrared OPO system. The system is pumped by an injection seeded Nd:YAG laser at 1064 nm. The oscillator downconverter lases from 710 to 845 nm and pumps the amplifier difference frequency mixer. The amplifier stage lases from 2000 to 4400 cm^{-1}.

2.5 References

[1] *Atomic and Molecular Beam Methods*, ed. G. Scoles, Oxford Univ. Press, NY 1988.

[2] T.G. Dietz, M.A. Duncan, D.E. Powers and R.E. Smalley, *J. Chem. Phys.*, **74**, 6511 (1981).

[3] *Physics and Chemistry of Small Clusters*, ed. P. Jena, B.K. Rao and S.N. Khanna, Plenum Press, NY 1986.

[4] W.H. Breckinridge, C. Jouvet, B. Soep, *Advances in Metal and Semiconductor Clusters*, ed. M.A. Duncan, JAI Press, Greenwich, 1995.

[5] W.C. Wiley, I.H. McLaren, *Rev. Sci. Instrum.*, **26**, 1150 (1955).

[6] (a) D.S. Cornett, M. Peschke, K. LaiHing, P.Y. Cheng, K.F. Willey and M.A. Duncan, *Rev. Sci. Instrum.*, **63**, 2177 (1992); (b) K. LaiHing, R.G. Wheeler, W.L. Wilson and M.A. Duncan, *J. Phys. Chem.*, **87**, 3401 (1987).

[7] K. LaiHing, R.G. Wheeler, W.L. Wilson and M.A. Duncan, *J. Chem. Phys.*, **87**, 3401 (1987).

[8] J.E. Reddic and M.A. Duncan, *Chem. Phys. Lett.*, **264**, 157 (1997).

[9] T.E. Adams, B.H. Rockney, R.J.S. Morrison and E.R. Grant, *Rev. Sci. Instrum.*, **52**, 1469 (1981).

[10] W. Demtroder, *Laser Spectroscopy*, Springer-Verlag, Berlin, 1996.

[11] S.E. Harris, *Proc. IEEE*, **57**, 2096, 1969.

Chapter 3

Laser Vaporization And Cluster Growth

The technique of laser vaporization has proven highly effective at facilitating the study of metal ion-molecule complexes[1] in the gas phase. Many factors affect the the growth of metal-containing clusters in our experiment and the processes are complex and not well understood. On the other hand, these many variables give us a number of handles on the experiment allowing us to control and empirically optimize the growth process to achieve desired results. These considerations depend dramatically on the nature of the cluster we wish to observe. A number of examples will be discussed that shed light on these processes and yield informative results.

3.1 Laser Vaporization Combined With Supersonic Expansion

Pulsed laser vaporization is utilized in these experiments because this allows for the study of a multitude of chemical elements, including alloys and nonmetals to be studied. Other methods have severe limitations in their application. Heated oven cells work only for low melting metals. Hollow cathode sources require the material to be an electrical conductor. Other means include seeding volatile organometallic complexes into the beam, however only select metals form such complexes. Laser vaporization is the simplest and most widely applicable method for producing clusters in the gas phase.

As discussed above, the vaporization laser generates an extremely hot plasma at the surface of the sample rod. The plasma as a whole is electrically neutral, but contains cations, anions and a balance of hot electrons as well as uncharged species. Metal vapor produced in this way is far too hot to allow for a substantial amount of clusters to exist, and therefore must be cooled to allow condensation to take place. Cooling is also necessary to allow bonds to form, since the kinetic energy must be released in order for the atoms to stick to each other. To solve this problem, we combine laser vaporization with a pulsed supersonic jet expansion[1] to cool the

metal vapor to cryogenic temperatures. The pulse of gas entrains the metal vapor and rapidly quenches the plasma down to nozzle temperature ∼300 K. The vapor-containing pulse is then allowed to expand into the first vacuum chamber of our instrument described in detail in Chapter 2.

Collisions with the buffer gas in the high density region of expansion redistribute internal energy modes among collision partners. This redistribution may not reach thermodynamic equilibrium, however, because the rates of rotational, vibrational and translational energy transfer are different. Translational energy transfer is the most efficient process, and this process quickly accelerates the metal atoms and clusters to the average linear speed of the buffer gas at room temperature.[2] Transfer of energy from internal degrees of freedom into translational motion is the next most efficient process and the one that leads to the energy being irreversibly removed from the system. Rotational energy transfer is the more efficient of these, followed by vibrational transfer.

The actual rates of these processes depend on the nature of the collision gas. For monatomic buffer gases, such as the noble elements, the efficiency of transfer per collision goes up with increasing mass, thus xenon cools much more efficiently per collision than helium. However, the collision frequency goes down inversely with the (square root of) mass of the gas atom leading to a compromise in total cooling. This tradeoff reaches an optimal balance with neon which is found to be the best at cooling of the noble gases. Diatomic and polyatomic gases possess internal degrees of freedom, and thus have energy levels that increase the state density in the vicinity of the internal modes of the clusters. The presence of these low lying energy states greatly enhances the ability of the collision gas to transfer vibrational and rotational energy out of the clusters beyond that of a monatomic gas. Expansion gases like nitrogen and carbon dioxide produce large amounts of cold clusters.

The clusters must be maintained intact on a timescale that allows us to study them. This is achieved by entraining them in a collision free molecular beam. Once the gas pulse leaves the rod holder region, it expands at a velocity greater than the local speed of sound, hence the gas flow is described as supersonic. Although the mathematics needed to describe the flow in a pulsed supersonic expansion are complex, we can attempt to treat the middle of the gas pulse as a quasi-continuous flow.[3] Supersonic expansions are characterized by their Mach Number, which is the speed of the expansion relative to the local speed of sound under those conditions. The speed of sound in a medium is defined as the speed that pressure waves propagate through that medium. A continuous flow establishes a boundary layer defined by a standing shockwave. The region contained by this shockwave is known as the "zone of silence" which physically extends a distance to the forward boundary called the Mach disk. The Mach disk appears at a distance x_m from the source of expansion given by

$$x_m = \left(\frac{2}{3}\right) d \left(\frac{P_b}{P_0}\right)^{\frac{1}{2}}, \tag{3.1}$$

where d is the nozzle diameter, P_b is the nozzle backing pressure and P_0 is the pressure of the source chamber. Within this region the expansion moves faster than Mach 1 and thus cannot sense the walls of the chamber that contains it. For the experiments conducted here, typical values for these parameters are: d = 1 mm, P_b = 3040 torr and $P_0 = 10^{-6}$ torr, resulting in a Mach disc 37 meters from the source. This is much larger than the distance of the source to the skimmer cone (20 cm) and so no shock structure could be expected to exist under these conditions. Studies have shown that pulsed nozzles in fact are capable of lower ultimate temperatures than continuous free jets,[4] and in some cases temperatures as low as 1 mK have been reported. The result is that the clusters expand without interaction with the

background gas or contact with the surroundings and can be expected to survive for the duration of this experiment.

3.2 Statistical and Nonstatistical Cluster Abundance

The distribution of cluster sizes observed in the molecular beam is a product of several factors including the conditions of the cluster source, the intrinsic instrumental biases of the mass spectrometer and most importantly, the physical and chemical properties of the atoms, ions and molecules themselves. A purely random cluster size distribution should exhibit a smooth and uniform array of peaks in the mass spectrum governed by the two competing factors of increasing collision cross section vs. decreasing number density. When a particular cluster size stands out among its adjacent sizes it is considered evidence that it has some special character and is termed a "magic number" cluster. This evidence is corroborated if the cluster appears prominently under a variety of source conditions, mass spectrometer focussing settings and/or ionization laser wavelengths and fluences.

3.3 Electrostatic Complexes

An example of a mass spectrum that exhibits magic numbers is $Mg(Ar)_n^+$ shown in Figure 3.1. These clusters were formed with a cutaway rod holder with a pure argon expansion and the ions are formed directly in the jet. The spectrum shows a distribution of clusters of a single magnesium ion with incremental addition of argon atoms. The distribution shows distinct peaks for 12, 18, 45 and 54 argon atoms and others. These numbers occur at a size one atom less than the pure rare gas ion clusters that have been observed many times before.[5] The pure rare gas magic numbers occur at sizes that correspond to geometric packing of the perfectly spherical atoms based on icosahedra that maximize the close contact attractive forces.[6] The magic number

sizes with magnesium ion are due to the fact that metal ion occupies the center position rather than an argon ion. Magnesium ion has a single valence electron in a spherical s orbital. Metals such as the transition metals can exhibit other magic numbers because they have nonspherical electron charge distributions.[10]

Introducing a mixture of ligand molecules into the source can provide insight into molecular electrostatic bonding to metal ion centers and the nature of intermolecular forces. Figure 3.2 shows an example of cobalt vaporized in an expansion containing hydrogen gas, water vapor, and argon. The clusters are sampled as ions out of the jet. This mixture combines a metal cation with molecules exhibiting each of the basic electrostatic interactions. The argon atom has no static multipole moments but has a large polarizability. The water molecule is predominantly surrounded by its dipole field. The hydrogen molecule possesses a quadrupole moment that is positive in value and would be expected to bond to an ion in a T-shaped orientation.[7] The electrostatic forces are strongly distance dependent and the strength of the force drops off faster with distance in the order:

charge-induced dipole > charge-quadrupole > charge-dipole

The respective binary binding energies of Co^+ with each of these have been measured previously and are listed in Table 3.1. Thus, the measured binding energies follow the predicted pattern in the strength of the electrostatic interaction.

Table 3.1:
Binding energies of cobalt ion with selected ligands. Values are taken from Freiser[8].

Co^+ - H_2O	38.5 kcal/mol
Co^+ - H_2	18.2
Co^+ - Ar	11.8

The lightest mass series in the spectrum belongs to $Co^+(H_2)_n$, where n=0-5. The intensity pattern shows a steady drop toward n=3 and then a sudden rise at n=4. The second grouping of peaks correspond to clusters of $Co^+(H_2O)$ successively attaching up to three H_2 molecules. Following this at higher mass is a set for Co^+Ar which adds up to five hydrogen molecules. At higher mass still is the four component cluster made of Co^+, Ar, H_2O and H_2 with H_2 going up to n=3. Finally at highest mass in the spectrum is cobalt with a pair of argon atoms and hydrogen molecules up to n=5. There is a noticeable absence of addition of atomic hydrogen attached to the metal ion. This would suggest that the metal is not breaking the H-H bond in the plasma during formation and that these are whole H_2 units adding to, or solvating, the metal ion.

The most stable configuration for an ion solvated by a particular type of molecule is to maximize the number of molecules that are in direct contact with it. Once this first sphere is closed, additional molecules will experience a significantly shielded electrostatic attraction. The first sphere for hydrogen on cobalt appears to close at five hydrogens because further addition is not observed. Measurements of binding energies in $Co^+(H_2)_n$ clusters have been made by equilibrium van't Hoff studies,[9] and are summarized in Table 3.2. The trend in binding energies shows a drop after n=2, n=4 and a sharp drop at six H_2 molecular units. The pattern of observed cluster signal follows the energy trend rather closely, as one might expect. However, there are notable differences between the observed intensity and the binding energy that occur for the n=3 and n=6 clusters where they appear in lower abundance than might be expected from the binding energy consideration. The n=6 cluster, likewise might be expected to occur in similar abundance as n=5 however it is not observed at all.

A water molecule will bind more strongly to the metal ion than hydrogen because it has a large dipole moment. The water would then be expected to displace some

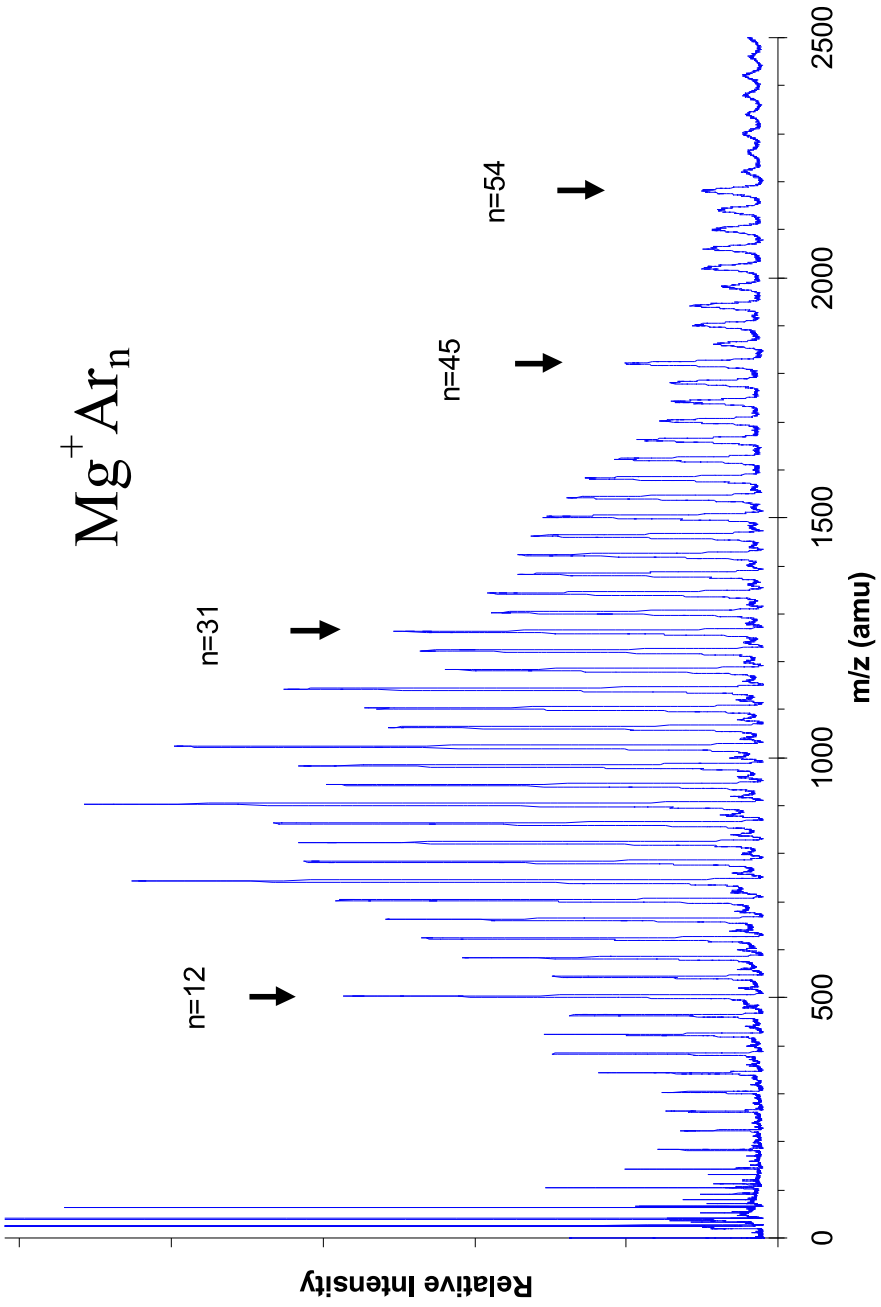

Figure 3.1:
A mass spectrum of magnesium argon clusters. The cluster distribution shows distinctive prominent peaks for certain cluster sizes. These special sizes have been observed in many cases and correspond to geometrical shell closings.

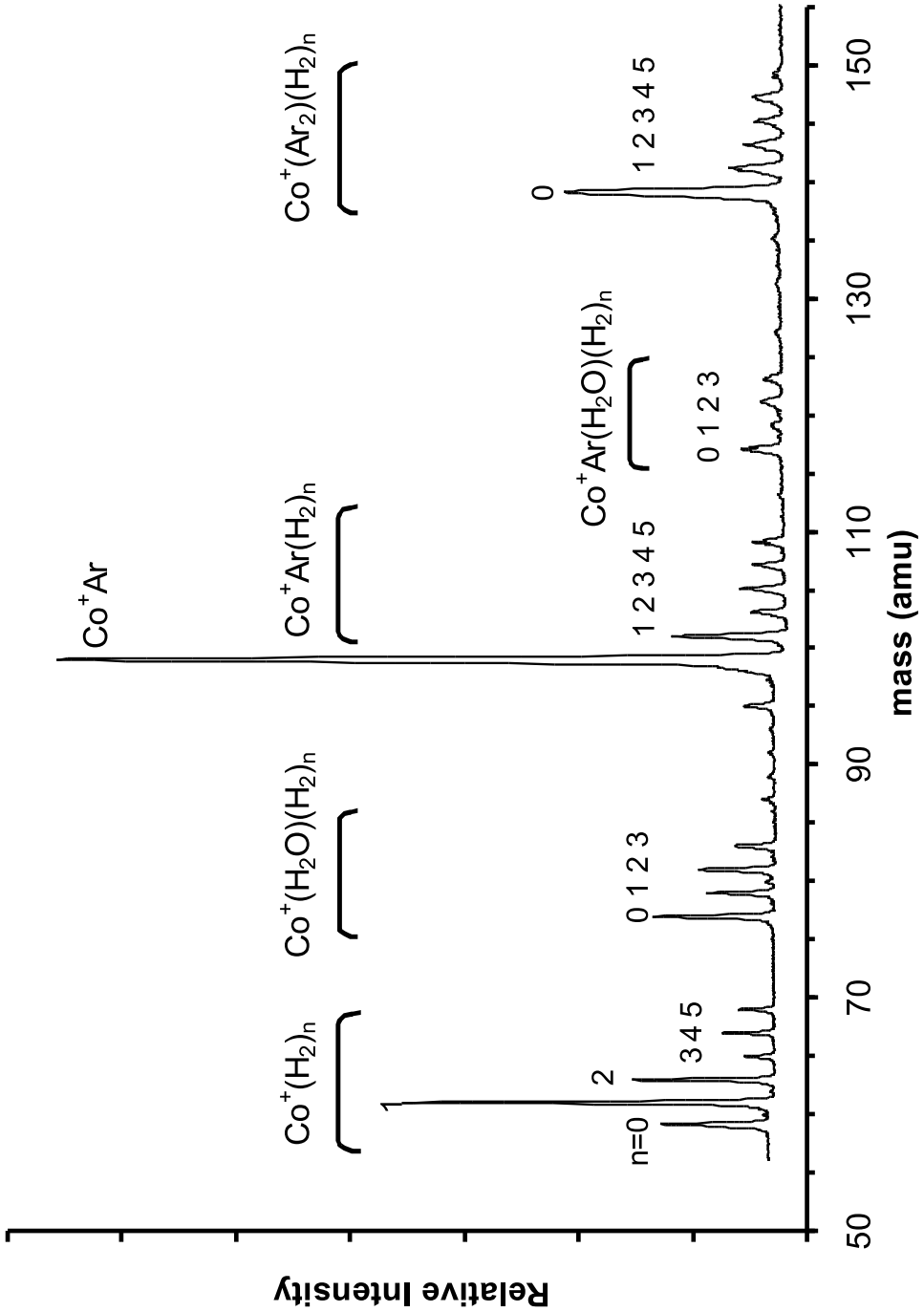

Figure 3.2:
A mass spectrum of mixed clusters of cobalt with hydrogen, water and argon.

Table 3.2:
Binding energies (in kcal/mol) of sequential removal of H_2 to Co^+. This is the energy of the reaction $Co^+(H_2)_n \Rightarrow Co^+(H_2)_{n-1} + H_2$. (Data from Refs. [8], [9])

n	D_0 (kcal/mol
1	18.2
2	17.0
3	9.6
4	9.6
5	4.3
6	04.0
7	0.8

hydrogen in the first solvation sphere. The clusters present in the mass spectrum for $Co^+(H_2O)(H_2)_n$ terminate after n=3, a dip at n=1, and the peak at n=2 shows some enhanced intensity. This pattern resembles that of the pure hydrogen clusters shifted down by two. Thus the water appears to displace a pair of hydrogen molecules due to its larger steric volume.

An argon atom can only bind to an ion by dispersion forces which in general are weaker than ion-dipole and ion-quadrupole interactions. The measured binding energy of Co^+H_2 is 18.2 kcal/mol whereas that of Co^+Ar is only 11.8 kcal/mol,[8] consistent with this expectation. When an argon atom is also present on the metal ion the peak for n=3 is larger than the adjacent sizes, just as n=4 was for pure hydrogen and n=22 was for water+hydrogen, which is consistent with argon occupying one site in the first sphere. However, one would expect that if the argon did occupy one site then the remainder of the distribution would terminate at n=4. This may mean that the clusters present represent a mixture of two structural isomers. One isomer would have argon directly in contact with the metal ion and gives rise to the enhanced n=3 peak. The other isomer would have the argon in the second sphere

of $Co^+(H_2)_n$ clusters that appear out to n=5. This explanation would account for the $Co^+(Ar_2)(H_2)_n$ distribution. In this case there would be four possible isomeric forms of argon occupying inner or outer positions, but only when both are outer sphere would there be a peak for n=5. The n=5 peak is present in this series, but at a fraction of its observed relative intensity for the other series with one or no argon.

It is also important to note that although we generally expect that the observed intensity somewhat follows binding strength, Co^+Ar appears with greater intensity than $Co^+(H_2O)$. This is easily explained, however, since argon is the backing gas in this experiment and occurs in much greater concentration than water which is seeded into it in small proportion. Therefore we can only use this argument in discussing the trends within the series of a particular ligand.

3.4 Strongly Bound Complexes

Strongly bound metal ion complexes are those which exhibit a significant degree of covalent bonding in their structure. The differences in bonding produce very different properties in the clusters. This radically affects the types of techniques needed to produce them in sufficient quantity in the cluster source.

In contrast to electrostatic complexes, where the electronic configuration of the metal primarily dictates the inter-electron repulsion governing stability of the complex, covalent systems adopt electronic configurations that maximize bonding orbital overlap. In covalent systems the electrons are more delocalized and the ionic charge can become distributed over a greater volume within the molecule. In order for the cluster to find the global minimum in the bonding potential energy surface it is often required that energy be put in to the system first so that more favorable overlaps can be obtained. This could be a relatively low energy process such as exciting the metal ion from its ground state to a state with a different electronic configuration.

Alternatively, it could be a process with a much higher barrier, like breaking covalent bonds in a molecular ligand and reforming those bonds around the metal to produce insertion products. Some examples of this may be $[H–Co–H]^+$ and $[V@C_{60}]^+$ (as opposed to $Co^+(H_2)$and $V^+–(C_{60})$.

The source conditions required to produce such clusters have certain features in common. Generally higher vaporization laser fluences are required, along with a backing gas that produces more collisions and is less efficient at cooling per collision, and an extended channel rod holder such as that shown in Figure 2.2. There are also features specific to each cluster in particular that must be taken into consideration as well. Some metal samples are quite soft and vaporize easily compared to other, more refractory metals. Some molecular ligands are involatile and must be applied to the metal rod in the vapor deposition rig ahead of time. These require careful attention to the coating thickness. This then factors in to the vaporization laser power required to produce a proper ratio of metal and ligand in the plasma.

The case of transition metal ions bound to aromatic and/or highly conjugated hydrocarbon molecules is illustrative of these considerations. Previous studies of metal-C_{60} systems[12] showed evidence for simple exhohedral bonding and the formation of alternating sandwich-type structures with C_{60} alternating with the metal atoms. Figure 3.3 shows the mass spectrum of clusters produced by co-vaporizing a rod of vanadium coated with C_{60}. The vaporization laser wavelength was chosen as 532 nm because the Nd:YAG laser produces much more intense light here than at 355 nm and the energy per photon is still moderately high. The most prominent peak belongs to $V(C_{60})^+$ followed by V^+ and $V(C_{60})_2^+$ Also prominent are a whole series of clusters belonging to vanadium carbides leading up to and terminating with $V_8C_{12}^+$.

The $V_8C_{12}^+$ species appearing in Figure 3.3, termed a "met-car", is a well known cluster that can be produced with many transition metals.[13] This cluster can be

produced readily by vaporizing metal in the presence of a source of carbon. In this case the source of carbon is C_{60}. C_{60} is a highly stable allotrope of carbon and requires a large amount of energy to rip apart. The plasma in the source was hot enough to allow the destruction of the fullerene cage which then allowed for the reformation of the met-car cluster with vanadium.

Figure 3.4 shows the mass spectrum obtained from laser vaporizing an iron rod in a helium expansion seeded with both benzene and coronene. While benzene has a high vapor pressure and the vapor can be seeded into the backing gas, coronene is a large, heavy polyaromatic molecule with low vapor pressure ($\sim 10^{-12}$ torr). This spectrum shows mixed clusters with proportions denoted by (x,y,z) where x is the number of benzene molecules, y is the number of iron atoms and z is the number of coronene. The labelled peaks show the presence of iron ion (0,1,0), coronene ion (0,0,1) and mixtures of these with benzene. Absent are any clusters of pure benzene or pure coronene.

In contrast to the conditions used in Figure 3.3, there is no indication that either benzene or coronene are being disrupted. This is a result of lower vaporization intensity. The clusters that appear are therefore likely to be simple addition products of metal with molecular ligands. The peaks for the two-ligand masses (2,1,0), (0,1,2) and (1,1,1) belong to "sandwich" structures where the metal atom resides between two molecular fragments, which allows for optimal sharing of the metal bonding interaction with both ligands. Photodissociation studies of these complexes[11] have been used to bracket the binding energies of these ligands to the metal ion. The findings showed that the order of binding energy with iron ion was coronene > benzene > C_{60}.

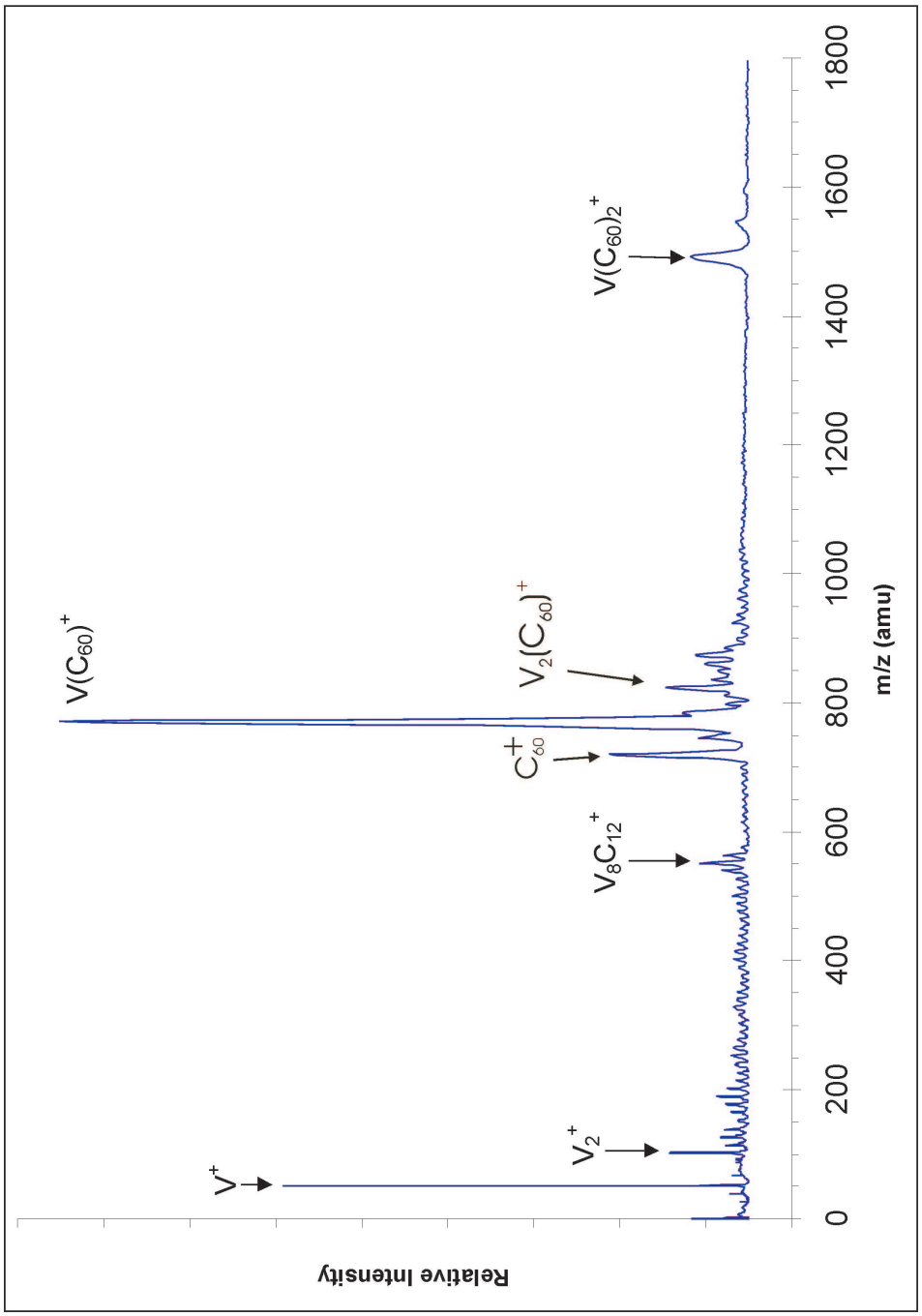

Figure 3.3:
Mass spectrum of vanadium C_{60} produced from a coated metal rod. The vaporization conditions were exceptionally hot, this allows for vanadium to break the C_{60} cage and form carbides. Visible is the $(V_8C_{12})^+$ "Met-Car" cluster.

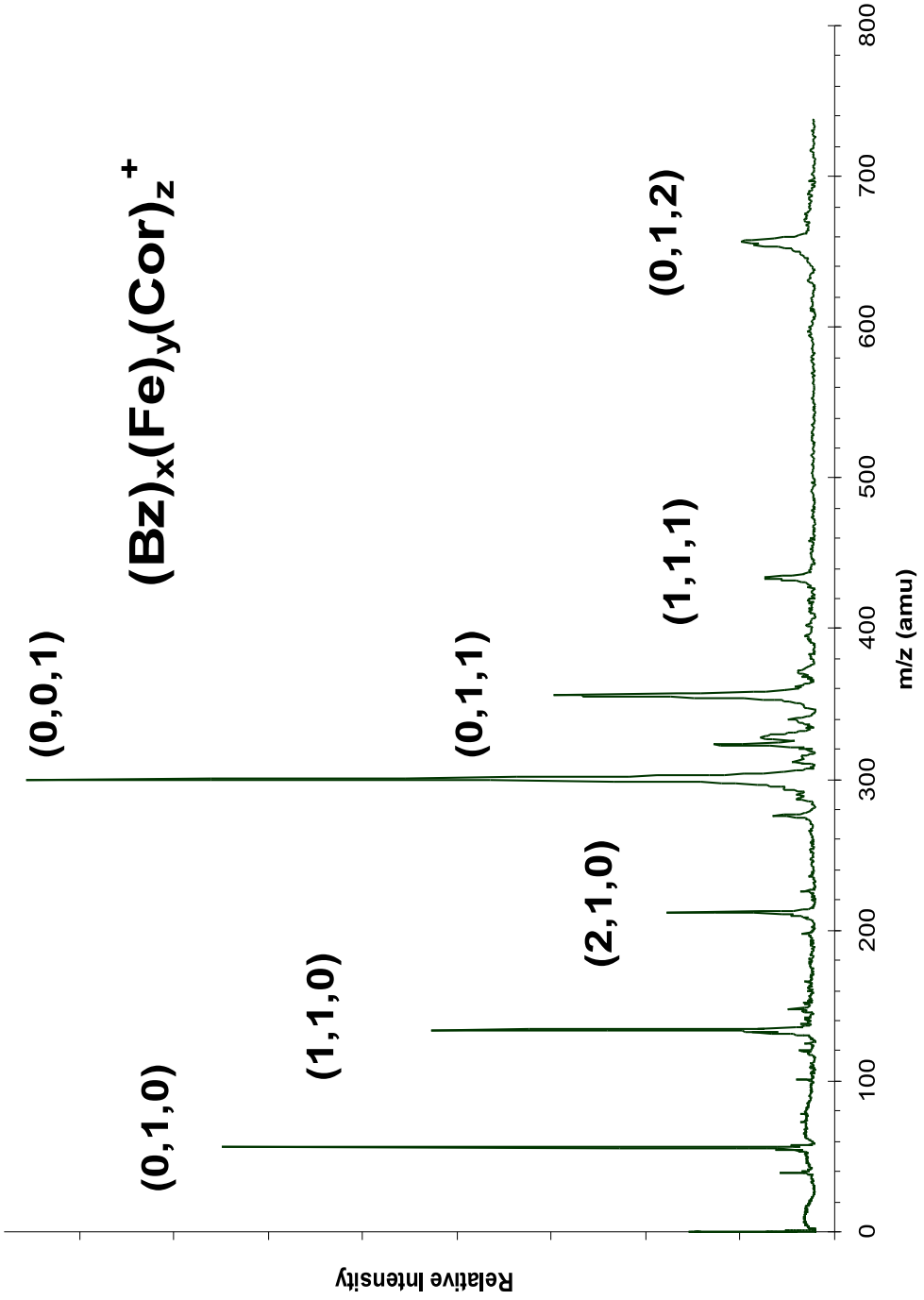

Figure 3.4:
Mass spectrum of mixed coronene and benzene with iron produced by using both a coated metal rod and a volatile seeded into the expansion gas.

3.5 References

[1] T.G. Dietz, M.A. Duncan, D.E. Powers and R.E. Smalley, *J. Chem. Phys.*, **74**, 6511 (1981).

[2] Heavier clusters may not obtain the full acceleration due to the finite number of collisions. This is known as "slippage", and can be utilized in the separation of larger clusters by controlling experimental timing.

[3] *Atomic and Molecular Beam Methods*, ed. G. Scoles, Oxford Univ. Press, NY 1988.

[4] *Jet Spectroscopy and Molecular Beams*, ed. J.M. Hollas and D. Phillips, Blackie Academic and Professional Press, Glasgow, UK 1995.

[5] (a) O. Echt, K. Sattler, E. Recknagle, *Phys. Rev. Lett.*, **47**, 1121 (1981); (b) A. Ding, J. Hesslich, *Chem. Phys. Lett*, **94** 54 (1983); (c) P.W. Stephens, J.G. King, *Phys. Rev. Lett.*, **51**, 1538 (1983).;(d) A.L. Mackay, *Acta. Crit.*, **15**, 916 (1967).

[6] *Clusters of Atoms and Molecules, V.1* ed. H. Haberland, Springer-Verlag, Berlin 1994.

[7] *The Forces Between Molecules* M. Rigby, E.B. Smith, W.A. Wakeham, G.C. Maitland, Oxford Science Publications, UK 1986.

[8] *Organometallic Ion Chemistry*, ed. B. Freiser, Kluwer Academic Publishers, 1996.

[9] P.R. Kemper, J. Bushnell, G. von Helden, M.T. Bowers, *J. Phys. Chem.*, **97**, 52, (1993).

[10] M. Velegrakis, *Advances in Metal and Semiconductor Clusters*, ed. M.A. Duncan, Elsevier Press, New York, 2001.

[11] J.W. Buchanan, G.A. Grieves, J.E. Reddic and M.A. Duncan, *Intl. J. Mass Spectrom.*, **182/183** 323-333 (1999).

[12] (a) G.A. Grieves, J.W. Buchanan, J.E. Reddic and M.A. Duncan, *Intl. J. Mass Spectrom.*, **204(1-3)**, 223-232 (2001); (b) J.E. Reddic, J.C. Robinson and M.A. Duncan, *Chem. Phys. Lett.*, **279(3,4)**, 203 (1997).

[13] B. C. Guo, S. Wei, J. Purnell, S. Buzza and A. W. Castleman, Jr., *Science*, **256**, 515-516 (1992).

Chapter 4

Metastable Doubly Charged Metal Ion-Molecule Complexes Observed with Laser Vaporization

4.1 Introduction

Metal cations are of ubiquitous importance in many areas of physical science including most solution phase chemistry, geology, atmospheric science, biology and anywhere salts in solution play a role. Because of this widespread occurrence, their interactions with solvent molecules have been studied extensively in the gas phase. Gas phase production methods, however, are heavily biased toward the single positive ion due to difficulties in producing multiply charged species. Most metals prefer an oxidation state[1] greater than 1 and therefore further research is needed to achieve broad understanding of metal ion solvation. Recent advances in techniques have allowed for the improved study of doubly and triply charged cations in the gas phase through various means.[2–16] However laser vaporization is a well established and facile method that has not as yet been applied generally toward producing species with double charge. This is the first successful application of the laser vaporization method toward generating a wide range of doubly charged metal cluster molecules.

The energetics of a doubly charged metal ion complex are governed by the difference between the second ionization potential, IP(M^+) and the first ionization potential, IP(L) of the ligand molecule:[19]

$$\Delta IP = IP(M^+) - IP(L). \tag{4.1}$$

If $\Delta IP < 0$ then the doubly charged complex is stable at all values of the internuclear separation r as depicted in Figure 4.1a. However, if $\Delta IP > 0$ then it is more stable at long range for the system to transfer charge from the +2 metal to the neutral ligand molecule, as in

$$M^{2+} + L \longrightarrow M^+ + L^+ + K.E. \tag{4.2}$$

Commonly referred to as "Coulomb explosion," this charge transfer event produces a pair of highly repelled positively charged fragments in close proximity to each

other. For a stable doubly charged complex to exist in this case, the potential energy surfaces must cross like that shown in Figure 4.1b.

Laser vaporization was largely assumed to be inefficient at producing doubly charged species. This is because the assumed mechanism of cluster growth in a laser vaporization source involves taking a bare metal ion and attaching ligands to it. The other methods for generating doubly charged ions involve starting with a metal salt solution already fully solvated[2−12] or second ionization of large singly charged clusters.[13−16] Dications are expected to be relatively short lived in the source due to the high abundance of free electrons available. Since most metals have a high second IP, charge transfer is expected to occur before the complex can form. Only in the presence of a certain number of solvent molecules does this situation become inverted and the higher charged metal becomes the preferred state. Despite this, we have observed multiply charged metal ion complexes in the gas phase by laser vaporization that are thermodynamically metastable.

4.2 Experimental

Doubly charged metal-ligand complexes are generated in a pulsed supersonic jet laser vaporization cluster source described in detail in Chapter 2. In brief, a gas mixture containing the ligand is pulsed with a high speed valve (General Valve Series 9) over the surface of rod of the appropriate metal of interest. The metal is vaporized into the gas pulse with the fundamental, second or third harmonic (1064 nm, 532 nm, 355 nm respectively) of a pulsed Nd:YAG laser (Spectra Physics Indi-30). The laser is focussed onto the sample rod with a 30 cm focal length lens. A backing gas of pure CO_2 or pure Ar was used to generate complexes of those ligands. For solvents that are liquid at room temperature a reservoir is installed on the line feeding the nozzle and argon passed through it. A backing pressure of 40-60 psi is used. The

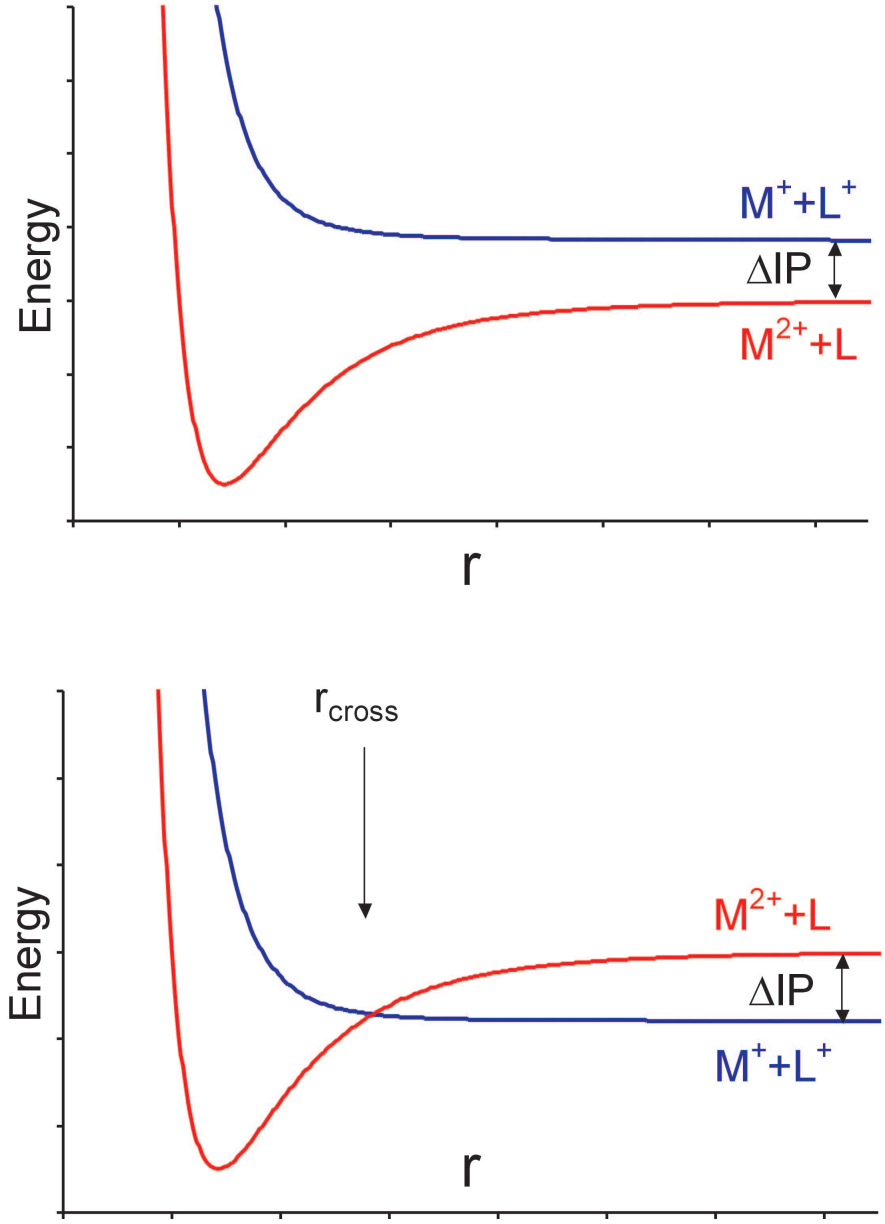

Figure 4.1:
a.) (above) Representation of potential energy curves for a doubly charged complex that is stable to charge transfer. b.) (below) The same for a complex that is metastable to charge transfer.

expansion is skimmed into a differentially pumped chamber containing a reflectron time-of-flight mass spectrometer used for analysis.

Ions observed in time-of-flight mass spectrometry are resolved based on the ratio of mass (m) to their electrostatic charge (q). This is due to the energy relation equating their kinetic energy of flight ($KE = (1/2)mv^2$) to the potential energy given to them by the field ($PE = qV$) on the mass spec plates. A cluster of given mass with two units of charge will be given the same kinetic energy as a singly charged cluster of half that mass. This can pose a problem in the assignment of the mass spectra due to flight time coincidences, however there are two properties that allow us to positively identify clusters with +2 charge. The first is that doubly charged ions with odd mass number will appear at half-integer positions in the mass spectrum which is not possible for singly charged species. Secondly, doubly charged species with multiple isotopes will exhibit the same relative isotope abundances, but the distribution will be compressed to a half unit scale.

4.3 Results

$Mg^{2+}L_n$ Complexes

Occasionally mass peaks appear in our laser vaporization experiment corresponding to doubly charged metal cations, especially in studies of alkaline earth metals. In certain instances we have observd stable clusters of these metal ions, such as $Ca^{2+}(H_2O)$.[26] During recent studies of singly charged carbon dioxide clusters on magnesium we detected the appearance of $Mg^{2+}(CO_2)$ which is an asymptotically unstable species, as defined above. This prompted a more systematic investigation of other "metastable" species that could be produced by laser vaporization. Cluster experiments were conducted using the following ligands: Ar, H_2O, NH_3, CH_3CN, C_4H_8O (THF), CH_3OH, $(CH_3)_2CO$, C_6H_6 and C_2H_5OH. Complexes of CO_2, Ar and

H_2O were found with Mg^{2+} but not with the other ligands. Table 4.1 lists the relevant ionization energetics of all species presented in this work.

The mass spectrum of $Mg(CO_2)_n^{2+}$ is shown in the upper trace of Figure 4.2. Doubly charged clusters are assigned based on their half integer m/z values as well as the half integer spacing of the isotopes of magnesium. The relative abundances of the isotopes are also consistent with this assignment. Doubly charged clusters appear interspersed with singly charged clusters and occur with about one fifth the intensity. The large singly charged peaks appear broadened in the spectrum due to space charge effects related to the high ion density. Doubly charged clusters appear out to n=5.

The lower trace of Figure 4.2 shows the mass spectrum obtained for H_2O and Ar clusters with Mg^{2+}. Clusters are observed for up to three argon atoms, but only one water molecule. The $Mg^{2+}Ar$ cluster is stable at all values of internuclear separation, but $Mg^{2+}(H_2O)$ is asymptotically unstable by about 2.4 eV. The conditions used to produce this spectrum are similar to those of the carbon dioxide clusters, except that a pure argon expansion seeded with water vapor was used. Attempts at using helium or a 70-30 neon-helium mix met with no success. Fuke and coworkers[27] reported that singly charged clusters of the type $[Mg(OH)]^+(H_2O)_{n-1}$ occur with greater abundance than the corresponding $Mg^+(H_2O)_n$ for $n > 5$. Competition with this intracluster reaction could be occurring in our experiment as well, but the clusters would appear near the singly charge magnesium water peaks and be obscured by congestion in the mass spectrum.

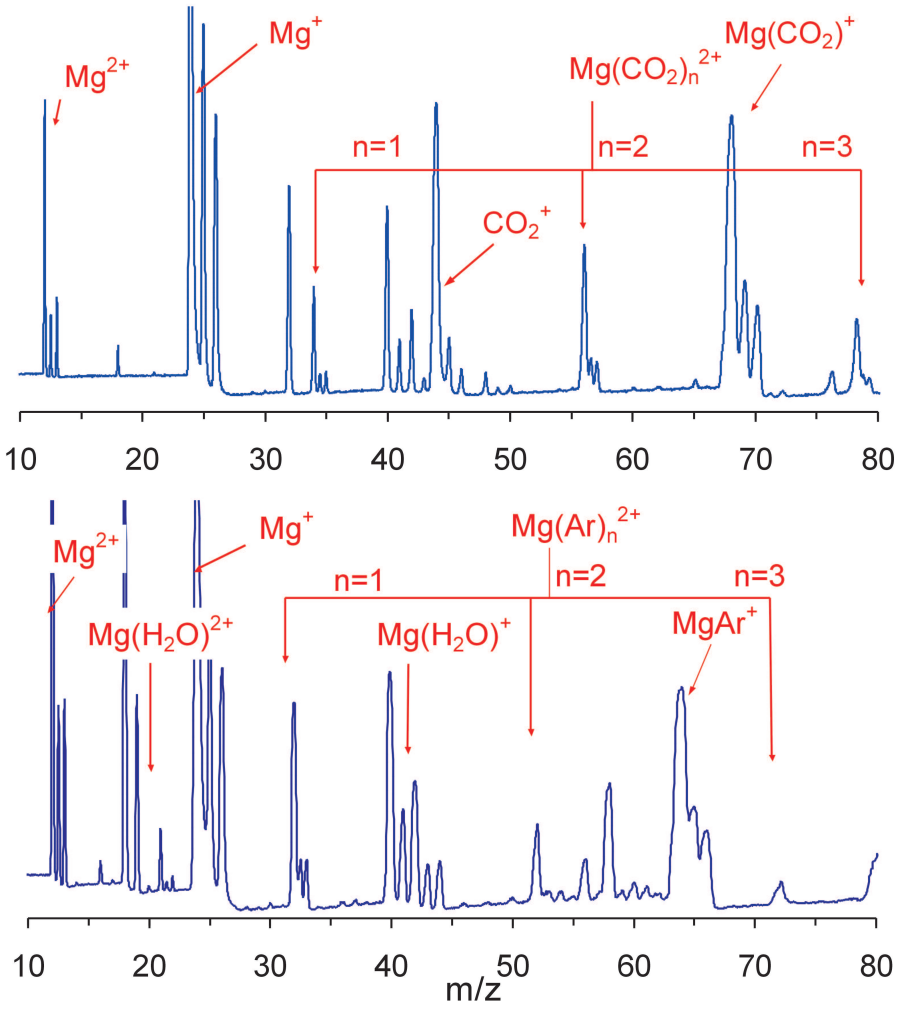

Figure 4.2:
The measured mass spectra for doubly charged magnesium ion with carbon dioxide, argon and water.

Table 4.1: Ionization energies and computed crossing distances for selected small metal ion-molecule complexes.

Complex	I.P.(M^+)	I.P.(L)	μ(L)	α(L)	r_{cross}(Å)
$Mg(Ar)^{2+}$	15.031	15.8	-	1.64	-
$Fe(Ar)^{2+}$	16.18	15.8	-	1.64	37.8
$Si(Ar)^{2+}$	16.34	15.8	-	1.64	26.7
$Co(Ar)^{2+}$	17.05	15.8	-	1.64	11.6
$Ti(CO_2)^{2+}$	13.57	13.8	-	2.63	-
$Mg(CO_2)^{2+}$	15.031	13.8	-	2.63	11.7
$Fe(CO_2)^{2+}$	16.18	13.8	-	2.63	6.1
$Co(CO_2)^{2+}$	17.05	13.8	-	2.63	4.6
$Mg(H_2O)^{2+}$	15.031	12.6	1.85	1.48	6.2
$Co(H_2O)^{2+}$	17.05	12.6	1.85	1.48	3.7
$Mg(CH_3CN)^{2+}$	15.031	12.2	3.92	4.4	5.89
$Mg(C_4H_8O)^{2+}$	15.031	9.2	1.75	~ 9	3.32
$Mg(CH_3OH)^{2+}$	15.031	10.8	1.71	3.23	3.89
$Mg((CH_3)_2CO)^{2+}$	15.031	9.7	2.88	6.39	3.34
$Mg(C_2H_5OH)^{2+}$	15.031	10.47	1.69	5.41	3.76

$Ti(CO_2)_n^{2+}$

Once we were able to produce "metastable" doubly charged species in the laser vaporization source, we turned our attention to transition metals. Titanium has a low second IP, and thus should produce many stable doubly charged clusters. The lower trace in Figure 4.3 shows a mass spectrum obtained for titanium with CO_2. Once again, the doubly charged clusters are assigned by their m/z ratios, their isotope spacings and relative abundances. These clusters are asymptotically stable, but this is the first reported observation of these clusters produced by laser vaporization.

$Co(L)_n^{2+}$ Complexes

The second IP of cobalt is higher than the first IP of any of the ligands used in this study, therefore any complex produced must be "metastable" to charge transfer. The ligand with the highest IP, and thus least likely to form an unstable complex,

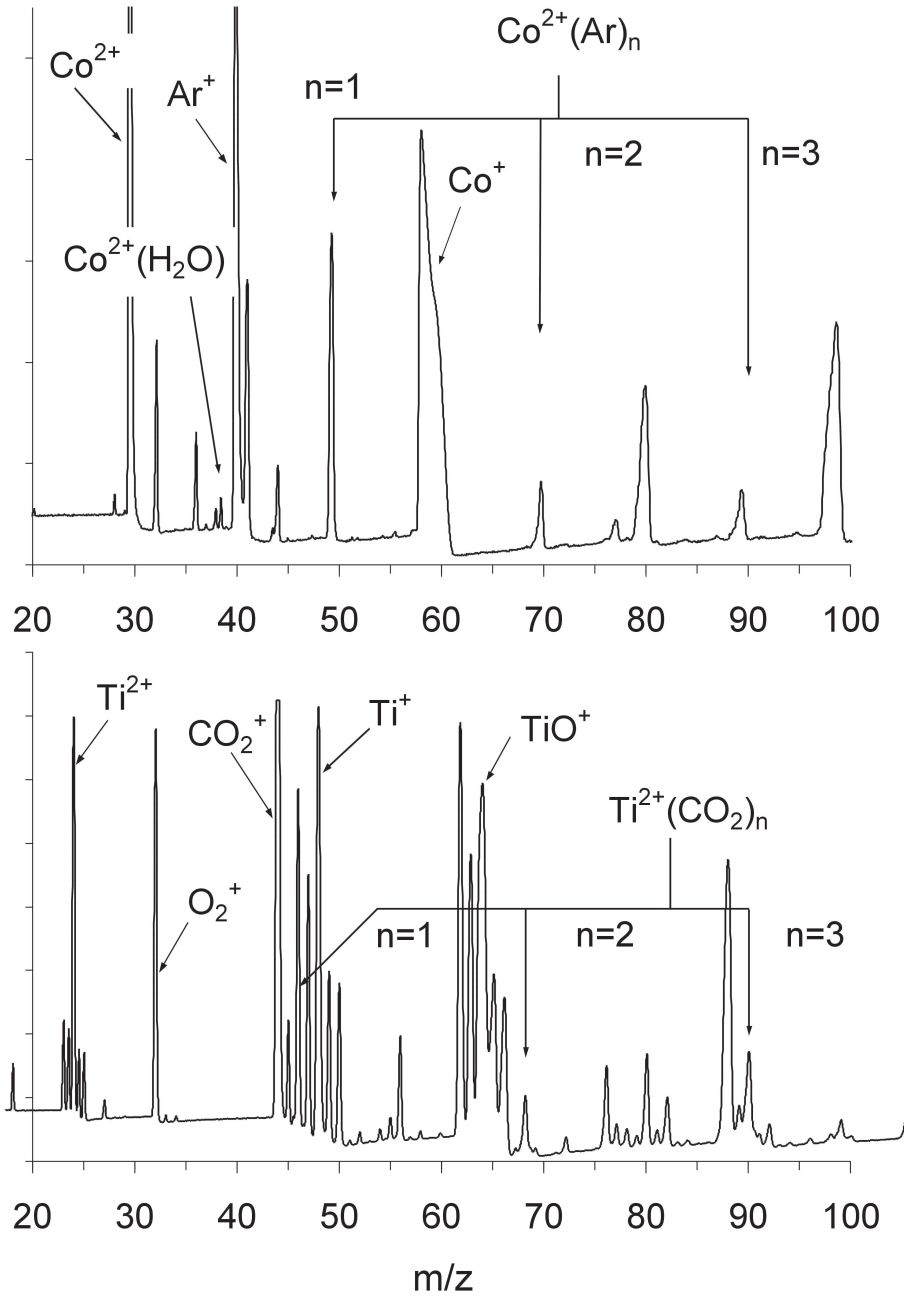

Figure 4.3:
The mass spectra for doubly charged transition metal complexes of cobalt and titanium.

is argon. The mass spectrum obtained for $Co^{2+}Ar_n$ clusters is shown as the upper trace in Figure 4.3. The clusters are assigned as $Co^{2+}Ar$, $Co^{2+}Ar_2$ and $Co^{2+}Ar_3$ based on half integer m/z values. Cobalt is mono-isotopic and so isotope spacings do not provide confirmation of this assignment, however no other half integer peaks appear in the spectrum. We were also able to produce $Co^{2+}(H_2O)$ in this experiment, under similar conditions as those for $Mg^{2+}(H_2O)$. This peak falls at half the m/z value of the singly charged complex, which makes it half integer. Only the mono-ligand species was observed and was produced only in argon expansions, just as was found for magnesium. The clusters of $Co^{2+}(H_2O)_n$ have been studied previously, produced in an electrospray source and the electronic spectra for the $4 < n < 7$ clusters has been measured.[28] The ΔIP for this complex is greater than that of any other system in this study.

$Si(Ar)_n^{2+}$Complexes

In addition to alkaline earth and transition metals, we were able to produce clusters with silicon. The mass spectrum of $Si^{2+}Ar_n$ clusters is shown in Figure 4.4. Again, peak positions and isotope patterns allow the ready assignment of the doubly charged clusters. Clusters appear out to n=4.

Other Complexes

Several other metal ion-ligand systems were also investigated in this survey. Doubly charged iron with argon and CO_2 was observed, but mass coincidences precluded definite assignment. Also, Fe has even mass isotopes, so the m/z ratio for the doubly charged clusters would be integer numbers. Nickel and aluminum were attempted with argon, but no doubly charged clusters could be produced.

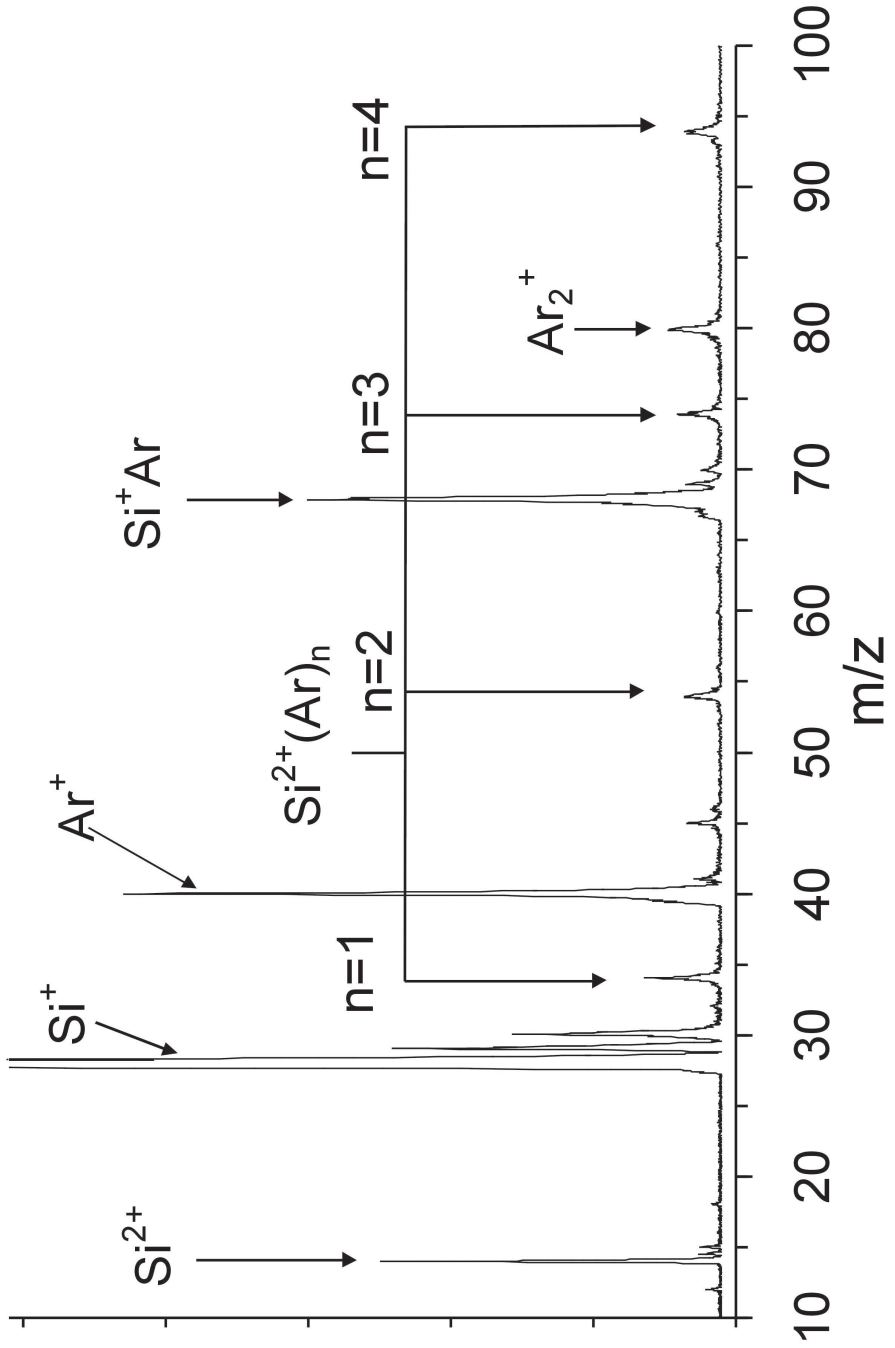

Figure 4.4:
The mass spectra for doubly charged silicon argon complexes.

4.4 Discussion

We have shown that a variety of doubly charged ion complexes can be produced using a laser vaporization cluster source. Although some of these clusters have been observed previously in sources specifically designed to produce multiply charged species,[1,3,6,11,15,20,21,23] for most of the clusters reported here this is the first observation by laser vaporization. Therefore it is important to consider how cluster growth occurs in this type of source.

Among several factors that we control in these experiments, two are distinctly different from the normal conditions used in generating singly charged clusters. These are the vaporization laser energy and the gas pulse duration. Normal laser energies employed are in the range of 5-10 mJ per pulse, whereas for optimal production of doubly charged clusters energies of 50-60 mJ per pulse were required. This relatively high power is believed to generate a hotter plasma with more energetic electron-metal collisions, promoting the higher energy ionization process. The cluster growth appeared to be essentially independent of the wavelength employed. Gas pulse durations found to be more effective were much shorter (160-200 μs) than typically used for singly charged clusters (200-250 μs). Additionally, the doubly charged clusters appeared earlier in the gas pulse as it entered the extraction region of the time-of-flight. For example, with an argon expansion singly charged clusters nominally arrives around 950 μs after the pulse is fired, whereas we observed the doubly charged species approximately 100 μs earlier than this. Considering the high vaporization laser powers used, apparently the center of the gas pulse becomes superheated and cluster growth becomes inefficient there. Regions before and after the central vaporization zone contain metal vapor via diffusion. The leading part of the gas pulse spends less time at higher pressure, therefore the complexes experience fewer collisions on average.

Electron-ion recombination is a critical issue in the growth and survival of ionized complexes in these experiments. The vaporized plasma is electrically neutral as a whole, and neutral clusters in general are the major component of a vaporization plasma. Recombination has been shown to be quite efficient at the low temperatures of supersonic expansions.[29] With certain adjustments however, we can enhance the production of ions relative to neutrals. It has been reported previously that pulsing the vaporization laser at the leading edge of the gas pulse produces more ions. This is believed to be due to greater electron mobility in the lower density area of the gas, allowing electrons to migrate outward away from the heavier ions resulting in less neutralization. This speculation is difficult to prove, but the empirical result remains. Another factor affecting ion yields is the presence of trace amounts of water in the expansion gas. Apparently water acts as an electron scavenger,[30] producing hydroxide anions and clusters which indeed have been observed under the same conditions found to produce good metal cation clusters.

Even with these adjustments of the source, it is still not possible to produce all the doubly charged metal ion complexes that we attempted to make. Some of the other considerations for the growth and stabilization of doubly charged metal ion complexes have been discussed previously by other groups active in this area.[19,15,1] Figure 4.1 shows the relevant potential energy curves that govern the stability of these complexes. For so-called "stable" complexes (upper trace), the second IP of the metal is less than the first IP of the ligand, and metal-ligand binding is possible without charge transfer at all internuclear distances. $Mg(Ar)_n^{2+}$ or $Ti(CO_2)_n^{2+}$ complexes fall into this category. For asymptotically unstable complexes, IP(M^+)>IP(L) and the lowest energy potential at long metal-ligand separations is that for the $M^+ + L^+$ species, which has a repulsive interaction. $Mg(CO_2)^{2+}$, $Mg(H_2O)^{2+}$, $Co(Ar)^{2+}$, $Co(H_2O)^{2+}$ and $Si(Ar)^{2+}$ complexes fall into this category. If a doubly charged metal ion approaches a neutral ligand, the $M^{2+} + L$ potential crosses that of $M^+ + L^+$

and charge transfer is possible, leading to dissociation of the complex. It is these complexes that are difficult to form and stabilize. However, at small values of r (internuclear separation), the interaction between M^{2+} and L lies at lower energy than that between M^{+} and L^{+} owing to the attractive ion-induced dipole interaction. If a complex can be produced on this inner bound portion of the potential, stable or "metastable" complexes can be formed and stabilized. The electrospray[3] source accomplishes this by desolvation of ions already existing in solution, while the "pick-up" method[1,15] accomplishes this using fragmentation or ionization of pre-formed neutral $M(L)_n$ and/or $M(L)_n(Ar)_m$ clusters. The "charge stripping" method[19,24] depends upon the ionization of a given singly charged species following impact with a neutral species. In each case ionization occurs after the complex components are already in close contact with one another. Even growth from separated components may also be possible if charge transfer is inefficient. In a study of the approach of Ti^{2+} to various alkenes by Weisshaar,[25] it was concluded that electron transfer occurred efficiently only when the potential energy surfaces cross at distances below 7 Å. Spears and co-workers[31] had earlier suggested that the comparatively large value of $r_{(cross)}$ might account for the extremely slow rate constant measured for charge transfer during collisions between Mg^{2+} and CO_2. Stace and coworkers[1,15] have since used a simple electrostatic model to calculate r_{cross} from the difference in ionization potentials between the metal and ligand, the dipole moment and polarizability of the ligand. They showed that Mg^{2+} complexes where the potential energy surfaces cross at longer distances have a tendency to be stable at smaller cluster sizes. So, in this previous work, the crossing distance seems to be important for both the growth of doubly charged complexes and their stabilization in environments where many collisions are present.

The formation of multiply charged clusters in the laser vaporization source appears to have less in common with electrospray sources and more features in

common with the pick-up source. In every case that doubly charged clusters are produced, there is already a large density of neutral and singly charged complexes present. In the laser vaporization process, a hot plasma is produced and energetic electrons are present from the metal vaporization process. The conditions are more extreme at high laser pulse energies, which are employed here. It thus seems likely that electron impact or Penning ionization of pre-grown neutral or singly ionized clusters could account for the formation of the doubly charged species seen here. Ionization of neutrals or singly charged ions produces the doubly charged species when the ligands are already bound at close range, thus bypassing the opportunity for charge transfer in traversing the curve crossing region. However, as noted before by Stace and others,[1,15] there is correlation with the complexes that we can produce and stabilize and the potential curve crossing point. Table 1 shows the crossing distances for each of the complexes studied here, which are calculated according to the model provided by Stace and coworkers.[1,15] The complexes of $Mg(CO_2)_n^{2+}$, $Mg(Ar)_n^{2+}$, $Co(Ar)_n^{2+}$ and $Si(Ar)_n^{2+}$ which we are able to produce all have crossing distances that are greater than 11 Å. This figure is significantly greater than the upper limit suggested by Weisshaar[25] to be necessary for charge transfer to occur. The $M(L)_n^{2+}$ complexes which we were not able to produce (Mg^{2+} with NH_3, CH_3CN, C_4H_8O (THF), CH_3OH, $(CH_3)_2CO$, C_6H_6 and C_2H_5OH; Co^{2+} with CO_2) all have extremely short crossing distances. It makes sense that these complexes are difficult to produce initially or they are hard to stabilize under the collisional environment in our source.

The successful generation of complexes of $Mg(H_2O)^{2+}$ and $Co(H_2O)^{2+}$ is surprising, since the surfaces described by these reactants cross at much shorter distances. However, both of these ions exhibited unusual behavior in that only the n=1 complexes were seen and argon expansions were necessary for their growth. Both $Mg(H_2O)^{2+}$ and $Co(H_2O)^{2+}$ are produced with weaker intensity than $Mg(Ar)_n^{2+}$ and

$Co(Ar)_n^{2+}$, which are simultaneously present in the respective mass spectra and it is not possible to form these ions except when the argon complexes are present. One explanation for this is that these water complexes are formed via substitution reactions with existing $M(Ar)_n^{2+}$ complexes. Argon atoms may then be ejected during the subsequent fragmentation of the cluster, yielding $M(H_2O)^{2+}$. No mixed complexes of $M(H_2O)(Ar)_n^{2+}$ or complexes of $M(H_2O)_n^{2+}$ with $n > 1$ are present in either mass spectrum. However, the intensity of peaks corresponding to $Mg(H_2O)^{2+}$ and $Co(H_2O)^{2+}$ are quite weak and these larger complexes could be present in smaller amounts and not detected with our sensitivity.

4.5 Conclusions

Several examples of both stable and asymptotically unstable doubly charged metal ion complexes (and those with silicon) are produced by a laser vaporization cluster source.[32] Examples in this initial survey include $Mg(CO_2)_n^{2+}$, $Mg(H_2O)^{2+}$, $Co(Ar)_n^{2+}$, $Co(H_2O)^{2+}$, $Si(Ar)_n^{2+}$ and $Ti(CO_2)_n^{2+}$ complexes. Plausible mechanisms can explain the cluster growth in this environment, and the growth and stability patterns seen make sense in light of previous ideas (crossing point position) about these complexes. Several complexes are produced that have been seen previously with other sources, and some new complexes are reported for the first time. Argon and CO_2 complexes are formed with several ions, consistent with the relative stability expected for these complexes because of their long range charge-transfer curve crossing points. Water complexes with Mg^{2+} and Co^{2+} are proposed to form by substitution reactions with an existing doubly charged complex of $M(Ar)^{2+}$. The laser vaporization source provides a convenient alternative to other sources that produce multiply charged ions in the gas phase. It is inherently a pulsed source, and so the ions provided come in intense packets suitable for interrogation with pulsed laser spectroscopy (e.g., pho-

todissociation). The intensities of the ion signals seem to be comparable to those provided with other sources. Like the pick-up method, the laser vaporization source provides an advantage over electrospray sources in that complexes with non-solvent ligands (Ar, CO_2, etc.) can be produced. The laser source also provides a more general method with which to obtain clusters from a wide variety of refractory materials. We have found that many variables determine the optimization of this source, but the initial results are promising in that many complexes were produced. Further investigations of this method are clearly warranted for the study of photodissociation spectroscopy, collision induced dissociation and/or ion-molecule reactions.

4.6 References

[1] A.J. Stace, *J. Phys. Chem. A*, **106** 7993 (2002).

[2] A. T. Blades, P. Jayaweera, M.G. Ikonomou, P. Kebarle, *Intl. J. Mass Spectrom. Ion Proc.*, **102**, 251 (1990).

[3] A. T. Blades, P. Jayaweera, M.G. Ikonomou, P. Kebarle, *J. Chem. Phys.*, **92**, 5900 (1990).

[4] M. Peschke, A.T. Blades, P. Kebarle, *J. Phys. Chem. A*, **102**, 9978 (1998).

[5] S. E. Rodrigeuz-Cruz, R.A. Jockusch, E. R. Williams, *J. Am. Chem. Soc.*, **120**, 5842 (1998).

[6] S. E. Rodrigeuz-Cruz, R.A. Jockusch, E. R. Williams, *J. Am. Chem. Soc.*, **121**, 1986 (1999).

[7] S. E. Rodrigeuz-Cruz, R.A. Jockusch, E. R. Williams, *J. Am. Chem. Soc.*, **121**, 8898 (1999).

[8] T.G. Spence, T.D. Burns, G.B. Guckenberger, L.A. Posey, *J. Phys. Chem. A*, **101**, 1081 (1997).

[9] T.G. Spence, B.T. Trotter, L.A. Posey, *J. Phys. Chem. A*, **102**, 7779 (1998).

[10] C.J. Thompson, J. Husband, F. Aguirre, R.B. Metz, *J. Phys. Chem. A*, **104**, 8155 (2000).

[11] K.P. Faherty, C.J. Thompson, F. Aguirre, J. Michne, R.B. Metz, *J. Phys. Chem. A*, **105**, 10054 (2001).

[12] M. Peschke, A.T. Blades, P. Kebarle, *J. Am. Chem. Soc.*, **122**, 1492 (2000).

[13] A.J. Stace, N.R. Walker, S. Firth, *J. Am. Chem. Soc.*, **119**, 10239 (1997).

[14] N.R. Walker, R.R. Wright, A.J. Stace, *J. Am. Chem. Soc.*, **121**, 4837 (1999).

[15] N.R. Walker, M.P. Dobson, R.R. Wright, P.E. Barran, J.N. Murrell, A.J. Stace, *J. Am. Chem. Soc.*, **122**, 11138 (2000).

[16] R.R. Wright, N.R. Walker, S. Firth, A.J. Stace, *J. Phys. Chem. A*, **105**, 54 (2001).

[17] *The Forces Between Molecules* M. Rigby, E.B. Smith, W.A. Wakeham, G.C. Maitland Oxford Science Publications, UK 1986.

[18] S. Petrie, *J. Phys. Chem. A*, **106**, 7034 (2002).

[19] D. Schröder, H. Schwarz, *J. Phys. Chem. A*, **103**, 7385 (1999).

[20] J.S. Pilgrim, K.R. Berry and M.A. Duncan, *J. Chem. Phys.*, **100** 7945 (1994).

[21] A.J. Stace*, Adv. Metal Semicond. Clusters 5*, 121 (2001).

[22] (a)D. Lessen, P.J. Brucat, *Chem. Phys. Lett.*, **149**, 10 (1988); (b) D. Lessen, P.J. Brucat, *J. Chem. Phys.*, **90**, 6296 (1989).

[23] A.A. Shvartsburg, K.W.M. Siu, *J. Am. Chem. Soc.*, **123**, 10071 (2001).

[24] D. Schröder, H. Schwarz, J. Wu, C. Wesdemiotis, *Chem. Phys. Lett.,* **343, 258 (2001).**

[25] (a) R. Tonkyn, J.C. Weisshaar, *J. Am. Chem. Soc.*, 108, 7128 (1986); (b) J.C. Weisshaar, *Acc. Chem. Res.*, 26, 213 (1993).

[26] J.S. Pilgrim, M.A. Duncan, unpublished results.

[27] (a) M. Sanekata, F. Misaizu, K. Fuke, S. Iwata, K. Hashimoto, J. Am. Chem. Soc. 117 (1995) 747.; (b) J.M. Martinez, R.R. Pappalardo, E.S. Marcos, J. Am. Chem. Soc. 121 (1999) 3175.

[28] K.P. Faherty, C.J. Thompson, F. Aguirre, J. Michne, R.B. Metz, *J. Phys. Chem. A*, 105 10054 (2001).

[29] Y. Hahn, *Rep. Prog. Phys.*, 60, 691 (1997).

[30] M.A. Duncan, *Ann. Rev. Phys. Chem.*, 48, 69 (1997).

[31] K.G. Spears, G.C. Fehsenfeld, M. McFarland, E.E. Ferguson, *J. Chem. Phys.*, 56, 2562 (1972).

[32] N.R. Walker, G.A. Grieves, J.B. Jaeger, R.S. Walters and M.A. Duncan, *Intl. J. Mass Spectrom.*, *In Press.*

Chapter 5

Photodissociation Processes

Photodissociation of mass selected ions has been used extensively since its inception for probing the structures of gas phase complexes.[1,2] Fixed frequency photodissociation can provide clues to the structural composition of complexes that cannot be analyzed spectroscopically.[1] Large molecules, especially those containing transition metal atoms, exhibit extremely complicated electronic spectra that usually are far too complex to get structural information from. Additionally, it is not generally possible to perform resonant photodissociation spectroscopy on such clusters because the bonds are strong and there are many degrees of freedom for the energy to distribute among, so they don't dissociate in the timescale of the experiment. However, patterns in the fragmentation products of photodissociation at fixed frequency can show major binding motifs and provide information on the organization within a molecule.

Resonance enhanced photodissociation makes possible the acquisition of spectra for complexes that can only be observed in the gas phase in low densities,[2] as are the clusters that are the focus of this work. This is because the detection of ions is far more sensitive than photons, and measuring direct absorption of such a low density in the ion beam is impossible. Thus absorption is detected via the "action" of measuring dissociation. Electronic photodissociation spectroscopy has been used with great success for a wide range of metal ion-ligand complexes.[3−34] The major limitation of this, however, is that in most cases, it only provides sharp, interpretable structure for the single ligand species. Complexes with two or more ligands on a metal ion undergo fast predissociation in the excited electronic state and makes the spectrum a blur due to lifetime broadening. The excitation scheme is centered on the metal ion electronic state which affects the metal–ligand bond. In a vertical excitation scheme this only places favorable Franck-Condon overlap on transitions in the metal-ligand stretch coordinate. The electronic photodissociation spectra also usually only show resonances for the metal-ligand stretch coordinate and so little

information is gained about vibrations of the ligand itself. By taking advantage of new pulsed infrared laser technology, we can overcome these difficulties and probe the ligand directly. Vibrational excitation in the complex electronic ground state provides a direct measure of the influence the metal ion has on the structure and energetics of the ligand. Fast predissociation of multiligand complexes is also not a hindrance but rather an asset that allows us to observe the dissociation on the timescale of the experiment. Thus, the study of metal ions surrounded by many shells of solvating molecules becomes possible.

5.1 Nonresonant Fixed Frequency Photodissociation

Nonresonant visible or UV photodissociation, used extensively in the studies of the heavy, strongly bound metal-PAH and -C_{60} complexes,[1] relies on the fact that these clusters possess a large number of excited electronic states within the range of our laser. One or more photons of fixed frequency from a high power Nd:YAG laser can excite the cluster to these accessible states and deposit energy in the cluster. Nonresonant absorption can take place in these large polyatomic molecules because the vibrational density of states increases very rapidly with energy, essentially forming a continuum of absorption frequencies.[36] Once excitation takes place the energy in the cluster can migrate to different internal coordinates through the mechanisms of Intramolecular Vibrational Redistribution (IVR), Internal Conversion (IC) or Intersystem Crossing (ISC).[35] In large PAH's, IC is usually the dominant mode of energy dissipation, however when heavy atoms, especially transition metals, are bound strongly to the molecule rates of ISC become competitive.[36] Radiative relaxation is very unlikely in these systems because IC and ISC occur extremely fast and irreversibly.[36] The cluster can also continue to absorb additional photons. These processes heat the cluster and increase the probability that this energy will couple to a

vibrational mode that lies along a pathway leading to the breaking of a bond, which we can detect. A tacit assumption of unimolecular decay kinetics is that the weakest bond in the cluster will break first. The rate of dissociation depends on the amount of energy deposited above the dissociation level as well as the density of states in the molecule in the vicinity of the excitation.[37] The molecule can actually undergo up to several thousand vibrational oscillations before dissociating.[35] Clusters remain suspended in the reflectron for about 2-3 μs and as long as the molecule dissociates while it is in the acceleration region of the reflectron the fragments will be mass resolved in the second flight tube and observed.

A photodissociation mass spectrum is represented by taking the difference between the spectrum with the fragmentation laser on and that spectrum with it off. This is illustrated in Figure 5.1 for bismuth clusters. First, the clusters are separated by their time of flight. Then the mass gate is activated, selecting a particular size cluster. The photodissociation laser is then synchronized with the cluster in the turning region of the instrument (Figure 2.1), the fragment signal appears and the parent cluster signal is diminished. In a series of data averaging sweeps, the laser is switched on and off in synchronization with the parent cluster. The spectra are then subtracted. This makes the parent appear as a negative peak indicating the depletion of this ion. Since the parent depletion is recorded, it is conclusive evidence that this cluster is the source of the fragments that appear.

There are several factors influencing the observed fragmentation products of clusters. As stated above, the molecule will separate at the weakest bond first. This is generally observed to be true, although in many cases there is adequate energy deposited in the cluster to break several bonds. In cases where the laser fluence is high, the fragments can also absorb light and subsequently fragment again. If a fragment is particularly stable (i.e. it forms a good leaving group) it is likely that the lower energy pathway to dissociation produces this fragment. For example, a

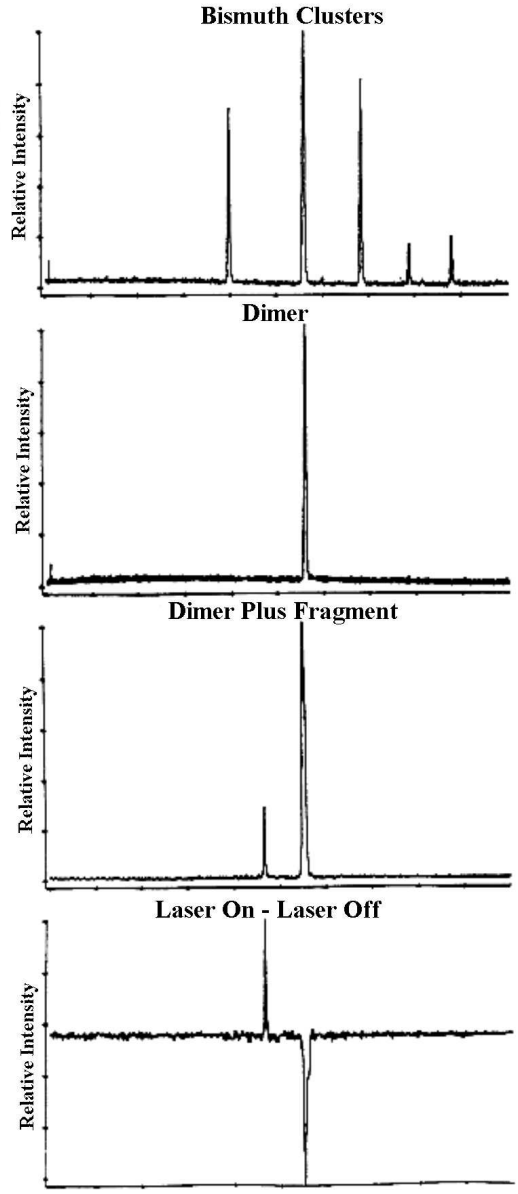

Figure 5.1:
Photodissociation spectra are acquired from a time of flight mass spectrum. First the cluster of interest is mass selected using an electronic gate. The cluster is then intersected with the photodissociation laser, reducing the amount of parent and creating the fragment. Mass spectra with the laser off are subtracted from those with it on to generate the difference spectrum.

fragment that forms a closed shell molecule will be observed preferentially over one that cannot.

Conservation of charge is an important issue. Since the parent ions have a unit of electric charge, then a single cluster can only dissociate to produce one charged fragment. The fragment with the lowest ionization potential will usually be the one that takes the charge. In other words, a cluster (AB^+) undergoes dissociation into two fragments A^+, and B as in

$$AB^+ + h\nu \Rightarrow A^+ + B, \tag{5.1}$$

where the A species has a lower ionization potential than B. This is illustrated clearly for the case of metal C_{60} for cobalt and vanadium, as shown in Figure 5.2. Cobalt has an IP higher than C_{60} and so C_{60} is observed to be the charged fragment, whereas vanadium has an IP lower than C_{60} and the vanadium is seen as the carrier of the charge in that case. In some cases several fragment ions may be observed, but this must indicate that there is more than one process taking place. Either the fragments are subsequently ionized by the photodissociation laser after they have separated as in

$$\begin{aligned} AB^+ + h\nu &\Rightarrow A^+ + B \\ B + h\nu &\Rightarrow B^+, \end{aligned} \tag{5.2}$$

or there are alternate competing fragmentation pathways occurring simultaneously leading to product ions,

$$\begin{aligned} AB^+ + h\nu &\Rightarrow A^+ + B \\ AB^+ + h\nu &\Rightarrow A + B^+ \\ &\cdots \end{aligned} \tag{5.3}$$

which is illustrated in the example of $Ag_3^+C_{60}$ shown in Figure 5.3. In this case Ag_3^+ is a stable closed shell molecule[38] and would be expected to attach in a cluster-plus-cluster bonding scheme. The Ag_2 fragment peak is absent because it is lost as

a neutral fragment. Ag_2 is a closed shell molecule when it is neutral. Thus, both conservation of charge and the stability of the leaving group play an important role in the photofragmentation process.

Observing cluster fragmentation patterns not only tells us about the process of fragmentation, it can also give clues to the structure of the parent cluster itself. Figure 5.4 shows examples of photodissociation spectra for two vanadium C_{60} clusters. Since dissociation occurs in the vacuum and imparts some kinetic energy to the fragments, it is highly unlikely that rearrangement of individual vanadium atoms could occur to form a molecule during fragmentation. Therefore, if the vanadium atoms were separated across the surface of the C_{60} molecule, one would only expect to see individual vanadium atoms as fragments. The appearance of a V_3^+ molecular fragment indicates that the vanadium most likely exists as a trimer cluster attached to the C_{60} unit. The fact that V_2^+ and V^+ are also present may indicate that there was enough laser power to subsequently fragment the V_3^+ ion.

Another example of competing fragmentation pathways occurs in systems that can undergo charge transfer. Figure 5.5 shows a difference mass spectrum in which the depletion of the selected parent ion and appearance of the photofragments are plotted. In this case when a doubly charged cluster undergoes charge transfer, both fragments obtain a +1 electrical charge, and are highly repelled by one another. The fragments observed include Co^{2+}, Ar^+ and Co^+. The latter has an m/z value that is greater than the parent ion. Apparently, there are low-lying electronic states of the complex that allow some dissociation via the Co^{2+} + Ar channel and some via the charge-transfer $Co^+ + Ar^+$ state. Another possibility is that absorption occurs to the charge transfer state and some branching into these two fragment channels occurs by electron transfer at the curve crossing as the species move apart. The fragment ion masses seen for Co^+ and Ar^+ are broader than our typical mass resolution, which would be consistent with some kinetic energy release in the photodissociation

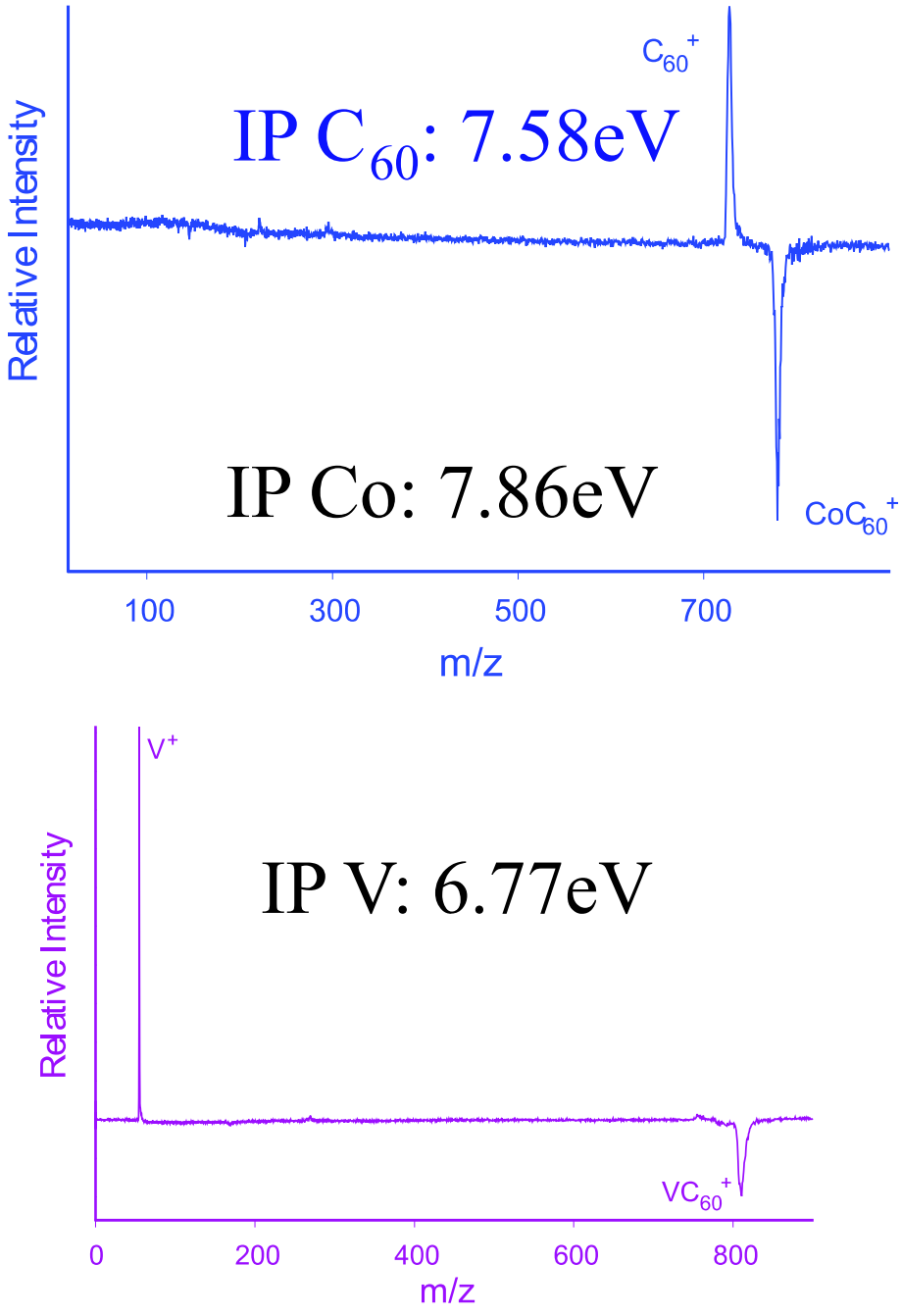

Figure 5.2:
Photodissociation of ion complexes yields observed fragment ions that possess the lower ionization energy.

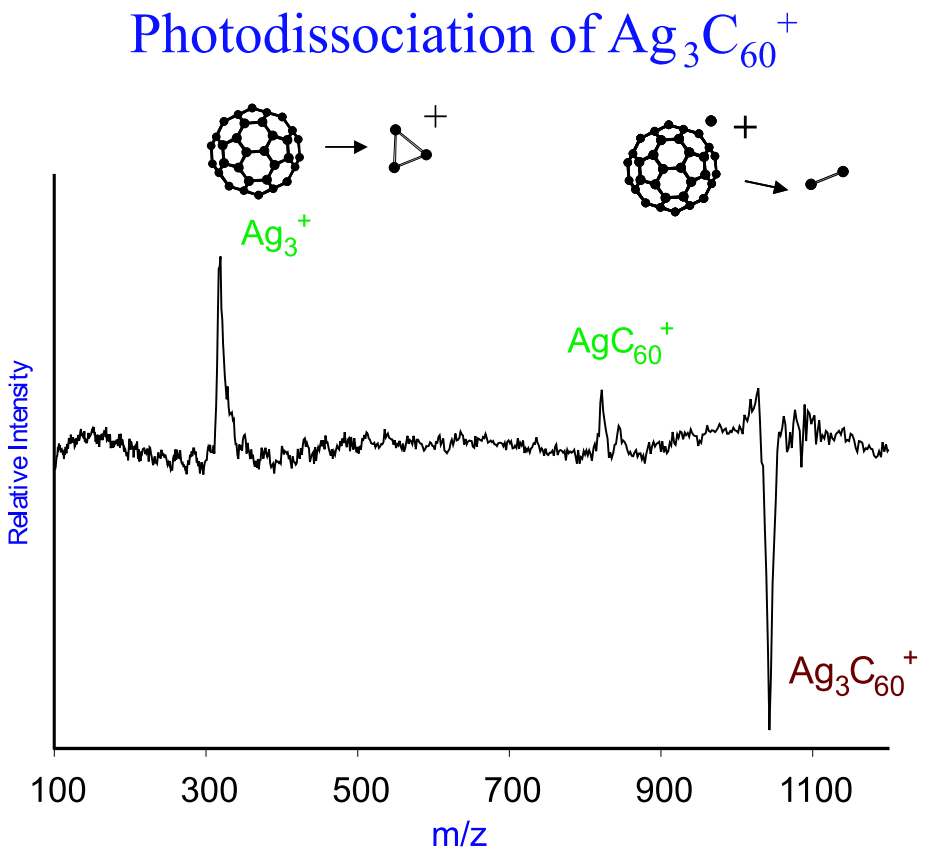

Figure 5.3:
Photodissociation of $Ag_3^+C_{60}$ showing alternate competing pathways to fragmentation.

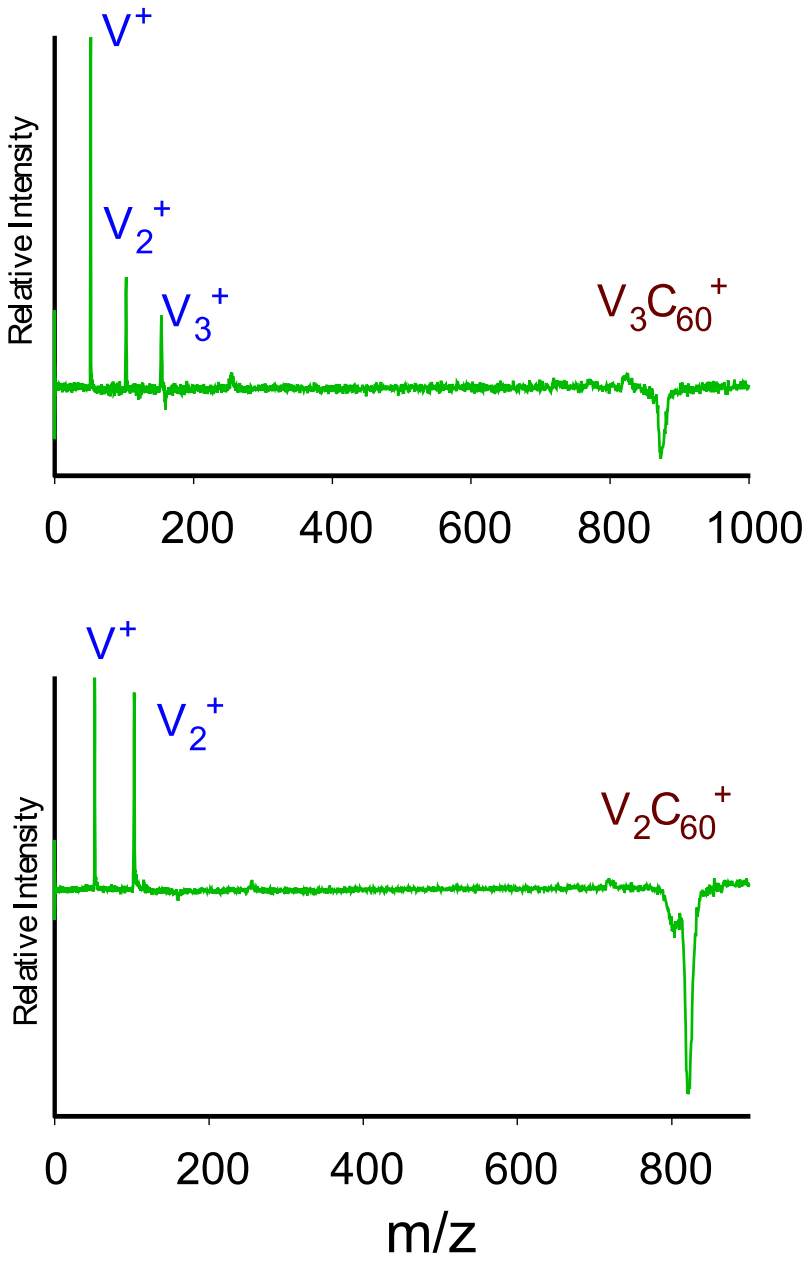

Figure 5.4:
Photodissociation spectra obtained for mass selected vanadium C_{60} clusters.

process. This behavior is expected for dissociation off the repulsive wall of the $Co^+ + Ar^+$ potential. Also consistent with this picture, the depletion of the parent ion is quite large, as indicated by the negative offscale peak. However, the fragment ions that make it to the detector represent a much smaller signal. Loss of fragment ion signal would also be expected if there is kinetic energy release into the fragments.

5.2 Resonance Enhanced Infrared Photodissociation Spectroscopy

The desire to study weakly bound metal ion clusters spans many disciplines, as outlined in Chapter 1. Studies using electronic photodissociation spectroscopy obtain important information about metal ion-ligand complexes but, as discussed above, this has certain limitations. Infrared spectroscopy can be used to gain information about larger cluster species, rather than just the mono-ligand clusters. Vibrational spectroscopy works on the cluster in the ground electronic state rather than probing excited states. We also use it to probe the effects the metal ion has on the ligand as opposed to spectroscopy that centers on the metal ion itself. The technique rests on the fact that we can pump enough energy into a vibrational state on resonance to cause dissociation. This method has been applied in the past for nonmetal clusters, but interest in solvation, biochemistry, catalysis and other disciplines require knowledge of metal ion interactions.

The clusters are composed of a metal ion surrounded by molecular ligands that are chosen to resemble gas phase analogs of condensed phase systems of interest. We can study ligands that have vibrational transitions in the region of our IR OPO laser system (2000 cm^{-1} to 4000 cm^{-1}). The ligands attached to the metal are stable molecules and interaction with the metal ion center is expected to perturb them slightly. This perturbation can affect either the metal in such a way as to make alternate oxidation states accessible, or the ligand itself so as to distort its

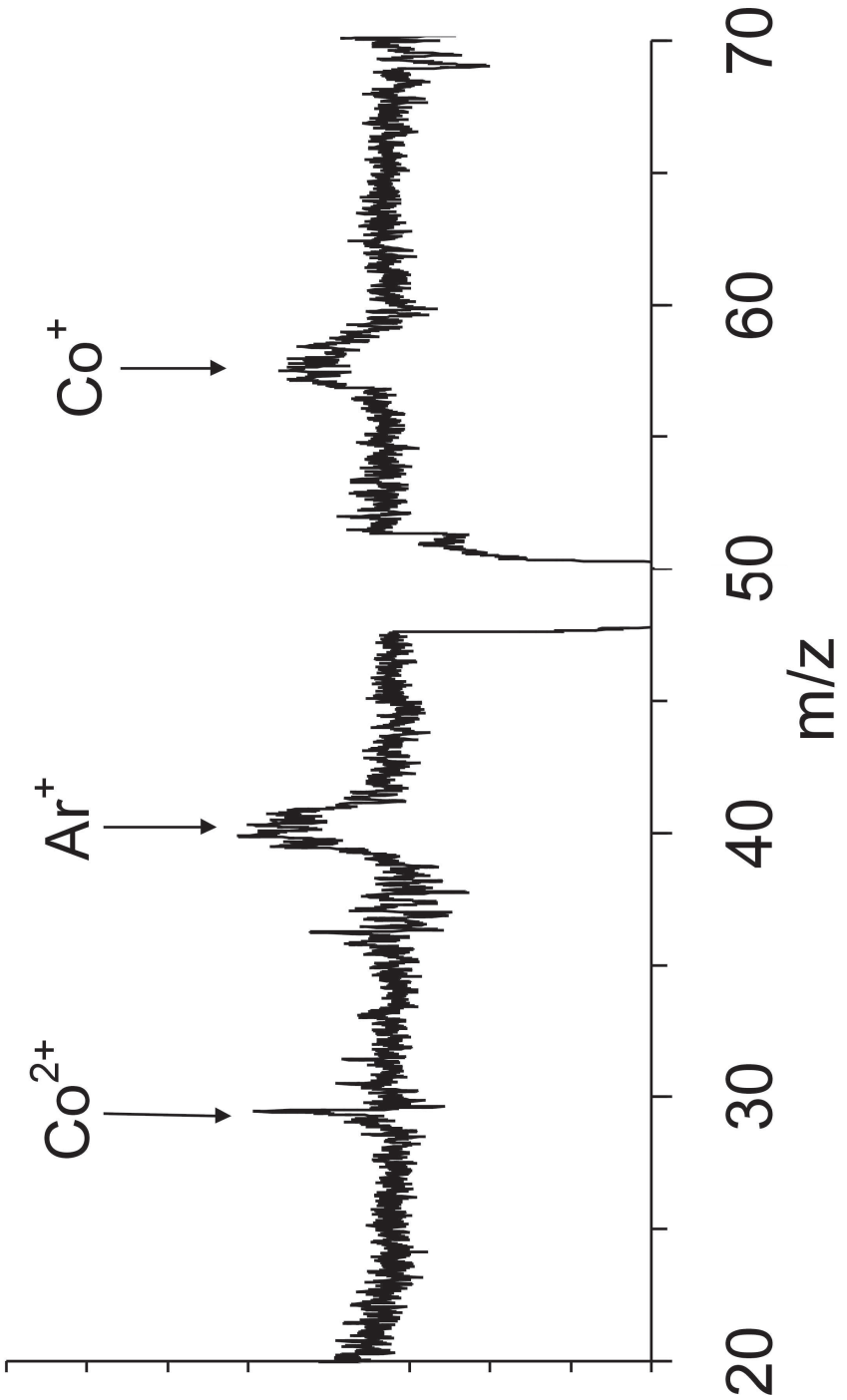

Figure 5.5:
The photodissociation spectrum of the doubly charged cobalt argon complex.

structure and/or enhance its chemical reactivity. Table 5.1 shows a comparison of binding energies to the vibrational frequencies of the free (gas phase) ligand that are accessible with our light source. In general, the mono-ligand complexes have binding energies that are greater than the energy of the vibrational state that we want to scan. Although binding energies generally decrease with increasing number of ligands, these still may not become lower than the vibrational energy until after many ligands are present. Therefore, dissociation by infrared excitation will have to be a multiphoton process. If we tune our laser to a resonance in the cluster, a photon will be absorbed. Due to anharmonicity, the next vibrational level in the progression of a given mode will be shifted lower in energy from where the fundamental falls. Thus a second photon generally will not be on resonance with the second transition. The cluster must have a relatively high density of other vibrational states in the vicinity of where the second photon falls for subsequent absorption to occur. For larger clusters with more ligands attached, the vibrational density of states increases faster, assisting this process. In addition, larger clusters have less strongly attached ligands, thus requiring fewer photons, or perhaps just one. As energy is deposited into the cluster, this energy redistributes throughout the system by the mechanisms of IVR. The rates of IVR are also enhanced by having a larger density of vibrational states. Therefore the larger clusters not only have an increased probability of absorbing enough photons, they also have an increased probability that the energy deposited will find its way to the dissociation coordinate.

We have often observed that the mono-ligand complexes do not dissociate,[39] presumably due to too low a density of states combined with too high a binding energy. To overcome this problem, we have made use of the technique of "rare gas tagging". As shown in Table 5.1, a rare gas atom binds much more weakly to a metal ion than a molecule. This is because the rare gas atom can only bind to the metal ion via the induced dipole force. If we can produce a mixed-ligand cluster of rare

gas-metal ion-ligand, then the cluster will have one significantly weaker bond that can dissociate. The rare gas will attach to the metal ion and is expected to be a very weak perturbation to the cluster, therefore it is expected not to produce any significant differences in the frequencies of vibration of the ligand. Another added benefit is that because the rare gas is so much more weakly bound the cluster can possess much less residual thermal energy. For instance, $Mg^+(H_2O)$ could possess up to a few thousand wavenumbers of residual heat, whereas Mg^+Ar could at most possess a few hundred wavenumbers. Excess internal energy in the clusters produces broad spectral peaks, so cool clusters will give narrow features. Rare gas tagging is therefore expected to provide better representation of the spectrum of the small clusters, with peaks essentially at the same locations, but much narrower linewidths and greater photodissociation signal intensity.

Table 5.1:
Comparison of binding energies to nominal ligand vibrational frequencies for selected complexes. Values from Freiser.[40]

Complex	**D_0(kcal/mol)**	**D_0(cm^{-1})**	**ν (cm^{-1})**	**type**
Mg^+ (CO_2)	14.7	5140	2349	asym. str.
Mg^+ (H_2O)	28.4	9940	3650/3750	sym./asym. str.
Mg^+ (H_2O) H_2O	22.4	7840	3650/3750	sym./asym. str.
Mg^+ $(H_2O)_2$ H_2O	17.3	6060	3650/3750	sym./asym. str.
Mg^+ $(H_2O)_3$ H_2O	11.5	4030	3650/3750	sym./asym. str.
Mg^+ Ar	3.25	1140	N/A	
Fe^+ (CO_2)	8	3000	2349	asym. str.
Fe^+ (H_2O)	30.6	10700	3650/3750	sym./asym. str.
Fe^+ (H_2O) H_2O	39.3	13800	3650/3750	sym./asym. str.
Fe^+ $(H_2O)_2$ H_2O	18.2	6400	3650/3750	sym./asym. str.
Fe^+ $(H_2O)_3$ H_2O	12.0	4200	3650/3750	sym./asym. str.
Fe^+ Ar	4	1400	N/A	

Dissociation of clusters containing more than one ligand molecule is more complex, but also provides us with more information about the structure of the cluster. Additional ligand molecules can be added directly to the metal ion, or they can build

upon each other in successive solvation spheres. Those that lie in the outer spheres will be bound by a smaller energy, and consequently exhibit a smaller frequency shift. The appearance of multiple shifted features in the spectrum of the cluster near the free molecule frequency indicates there are ligands in different environments in the cluster and tells us about its structure. There are two ways dissociation can be observed in this case. We can excite on resonance with the outer sphere ligand selectively due to its characteristic shift and it can break its bond to the inner sphere. On the other hand, we can excite the inner sphere ligand and IVR can carry the energy to either of the two weak bonds. Since the outer sphere molecule is bound much less tightly, it is more likely to break. The presence of more ligand molecules greatly increases the density of vibrational states in the cluster and significantly enhances the rate of dissociation. For relatively large clusters however (upwards of a dozen or more ligands), this also increases the number of modes the energy can redistribute to before finding a dissociation pathway and therefore the signal intensity for fragmentation decreases above this point.

5.3 References

[1] (a) N.R. Foster, J.W. Buchanan, N.D. Flynn and M.A. Duncan, *Chem. Phys. Lett.*, **341**, 476 (2001); (b) G.A. Grieves, J.W. Buchanan, J.E. Reddic and M.A. Duncan, *Intl. J. Mass Spectrom.*, **204**, 223 (2001); (c) N.R. Foster, G.A. Grieves, J.W. Buchanan, N.D. Flynn and M.A. Duncan, *J. Phys. Chem. A*, **104**, 11055 (2000); (d) J.W. Buchanan, G.A. Grieves, N.D. Flynn and M.A. Duncan, *Intl. J. Mass Spectrom.*, **185-187**, 617 (1999); (e) J.W. Buchanan, G.A. Grieves, J.E. Reddic and M.A. Duncan, *Intl. J. Mass Spectrom.*, **182**, 323 (1999); (f) J.W. Buchanan, J.E. Reddic, G.A. Grieves and M.A. Duncan, *J. Phys. Chem.*, **102**, 6390 (1998); (g) J.E. Reddic, J.C. Robinson and M.A. Duncan, *Chem. Phys.*

Lett., **279**, 203 (1997).

[2] (a) M.A. Duncan, *Annu. Rev. Phys. Chem.*, **48**, 69 (1997); (b) P.J. Brucat in *Advances in Metal and Semiconductor Clusters*, M.A. Duncan, Ed., Volume I, Chapter 7 (JAI Press, New York, 1991); (c) D. C. Sperry, A. J. Midey, J. I. Lee, J. Qian, J M. Farrar, *J. Chem. Phys.*, **111**, 8469 (1999); (d) J. Velasquez, J.E. Reddic and M.A. Duncan, *Chem. Phys. Lett.* **343**, 613 (2001); (e) M.A. Duncan, *Intl. J. Mass Spectrom.*, **200**, 545 (2000); (f) J.E. Reddic and M.A. Duncan, *J. Chem. Phys.*, **112**, 4974 (2000); (g) J.E. Reddic and M.A. Duncan, *Chem. Phys. Lett.*, **312**, 96 (1999); (h) J.E. Reddic and M.A. Duncan, *J. Chem. Phys.*, **110**, 9948 (1999); (i) M.R. France, S.H. Pullins and M.A. Duncan, *Chem. Phys.*, **239**, 447 (1998); (j) M.R. France, S.H. Pullins and M.A. Duncan, *J. Chem. Phys.* **109**, 8842 (1998); (k) M.R. France, S.H. Pullins and M.A. Duncan, *J. Chem. Phys.*, **108**, 7049 (1998); (l) S.H. Pullins, J.E. Reddic, M.R. France and M.A. Duncan, *J. Chem. Phys.*, **108**, 2725 (1998); (m) C.T. Scurlock, S.H. Pullins and M.A. Duncan, *J. Chem. Phys.*, **105**, 3579 (1996); (n) S.H. Pullins, C.T. Scurlock, J.E. Reddic and M.A. Duncan, *J. Chem. Phys.*, **104**, 7518 (1996); (o) C.T. Scurlock, S.H. Pullins, J.E. Reddic and M.A. Duncan, *J. Chem. Phys.*, **104**, 4591 (1996); (p) C.T. Scurlock, J.S. Pilgrim and M.A. Duncan, *J. Chem. Phys.*, **103**, 3293 (1995); (q) D.L. Robbins, L.R. Brock, J.S. Pilgrim and M.A. Duncan, *J. Chem. Phys.*, **102**, 1481 (1995); (r) J.S. Pilgrim, K.R. Berry and M.A. Duncan, *J. Chem. Phys.*, **100**, 7945 (1994); (s) C.S. Yeh, K.F. Willey, D.L. Robbins and M.A. Duncan, *J. Chem. Phys.*, **98**, 1867 (1993); (t) K.F. Willey, C.S. Yeh, D.L. Robbins, J.S. Pilgrim and M.A. Duncan, *J. Chem. Phys.*, **97**, 8886 (1992); (u) K.F. Willey, C.S. Yeh, D.L. Robbins and M.A. Duncan, *J. Phys. Chem.*, **96**, 9606 (1992).

[3] P. Kebarle, *Ann. Rev. Phys. Chem.*, **28**, 445 (1977).

[4] a) A. W. Castleman, P.M. Holland, D.M. Lindsay and K.I. Peterson, *J. Am. Chem. Soc.*, **100**, 6039 (1978); (b) A.W. Castleman, *Chem. Phys. Lett.*, **53**, 560 (1978); (c) P.W. Holland and A.W. Castleman, *J. Chem. Phys.*, **76**, 4195 (1982); (d) K.L. Glein, B.C. Guo, R.G. Keesee and A.W. Castleman, *J. Phys. Chem.*, **93**, 6805 (1989); (e) B.C. Guo, J.W. Purnell and A.W. Castleman, *Chem. Phys. Lett.*, **168**, 155 (1990); (f) B.C. Guo and A W. Castleman, *Chem. Phys. Lett.*, **181**, 16 (1991).

[5] T.F. Magnera, D.E. David and J. Michl, *J. Am. Chem. Soc.*, **111**, 4100 (1989).

[6] P.I. Marinelli and P.R Squires, *J. Am. Chem. Soc.*, **111**, 4101 (1989).

[7] F. Bouchard, J.W. Hepburn and T.B. McMahon, *J. Am. Chem. Soc.*, **111**, 8934 (1989).

[8] M.S. El-Shall, K.E. Shriver, R.L. Whetten and M.J. Mautner, *J. Phys. Chem.*, **93**, 7969 (1989).

[9] (a) R.H. Schultz and P.B. Armentrout, *J. Phys. Chem.*, **97**, 596 (1993); (b) Y.M. Chen and P.B. Armentrout, *Chem. Phys. Lett.*, **210**, 123 (1993); (c) N.F. Dalleska, B.L. Tjelta and P.B. Armentrout, *J. Phys. Chem.*, **98**, 4191 (1994); (d) N.F. Dalleska, K. Homma, L.S. Sunderlin and P.B. Armentrout, *J. Am. Chem. Soc.*, **116**, 3519 (1994).

[10] (a) C. Heinemann, J. Schwarz and H. Schwarz, *J. Phys. Chem.*, **100**, 6088 (1996); (b) R.C. Dunbar, S.J. Klippenstein, J, Hrusak, D. Stockigt and H. Schwarz, *J. Am. Chem. Soc.*, **118**, 5277 (1996).

[11] (a) R.L. Hettich and B.S. Freiser, *J. Am. Chem. Soc.*, **109**, 3543 (1987); (b) B.S. Freiser, *Chemtracts-Anal. and Phys. Chem.*, **1**, 65 (1989); (c) L.M. Lech, *Ph.D. Thesis*, Purdue University, 1988.; (d) R.L. Hettich, T.C. Jackson, E.M.

Stanko and B.S. Freiser, *J. Am. Chem. Soc.*, **108**, 5086(1986); (e) L. Operti, E.C. Tews and B.S. Freiser *J. Am. Chem. Soc.*, **110**, 3847 (1988); (f) L. Operti, E.C. Tews, T.J. MacMahon and B.S. Freiser, *J. Am. Chem. Soc.*, **111**, 9152 (1989); (g) Y.A. Ranasinghe and B.S. Freiser, *Chem. Phys. Lett.*, **200**, 135 (1992); (h) S. Afzaal and B.S. Freiser, *Chem. Phys. Lett.*, **218**, 254 (1994).

[12] (a) W.L. Liu and J.M. Lisy, *J. Chem. Phys.*, **89**,605 (1988); (b) T.S. Selegue, N. Moe, I.A Draves and I.M. Lisy, *J. Chem. Phys.*, **96**, 7268 (1992); (c) T. Selegue and J.M. Lisy, *J. Phys. Chem.*, **96**, 4143 (1992); (d) T.J. Selegue and J. M. Lisy, J. *Am. Chem. Soc.*, **116**, 4874 (1994); (e) C.J. Weinheirnerand J.M. Lisy, *J. Chem. Phys.*, **105**, 2938 (1996).

[13] (a) P.R Kemper and M.T. Bowers, *J. Phys. Chem.*, **95**, 5134 (1991); (b) P.R Kemper, M.T. Hsu and M.T. Bowers, *J. Phys. Chem.*, **95**, 10,600 (1991); (c) G. von Helden, P.R Kemper, M.T. Hsu and M.T. Bowers, *J. Chem. Phys.*, **96**, 6591 (1992); (d) P.R Kemper, J. Bushnell, G. von Helden and M.T. Bowers, *J. Phys. Chem.*, **97**, 52 (1993).

[14] (a) K.F. Willey, P.Y. Cheng, T.G. Taylor, M.B. Bishop and M.A. Duncan, *J. Phys. Chem.* 94, 1544 (1990); (b) K.F. Willey, P.Y. Cheng, M.B. Bishop and M.A. Duncan, *J. Am. Chem. Soc.*, **113,4721** (1991); (c) K.F. Willey, C.S. Yeh, D.L. Robbins and M.A. Duncan, *J. Phys. Chem.*, **96,9106** (1992).

[15] (a) M.H. Shen and I.M. Farrar, *J. Phys. Chem.* **93**, 4386 (1989); (b) M.H. Shen and J.M. Farrar, *J. Chem. Phys.*, **94**, 3322 (1991); (c) C.A. Schmuttenmaer, J. Qian, S.G. Donnelly, M.J. DeLucia, D.F. Varley, *et al*, J. Phys. Chem. **97**, 3077 (1993); (d) S.G. Donnelly and J.M. Farrar, *J. Chem. Phys.*, **98**, 5450 (1993); (e) J.M. Farrar, *Cluster Ions*, edited by C.Y. Ng, T. Baer and I. Powis (John Wiley

and Sons, New York), p. 243, (1993); (f) J. Qian, AJ. Midey, S.G. Donnelly, J.I. Lee and J.M. Farrar, Chem. Phys. Lett. **244**, 414 (1995).

[16] (a)D.E. Lessen and P.J. Brucat, *J. Chem. Phys.*, **90,6296** (1989); (b)D.E. Lessen and P.J. Brucat, *J. Chem. Phys.*, **91**, 4522 (1989); (c) D.E. Lessen, R.L. Asher and P.J. Brucat, *J. Chem. Phys.*, **93**, 6102 (1990); (d)D.E. Lessen, R.L. Asher and P.J. Brucat, *J. Chem. Phys.*, **95**, 414 (1991); (e)D.E. Lessen, R.L. Asher and P.J. Brucat, *Advances in Metal and Semiconductor Clusters*, edited by M.A. Duncan (JAI, Greenwich, CT, 1995), Vol. I; (f) R L. Asher, D. Bellert, T. Buthelezi and P.J. Brucat, *Chem. Phys. Lett.*, **227**, 623 (1994) (g) R L. Asher, D. Bellert, T. Buthelezi, G. Weerasekera and P. J. Brucat, *Chem. Phys. Lett.*, 228, 390 (1994); (h) R L. Asher, D. Bellert, T. Buthelezi and P. J. Brucat, *Chem. Phys. Lett.*, **228**, 599 (1994); (i) R L. Asher, D. Bellert, T. Buthelezi and P. J. Brucat, *Chem. Phys. Lett.*, **227**, 277 (1994); (j) R L. Asher, D. Bellert, T. Buthelezi, D. Lessen and P. J. Brucat, *Chem. Phys. Lett.*, **234**, 119 (1995); (k) T. Buthelezi, D. Bellert, V. Lewis and P.J. Brucat, *Chem. Phys. Lett.*, **242**, 627 (1995).

[17] (a)L. N. Ding, M. A. Young, P. D. Kleiber, W. C. Stwalley and A. M. Lyyra, *J. Phys. Chem.*, **97**, 2181 (1993); (b) L.N. Ding, P.D. Kleiber, Y.C. Cheng, M.A. Young and S.V. O'Neil, *J. Chem. Phys.*, **102**, 5235 (1995).

[18] (a) F. Misaizu, M. Sanekata, K. Tsukamoto, K. Fuke and S. Iwata, *J. Phys. Chem.*, **96**, 8259 (1992); (b) K. Fuke, M. Misaizu, M. Sanekata, K. Tsukamoto and S. Iwata, *Supplement to Z. Phys. D*, **26**, S 180 (1993); (c) F. Misaizu, M. Sanekata and K. Fuke, *J. Chem. Phys.* **100**, 1161 (1994); (d) M. Sanekata, F. Misaizu, K. Fuke, S. Iwata and K. Hashimoto, *J. Am. Chem. Soc.*, **117**, 747 (1995); (e) H. Watanabe, S. Iwata, K. Hashimoto, F. Misaizu and K. Fuke, *J.*

Am. Chem. Soc., **117**, 755 (1995); (f) M. Sanekata, F. Misaizu and K. Fuke, *J. Chem. Phys.*, **104**, 9768 (1996).

[19] S.I. Panov, J.M. Williamson and T.A. Miller, *J. Chem. Phys.*, **102**, 7359 (1995).

[20] (a) C.W. Bauschlicher, H. Partridge and S.H. Langhoff, *Chem. Phys. Lett.*, **165**, 272 (1990); (b) C. W. Bauschlicher and H. Partridge, *J. Phys. Chem.*, **95**, 3946 (1991); (c) C. W. Bauschlicher and H. Partridge, *J. Phys. Chem.*, **95**, 9694 (1991); (d) C. W. Bauschlicher and H. Partridge, *Chem. Phys. Lett.*, **181**, 129 (1991); (e) M. Sodupe, C. W. Bauschlicher and H. Partridge, *Chem. Phys. Lett.*, **192**, 185 (1992); (f) M. Sodupe, C. W. Bauschlicher, S.R. Langhoff, H. Partridge, *J. Phys. Chem.*, **96**, 2118 (1992); (g) C.W. Bauschlicher, M. Sodupe and H. Partridge, *J. Chem. Phys.*, **96**, 4453 (1992); (h) H. Partridge, C.W. Bauschlicher and S.R. Langhoff, *J. Phys. Chem.*, **96**, 5350 (1992); (i) M. Sodupe, C.W. Bauschlicher and H. Partridge, *Chem. Phys. Lett.*, **195**, 494 (1992); (j) C. W. Bauschlicher, *Chem. Phys. Lett.*, **201**, 11 (1993); (k) M. Sodupe and C. W. Bauschlicher, *Chem. Phys Lett.*, **203**, 215 (1993); (1) C.W. Bauschlicher and M. Sodupe, *Chem. Phys. Lett.*, **214**, 489 (1993); (m) H. Partridge and C.W. Bauschlicher, *J. Phys. Chem.*, **98**, 2301 (1994); (n) P. Maitre and C. W. Bauschlicher, *Chem. Phys. Lett.*, **225**, 467 (1994); (o) C.W. Bauschlicher, H. Partridge and S.R. Langhoff, *Advances in Metal and Semiconductor Clusters*, edited by M.A. Duncan (JAI, Greenwich, CT, 1994), Vol. II; (P) M. Sodupe and C.W. Bauschlicher, *Chem. Phys.*, **185**, 163 (1994); (q) C.W. Bauschlicher and H. Partridge, *Chem. Phys. Lett.*, **239,241** (1995).

[21] (a) J.S. Pilgrim, C.S. Yeh and M.A. Duncan, *Chem. Phys. Lett.*, **210**, 322 (1993); (b) J.S. Pilgrim, C.S. Yeh, K.R. Berry and M.A. Duncan, *J. Chem. Phys.*, **100**, 7945 (1994); (c) C.S. Yeh, K.F. Willey, D.L. Robbins and M.A. Duncan, *Intl. J. Mass Spectrom. Ion Proc.*, **131**, 307 (1994); (d) C.S. Yeh, J.S.

Pilgrim, K.F. Willey, D.L. Robbins and M.A. Duncan, *Intl. Rev. Phys. Chem.*, **13**, 231 (1994).

[22] (a) K.F. Willey, C.S. Yeh, D.L. Robbins and M.A. Duncan, *Chem. Phys. Lett.*, **192**, 179 (1992); (b) C.S. Yeh, K.F. Willey, D.L. Robbins, J.S. Pilgrim and M.A. Duncan, *J. Chem. Phys.*, 98, 1867 (1993); (c) C.S. Yeh, K.F. Willey, D.L. Robbins and M.A. Duncan, *J. Phys. Chem.*, **96**, 7833 (1992).

[23] D.L. Robbins, L.R. Brock, J.S. Pilgrim and M.A. Duncan, *J. Chem. Phys.*, **102**, 1481 (1995).

[24] (a) C.S. Yeh, K.F. Willey, D.L. Robbins, J.S. Pilgrim and M.A. Duncan, *Chem. Phys. Lett.*, **196**, 233 (1992); (b) K.F. Willey, C.S. Yeh, D.L. Robbins, J.S. Pilgrim and M.A. Duncan, *J. Chem. Phys.*, **97**, 8886 (1992).

[25] J. Chen, T.H. Wong, Y.C. Cheng, K. Montgomery and P.D. Kleiber, *J. Chem. Phys.*, **108**, 2285 (1998).

[26] S.H. Pullins, C.T. Scurlock, J.E. Reddic and M.A. Duncan, *J. Chem. Phys.*, **104**, 7518 (1996).

[27] C.T. Scurlock, S.H. Pullins and M.A. Duncan, *J. Chem. Phys.*, **105**, 3579 (1996).

[28] S.H. Pullins, J.E. Reddic, M.R France and M.A. Duncan, *J. Chem. Phys.*, **108**, 2725 (1998).

[29] C.T. Scurlock, S.H. Pullins and M.A. Duncan, *J. Chem. Phys.*, **104**, 4591 (1996).

[30] M.R. France, S.H. Pullins and M.A. Duncan, *J. Chem. Phys.*, **108**, 7049 (1998).

[31] C. Luder, D. Prekas, A. Vourliotaki and M. Velegrakis, *Chem. Phys. Lett.*, **267**, 49 (1997).

[32] C. Luder and M. Velegrakis, *J. Chem. Phys.*, **105**, 2167 (1996).

[33] D. Prekas, B. Feng and M. Velegrakis, *J. Chem. Phys.*, **108**, 2712 (1998).

[34] C.T. Scurlock, J.S. Pilgrim and M.A. Duncan, *J. Chem. Phys.*, **103**, 3293 (1995); Erratum. *J. Chem. Phys.*, **105**, 7876 (1996).

[35] *Photodissociation Dynamics*, R. Schinke Cambridge University Press, UK 1993.

[36] M. Klessinger and J. Michl, *Excited States and Photochemistry of Organic Molecules*, VCH Publishers, Inc., New York 1995.

[37] *Unimolecular Reaction Dynamics*, T. Baer, W. Hase, Oxford University Press, NY 1996.

[38] K. LaiHing, P.Y Cheng and M.A. Duncan, *Zeitschrift fuer Physik D: Atoms, Molecules and Clusters*, **13(2)**, 161 (1989).

[39] (a) R.S. Walters, T.D. Jaeger and M.A. Duncan, *J. Phys. Chem.*, in press.; (b) G. Gregoire, N.R. Brinckmann, H.F. Schaefer and M.A. Duncan, *J. Phys. Chem.*, in press.; (c) G. Gregoire and M.A. Duncan, *J. Chem. Phys.*, **117**, 2120 (2002); (d) G. Gregoire, J. Velasquez and M.A. Duncan, *Chem. Phys. Lett.*, **349**, 451 (2001).

[40] *Organometallic Ion Chemistry*, ed. B.Freiser, Kluwer Academic Publishers, 1996.

Chapter 6

Photodissociation Studies of Rare Earth Lanthanide Metal-Cyclooctatetraene

Prompted by the chemistry of well known organometallic complexes such as ferrocene[1] and dibenzene chromium,[2] previous investigations have explored the possibility of extended stacking motifs in the structures of transition metal ion complexes with benzene[5], cyclopentadiene,[6] coronene[7] and C_{60}.[8,9] These studies were conducted in the gas phase to avoid problems often faced in solution with interfering solvent effects and precipitation of large molecules. In each of these cases for certain transition metals, evidence was found for multi-decker "sandwich" structures. Uranocene, discovered in 1968 by Streitwieser and Muller-Westerhoff,[10] is analogous to ferrocene but utilizes the rare earth actinide metal uranium, sandwiched with two cyclooctatetraene (COT) moieties. In a natural extension of these ideas, Kaya and coworkers performed studies in the gas phase to see if an extensible stacking motif would also occur for lanthanide metals with COT.[11] Using laser vaporization coupled with time-of-flight mass spectrometry they discovered a strong pattern of magic numbers corresponding to the clusters $M_n^+(COT)_{n+1}$, (M=Ce, Nd, Eu, Ho, Yb) which is exactly what is expected for sandwich structures. Further, they also performed photoelectron spectroscopy studies of such complexes and found further confirmation based on the electronic structure of these complexes. Our aim is to provide additional evidence of the existence of multi-decker sandwich or other structural motifs in lanthanide ion-COT clusters.

Previous experimental[12] and theoretical[13] studies confirmed that lanthanide COT complexes bond very differently than the corresponding actinide complexes. Actinides commonly are able to adopt a +4 oxidation state, which makes them ideally suited to form the sandwich structure with COT by donating two electrons to each COT ligand. This produces $M^{4+}(COT^{-2})_2$ structures that exhibit directional bonding utilizing the valence 5f orbitals in a mostly covalent interaction. Lanthanides are not able to do this. In fact, their strong trivalency overcomes the aromaticity of COT^{-2} leading to more ionic, nondirectional bonding of the type $M^{3+}(COT^{-1.5})_2$.

6.1 Experimental

Rare earth lanthanide complexes are generated in a pulsed supersonic jet laser vaporization cluster source described in detail in Chapter 2. In brief, a gas mixture containing volatile 1,3,5,7-cyclooctatetraene (COT) is pulsed with a high speed valve (General Valve Series 9) over the surface of rod of the appropriate metal, in this case either dysprosium, samarium or neodymium. Complexes grow by recombination in a gas channel extension to the rod holder that is 1-2 cm in length. The metal is vaporized into the gas pulse with the second or third harmonic (532 nm, 355 nm respectively) of a pulsed Nd:YAG laser (Spectra Physics GCR-11). The laser is focussed onto the sample rod with a 30 cm focal length lens. A backing gas of argon or helium was used to generate complexes of those ligands. Since COT is a liquid at room temperature a reservoir is installed on the line feeding the nozzle and argon passed through it. A backing pressure of 40-60 psi is used. The expansion is skimmed into a differentially pumped chamber containing a reflectron time-of-flight mass spectrometer used for analysis. The clusters are produced as neutrals and are photoionized with 195 nm from an ArF excimer laser (Lambda Physik Compex).

Photodissociation is performed in the turning region of the reflectron using fixed frequency second or third harmonic from another Nd:YAG (Spectra Physics DCR-11). The term "high power," as used below, indicates 50-100 mJ/cm^2, whereas low power refers to 1-10 mJ/cm^2.

6.2 Results and Discussion

The mass spectra of clusters obtained for the lanthanide metals neodymium, samarium and dysprosium are shown in Figure 6.1a-c. The peaks are labelled according to their assignment (x,y) corresponding to $M_x^+(COT)_y$. Noticeably absent in any of the spectra are signs of COT clusters or pure metal clusters. Clusters with neodymium shown in Figure 6.1a show addition of one and two COT ligands to a metal ion and up to three with two metals. Similarly for dysprosium in Figure 6.1c. With samarium we were able to produce clusters out to the (3,4) complex. The absence of a peak for the (1,3) cluster in these systems indicates that one metal atom will accept only two COT ligands at most. There are also no peaks corresponding to multiple metal atoms on a single coronene, also probably indicating that we are not forming metal clusters. Since neither ligand appears in excess of the other, the metal vapor and COT vapor appear to be present in about the same concentration. Some peaks appear broad due to the multiple metal isotopes, particularly the peaks for clusters with multiple metal atoms. The mass spectral resolution, however, is good enough to resolve some isotopes in the single metal complexes. In the spectra for both Nd and Dy a peak was also present that assigns to $M^+(C_5H_5)$, which is apparently generated from the breakdown of COT in the presence of these metals in the vaporization plasma. Kaya and coworkers observed much more pronounced magic numbers of $M_n^+(COT)_{n+1}$ than what we observe here.[11] They also observed larger clusters out to about n=5 for each metal they studied. We attribute the dif-

ference in our result as due to somewhat colder expansion conditions in our system. This tends to limit growth of large mutli-atom clusters because insufficient energy remains to overcome the activation energy for strongly bound clusters to form. Our spectrum for samarium in Figure 6.1(b) actually shows an inverted pattern in that the (2,1) and (2,3) peaks are weak while the (2,2) peak is strong. Samarium is the only metal in this study that is able to adopt either a +2 or a +3 oxidation state. Dysprosium is the only metal we observed a pronounced preference for the (1,2) and (2,3) cluster sizes.

Through the use of fixed frequency photodissociation we sought to obtain some information in the structures of these clusters. Figure 6.2 shows the photodissociation mass spectrum of $Sm^+(COT)$. The parent ion is shown as a negative peak indicating depletion due to fragmentation, while the fragments appear positive. The most prominent fragment is the metal ion itself. The ionization potential (IP) of samarium is 5.64 eV, whereas that of COT is 8.0 eV. When the cluster dissociates the fragment with the lower IP is observed as an ion, while the higher IP fragment is lost as a neutral and is not detected. Also apparent with smaller intensities are peak assigned to $Sm^+(C_2H_2)$ and $Sm^+(C_5H_5)$. The spectrum shown was obtained at higher photodissociation laser power at 355 nm. At lower power these fragments were not observed and the cluster dissociates cleanly into metal ion. Conventional mass spectrometry of COT shows that it fragments by loss of whole C_2H_2 molecules and primarily produces $C_6H_6^+$ and $C_4H_4^+$. These fragments are preferred due to the stability of benzene as an aromatic molecule, and C_4H_4 is prominent due to the stability of acetylene (C_2H_2) lost as a neutral closed shell molecule. The appearance of $Sm^+(C_5H_5)$ as a fragment is probably due to some acquired energy stabilization of this complex. A simple explanation would be that C_5H_5 exists in this cluster as the cyclopentadienyl anion as in $Sm^2+(C_5H_5)^-$ created by charge transfer. As noted above, there is no evidence for $Sm^+(C_5H_5)$ in the mass spectrum. The (1,1) cluster

of samarium most likely exists as a metal ion attached to a whole COT molecule without insertion or disruption of the carbon backbone of the ligand. The appearance of $Sm^+(C_5H_5)$ fragments probably occur due to a competing photoinduced pathway that has small quantum yield at this wavelength.

Photodissociation of $Sm^+(COT)_2$ at 355 nm yields the mass spectrum shown in Figure 6.3. The primary product is $Sm^+(COT)$, formed by cleanly dissociating a neutral COT molecule. This fragment then goes on to dissociate again by loss of neutral COT leaving the bare metal ion. The appearance of the (1,1) cluster as an ionic fragment indicates that it has an IP lower than that of COT (8.0 eV). Since the COT ligands would be expected to experience a greater attraction for the metal ion than for each other we would expect that this complex exists as a sandwich structure. The fragmentation pattern is consistent with the "peeling off" of layers if it is assumed that this is a stacked cluster. Also present is a small amount of $Sm^+(C_5H_5)$, not present at low laser fluence. This was observed above for the photodissociation of the (1,1) complex. This is a result of the high power used to photodissociate the (1,2) parent cluster leaving the (1,1) fragment with enough energy to undergo another fragmentation.

The photodissociation spectrum shown in Figure 6.4 shows a degree of complexity not seen in any of the other samarium spectra. This cluster breaks into clusters of $Sm_2^+(C_xH_x)$ (x = 2,4,6) which are due to loss of acetylene units. The (2,1) cluster also fragments into $Sm^+(COT)$, $Sm^+(C_2H_2)$ and Sm^+. There is no indication of Sm_2^+ among the fragments. The same fragmentation pattern occurs at both high and low laser fluence. The degree of fragmentation of the COT framework, even at low laser power suggests that cluster itself exists with metals inserting into the carbon-carbon framework of the ligand, but that the metals are probably not bound to each other. Since $Sm_2(COT)$ shows a fragmentation channel for the loss of a neutral Sm atoms, it must have an IP that is not only lower than that of COT, but lower than that

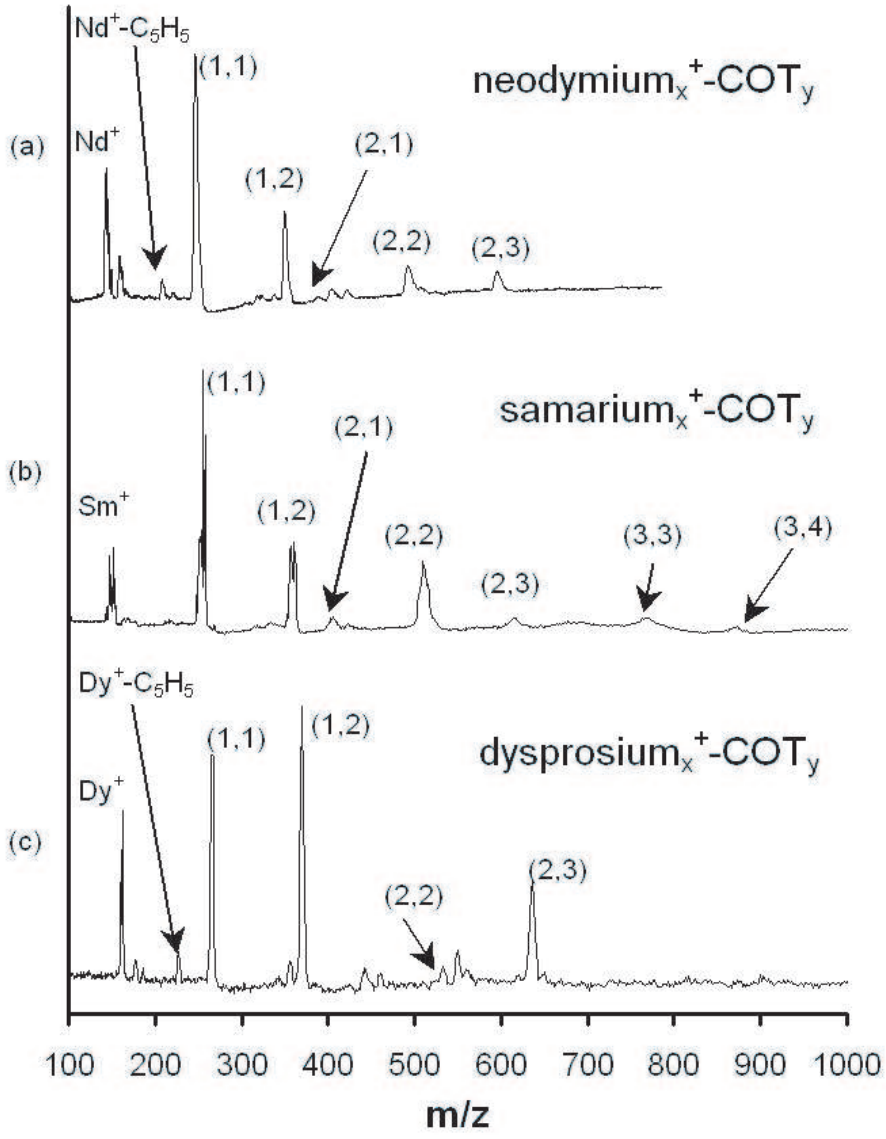

Figure 6.1:
Mass spectra of clusters of the lanthanide metals neodymium (a), samarium (b) and dysprosium (c) with cyclooctatetraene.

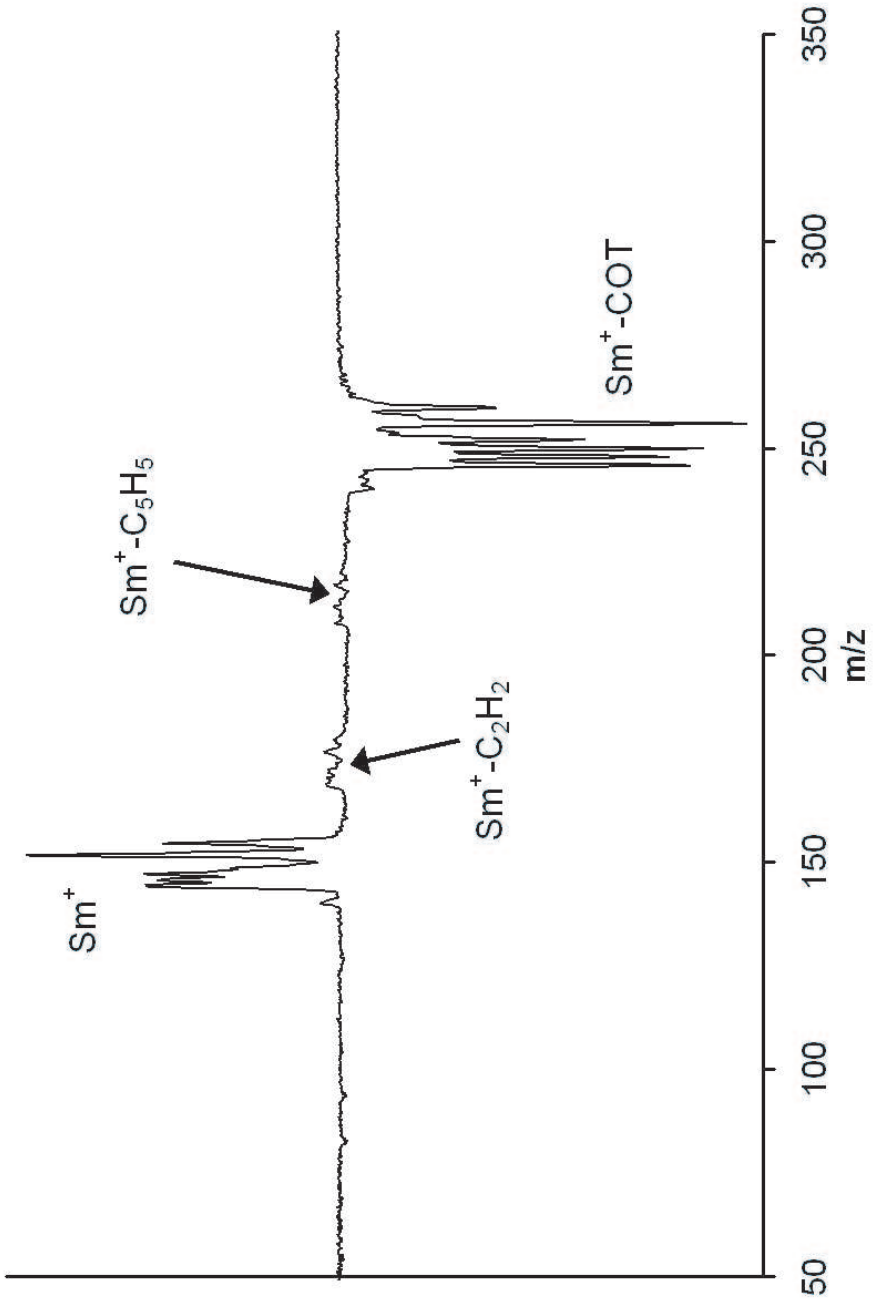

Figure 6.2:
Photodissociation spectrum of Sm^+(COT) fragmented at 355 nm and at high laser power (defined in text).

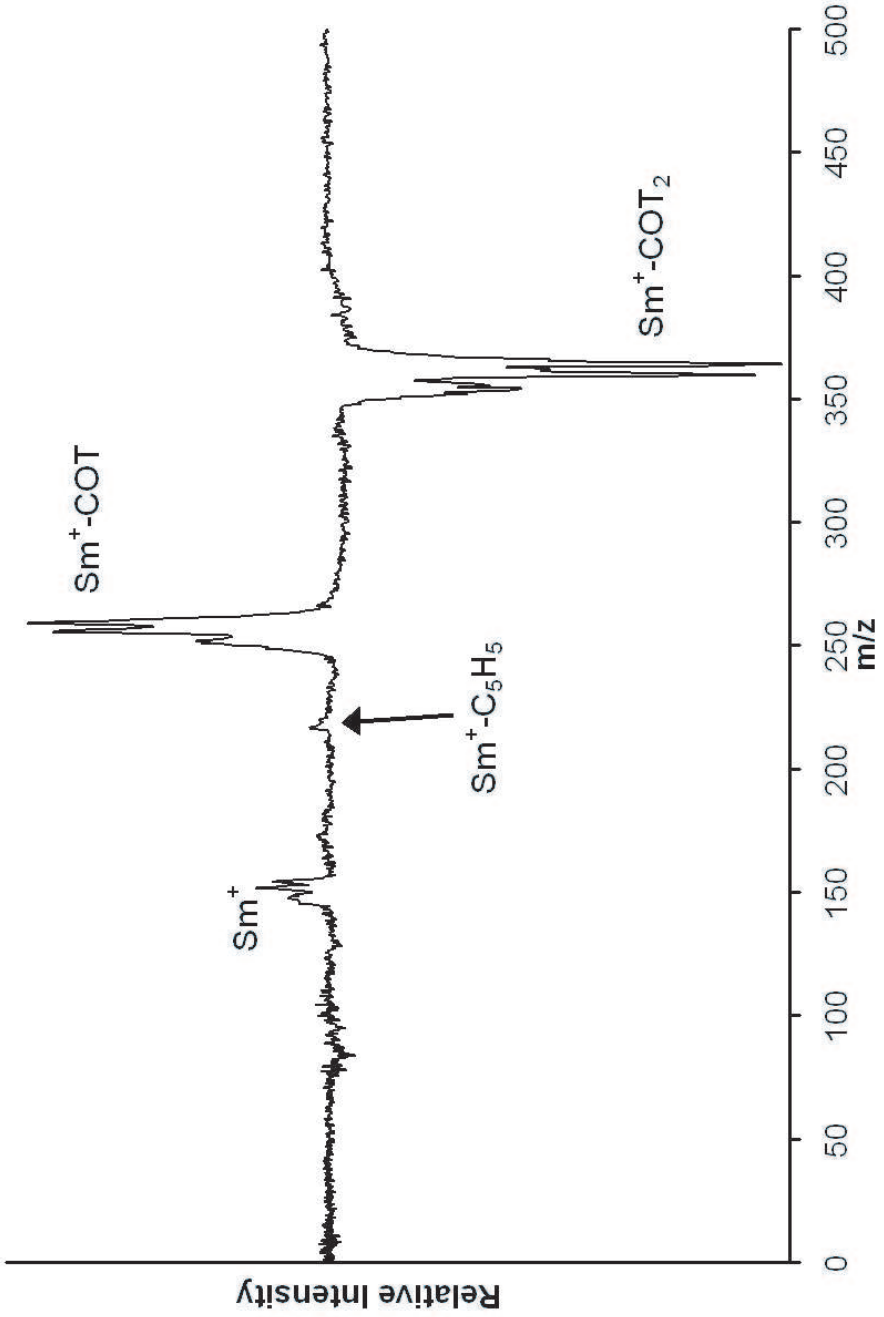

Figure 6.3:
Photodissociation spectrum of $Sm^+(COT)_2$ at 355 nm and at high laser power.

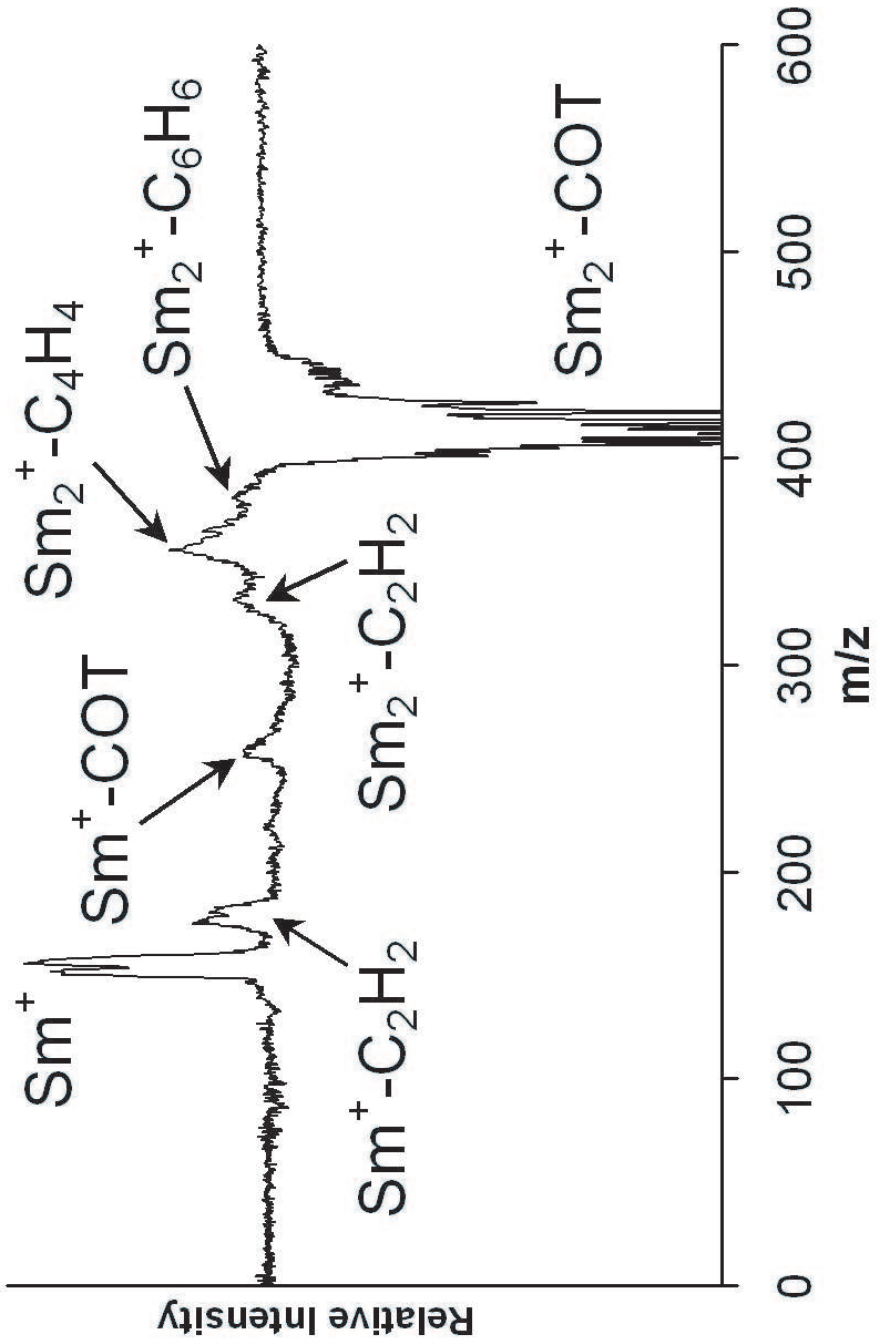

Figure 6.4:
Photodissociation mass spectrum of Sm_2^+(COT).

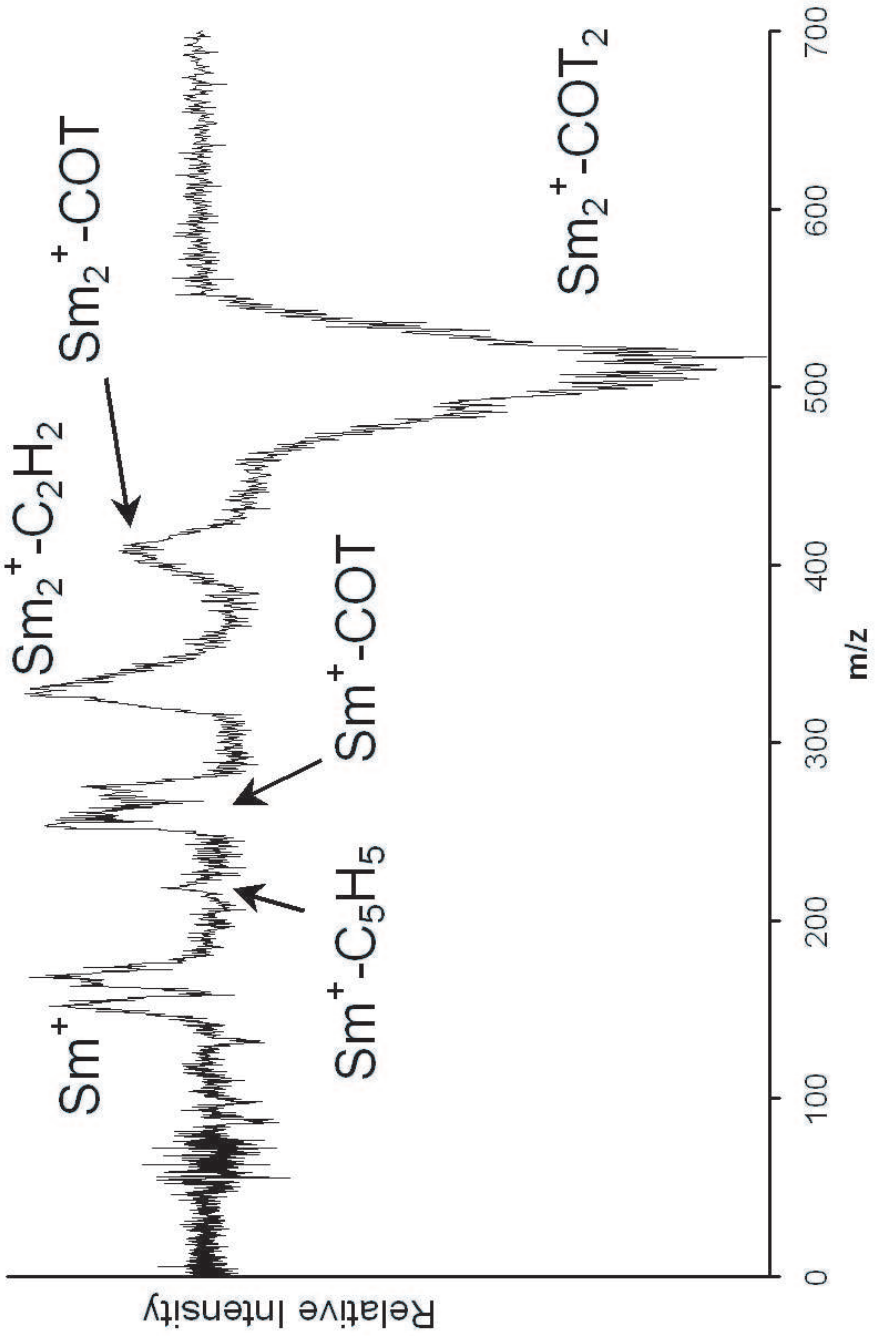

Figure 6.5:
Photodissociation spectrum of $Sm_2^+(COT)_2$.

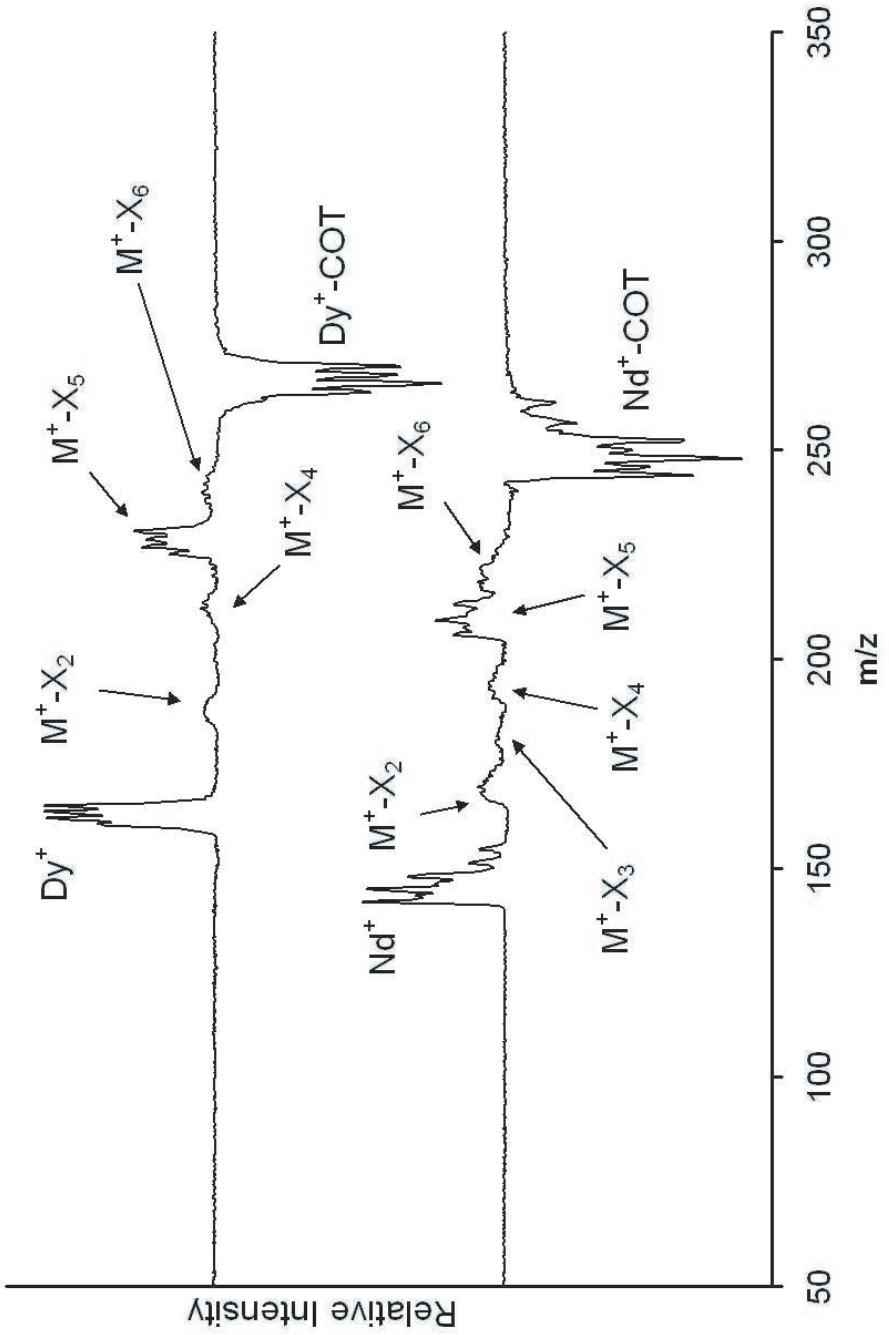

Figure 6.6:
Photodissociation spectrum of M^+(COT), M = Dy, Nd.

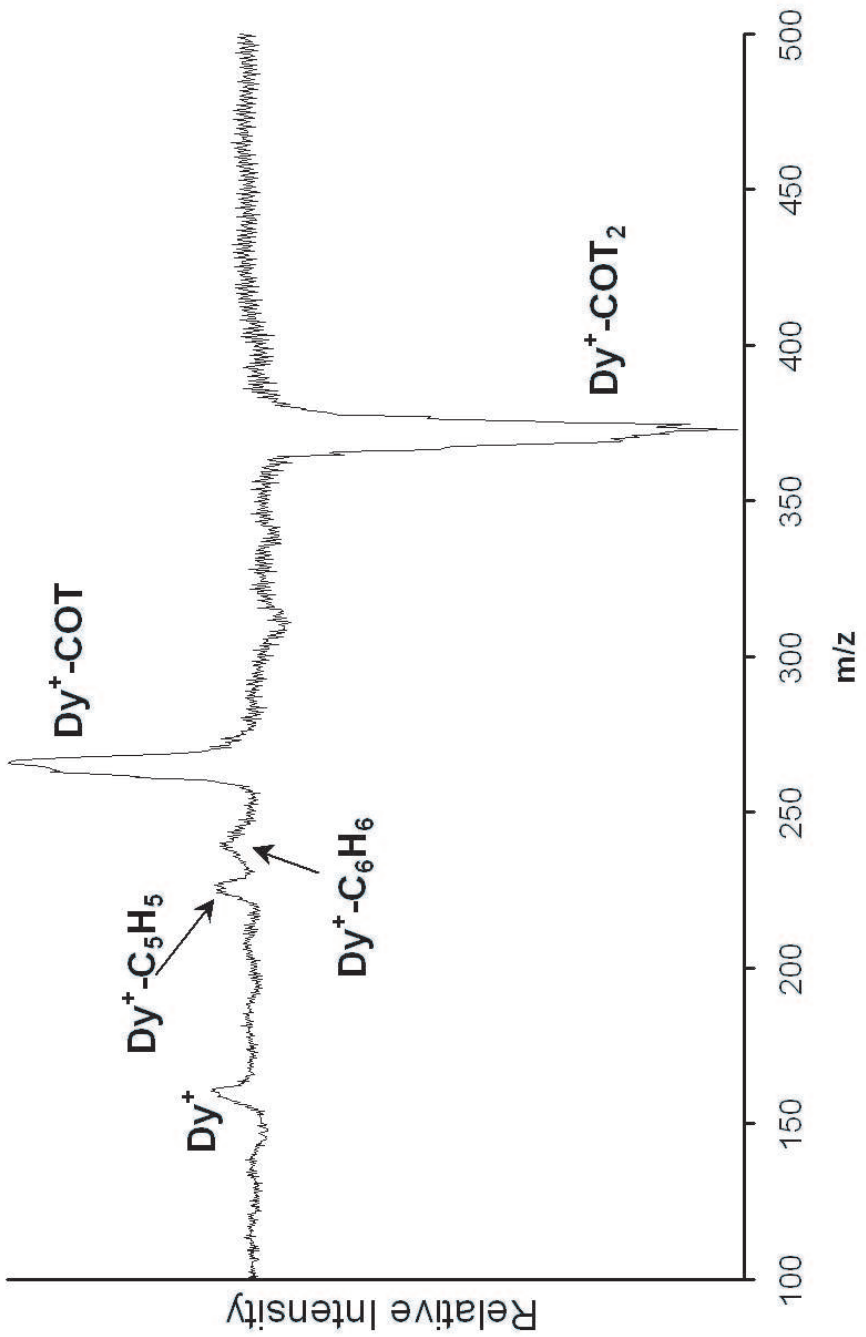

Figure 6.7:
Photodissociation spectrum for $Dy^+(COT)_2$.

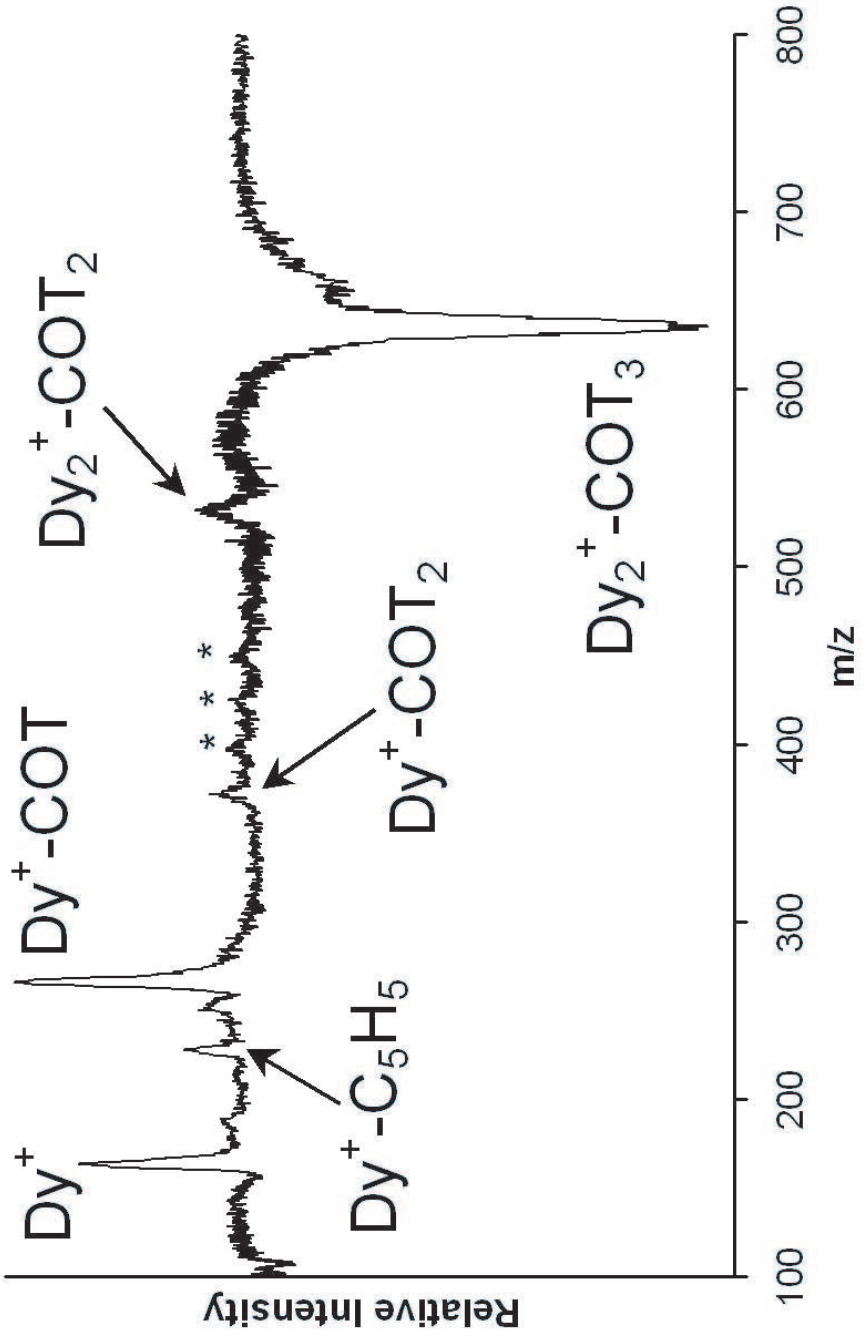

Figure 6.8:
Photodissociation spectrum for $Dy_2^+(COT)_3$.

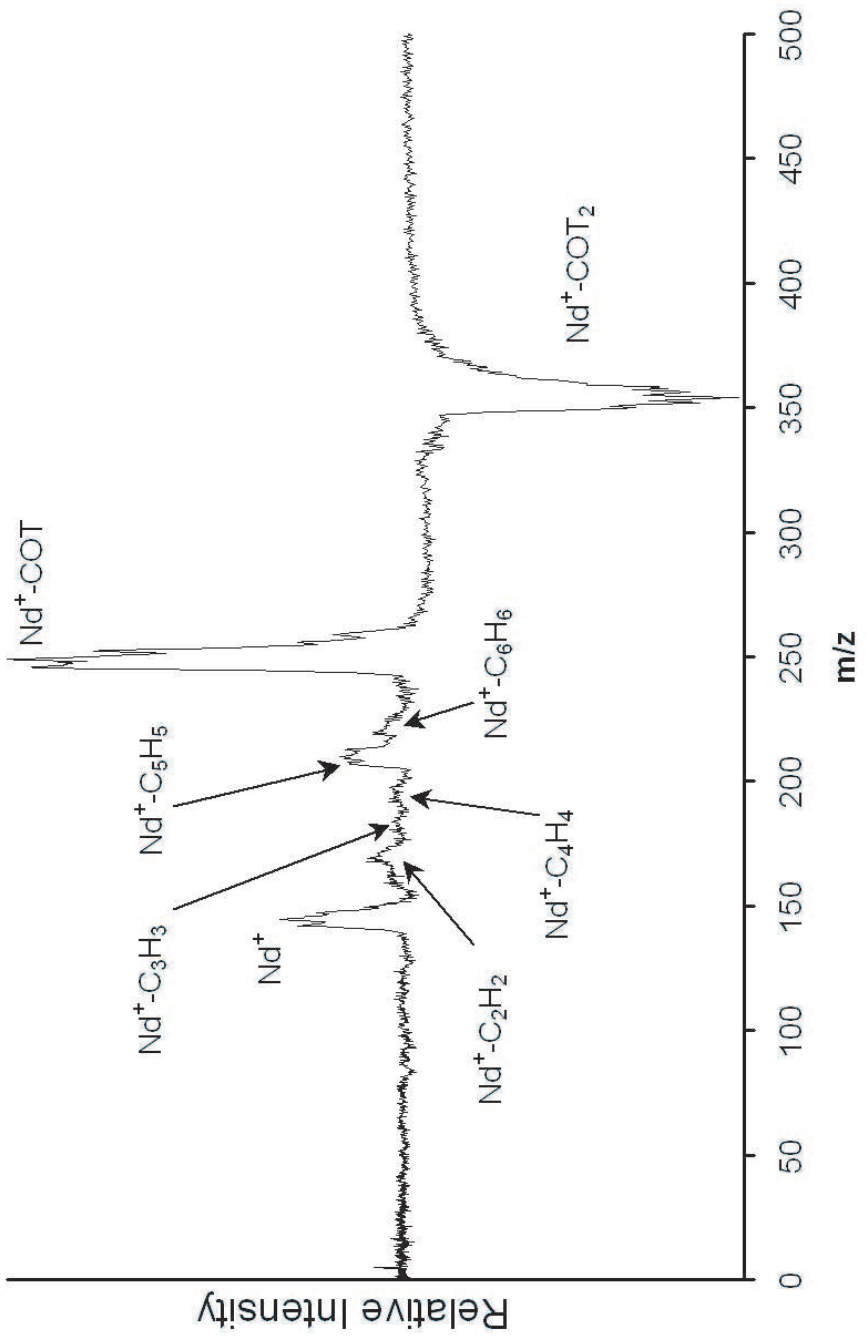

Figure 6.9:
Photodissociation spectrum for $Nd^+(COT)_2$.

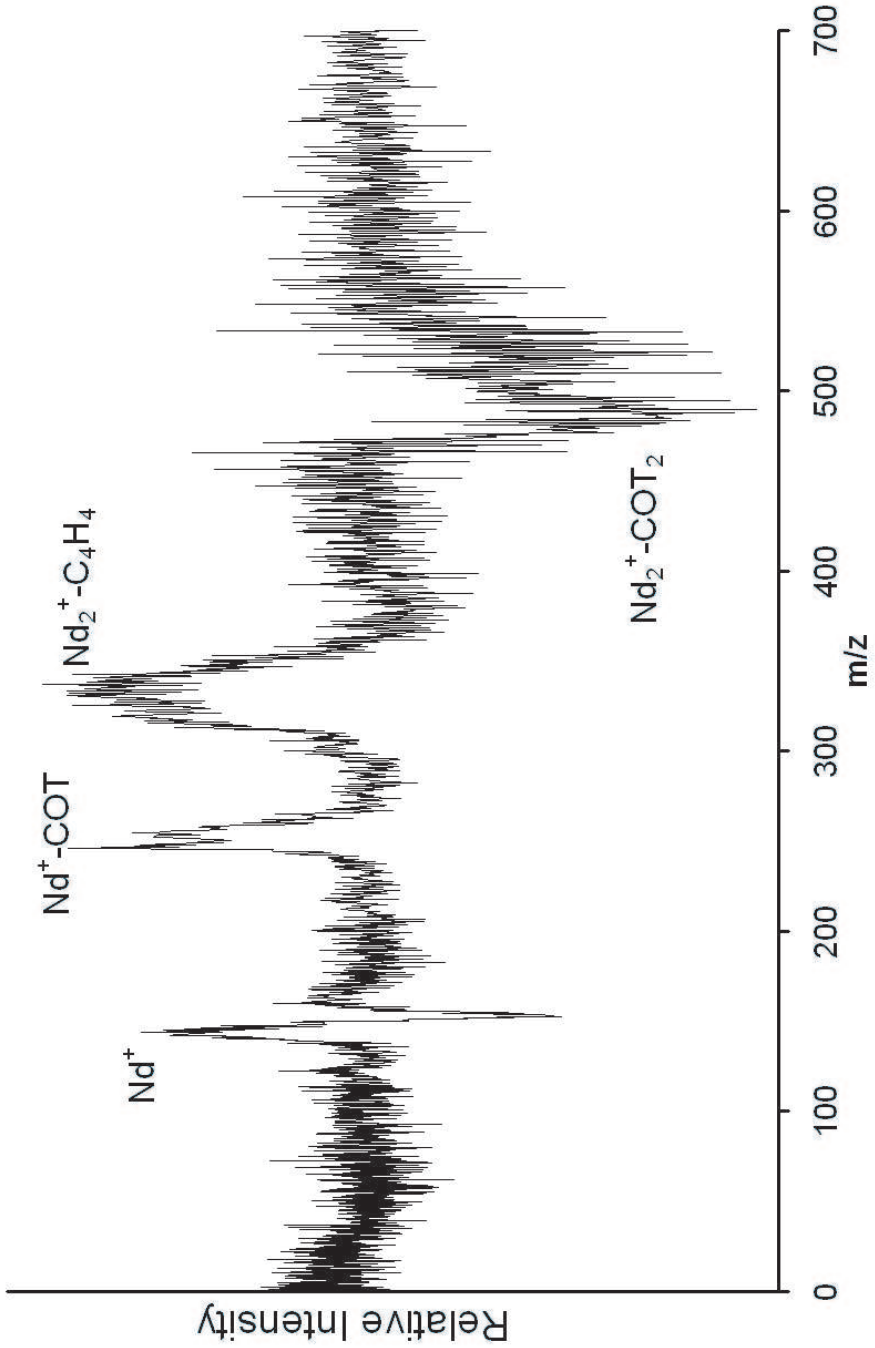

Figure 6.10:
Photodissociation spectrum for $Nd_2^+(COT)_2$.

of Sm at 5.64 eV. The $Sm^+(C_2H_2)$ cluster may result from fragmentation of the (2,1) itself or it may be a fragment of the $Sm_2^+(C_4H_4)$ cluster. The latter would be consistent with a bonding scheme in which the metals are attached to vicinal double bonds in an open ring fragment with samariums at each end:

$$\begin{array}{c} \text{Sm} \quad \text{Sm} \\ \text{C=C—C=C} \end{array}$$

This would account for the fragmentation into $Sm^+(C_2H_2)$ by simply breaking the C—C single bond.

The larger cluster $Sm_2^+(COT)_2$ could adopt several possible structural configurations. One such possibility is the layering of alternating metal-COT-metal-COT. Another configuration could be metal dimer sandwiched between two COT ligands. The photodissociation mass spectrum for the (2,2) cluster with samarium is shown in Figure 6.5. Lower signal intensity, decreased resolution at this higher mass, and the multitude of isotopes with two samarium atoms make the peaks look broad and noisy. The heaviest photofragment observed is loss of an entire COT ligand yielding the (2,1) cluster. From here we might expect a similar fragmentation pattern as that for the (2,1) cluster above, instead, however there is a prominent fragment for the (1,1) and Sm^+. This pattern bears strong resemblance to that observed in previous studies of multi-decker sandwich clusters, and is consistent with the idea of alternating layers. Present also are peaks that assign to $Sm_2(C_2H_2)^+$ and $Sm^+(C_2H_2)$. The former was present in the photodissociation of (2,1) but appears here as the most prominent peak in the spectrum. The latter was not present in the spectrum of (2,1) but was for (1,2) and (1,1). This pattern observed here may indicate that the cluster is a multi-decker sandwich type structure, although it is possible that an isomeric form exists comprised of an $Sm_2(COT)^+$ species with a COT ligand weakly attached.

The photodissociation mass spectra of the (1,1) complexes of neodymium and dysprosium are shown in Figure 6.6, grouped together because of their similarity. There is significantly more disruption of the carbon backbone of COT than has been seen for samarium. The most prominent peak for these is the M^+. Also apparent are a series of fragments corresponding to M^+X_n, where $X_n = C_nH_n$, n=2-6, the strongest of which is n=5. Dysprosium and neodymium are not known to exist in a +2 oxidation state, so the prominence of $M^+(C_5H_5)$, seen both here and in the mass spectra, is a mystery. The extensive fragmentation into metal-hydrocarbon clusters could indicate that the metal is inserting into the framework of COT and forming metal-carbon bonds.

The spectrum of the (1,2) complex of dysprosium is shown in Figure 6.7. Similar to the (1,2) complex of samarium, we see loss of whole COT ligands leaving the (1,1) and Dy^+. The ionization potential of Dy is 5.93 eV. A peak appears assigned to $Dy^+(C_5H_5)$ and is slightly more prominent that the peak assigned to $Dy^+(C_6H_6)$. This latter complex probably represents the metal ion bound to a benzene molecule, which is the major fragment of the free COT molecule absent of metal. The appearance of $Dy^+(C_5H_5)$ could represent a cyclopentadienyl-metal complex. Cyclopentadiene requires the donation of a single electron to become an aromatic ligand. Dysprosium strongly prefers a +3 oxidation state. The clusters have a net charge of +1 and if dysprosium donated one electron to the C_5H_5 ligand, it would have to be in a +2 oxidation state. As with samarium, this pattern likely means that this complex is a full sandwich type structure, with some photoinduced fragmentation into alternate products taking place.

The photodissociation spectrum of $Dy_2(COT)_3^+$ shown in Figure 6.8 is interesting because this cluster is the largest we observed that falls into the (n,n+1) pattern observed by Kaya. The major fragments produced at high laser power are the (2,2), (1,2), (1,1) and Dy^+. The main scheme of fragmentation appears here to strongly

suggest layering of metal and COT in a triple decker sandwich. Here we also see some new features in the minor fragments. To higher mass of the (1,2) complex are adducts of (1,2) with C_nH_n, where n=1-7 with an intensity preference for the even values of n. A small amount of $Dy^+(C_5H_5)$ is apparent as well.

We have observed similarities in the fragmentation patterns for neodymium and dysprosium, however when we turn to $Nd^+(COT)_2$ shown in Figure 6.9 we see a slightly different result. The cluster primarily loses an entire COT molecule, however below this there is a significant degree of fragmentation, just as was observed for the neodymium (1,1) complex. This seems to indicate, as stated before, that neodymium is breaking into the COT backbone and in this case, the inserted complex is then attaching to a complete COT molecule.

Spectra were also obtained for $Nd_2(COT)_2^+$ (Figure 6.10). Photofragments include Nd^+ and the (1,1) complex as well as $Nd_2(C_4H_4)^+$. There is no sign of Nd_2^+ nor of the (2,1) complex as was seen for samarium. The C_4H_4 group in this case cloud represent a cyclobutadiene ligand interacting with a pair of neodymium atoms. Cyclobutadiene exhibits a high ring strain, however there are many known cases of transition metal cyclobutadiene complexes where the presence of the metal stabilizes the ring.[3,14] Lanthanide metals often exhibit similar chemistry to the transition metals due to the contracted nature of the f orbitals, which prevents their participation in valence bonding.[3] With the exception of the metal hydrocarbon peak, this appears to be strongly indicative of of a multi-decker sandwich structure.

6.3 Conclusions

Lanthanide metal complexes of Sm, Dy and Nd with COT were produced by laser vaporization and studied by fixed frequency photodissociation. Mass spectral data shows that the clusters are formed by metal atoms, not clusters, attaching to COT

molecules. For Nd and Dy, some degree of metal insertion into the COT ring takes place in the source plasma to produce $M^+(C_5H_5)$. This result is intriguing because if the ligand is a cyclopentadienyl group, these metals must adopt a net +2 oxidation state, which they generally do not prefer. Photodissociation of the COT clusters with Dy and Nd also indicates that ring insertion into one COT ligand may be taking place, followed by the weak attachment of additional COT ligands. Samarium COT clusters were not observed to exhibit the (n, n+1) alternating pattern observed previously.[11] Photodissociation of samarium-COT clusters exhibited much less ring disruption except in clusters with more than one samarium atom. This suggests that Nd and Dy bind strongly to the COT ligand, whereas Sm is not so strongly bound. Clusters with two or more metal atoms exhibit a large degree of COT fragmentation, which may be present in the nascent parent cluster, or may be photoinduced upon fragmentation. The fragmentation patterns observed, however, still indicate at least the presence of an isomer that may exist in a multi-decker sandwich form. These systems exhibit some very interesting chemistry. Further study by infrared spectroscopy would be able to distinguish between COT that is weakly attached to a metal versus COT that has become aromatic by way of the distinct C-H stretch vibrations. By measuring this, the question of whether the metals are donating electrons to the COT ligands could be addressed and in doing so provide insights about the oxidation state of the metals. Also IR spectroscopy would be able to shed valuable insight on the nature of the lanthanide-hydrocarbon clusters to determine if they are open structures or rings in their attachment to the metals.

6.4 References

[1] (a) T.J. Kealy and P.L Paulson, *Nature*, **168**, 1039 (1951); (b) Fischer, *Angew. Chem.*, **67**, 475 (1955).

[2] A. Haaland, *Acta Chem. Scand.*, **19**, 41 (1965).

[3] F.A. Cotton and G. Wilkinson "Advanced Inorganic Chemistry." 3rd Ed., Wiley-Interscience, New York, 1972.

[4] G. Wilkinson, *J. Organometal. Chem.*, **100**, 273 (1975).

[5] (a) K. Hoshino, T. Kurikawa, H. Takeda, A. Nakajima and K. Kaya, *J. Phys. Chem.*, **99(10)**, 3053 (1995); (b) T. Kurikawa, H. Takeda, A. Nakajima and K. Kaya , *Zeitschrift fuer Physik D: Atoms, Molecules and Clusters*, **40(1-4)**, 65-69 (1997).

[6] S. Nagao, A. Kato, A. Nakajima and K. Kaya, *J. Am. Chem. Soc.*, **122(17)**, 4221 (2000).

[7] (a) M.A. Duncan, A.M. Knight, Y. Negeshi, S. Nagoa, Y. Nakamura, A. Kato, A. Nakajima and K. Kaya, *J. Phys. Chem. A* **105**, 10093 (2001); (b) N.R. Foster, J.W. Buchanan, N.D. Flynn and M.A. Duncan, *Chem. Phys. Lett.*, **341**, 476 (2001); (c) N.R. Foster, G.A. Grieves, J.W. Buchanan, N.D. Flynn and M.A. Duncan, *J. Phys. Chem. A* , **104**, 11055 (2000); (d) J.W. Buchanan, G.A. Grieves, N.D. Flynn and M.A. Duncan, *Intl. J. Mass Spectrom.*, **185-187**, 617 (1999); (e) J.W. Buchanan, G.A. Grieves, J.E. Reddic and M.A. Duncan, *Intl. J. Mass Spectrom.*, **182**, 323 (1999); (f) J.W. Buchanan, J.E. Reddic, G.A. Grieves and M.A. Duncan, *J. Phys. Chem.*, **102**, 6390 (1998).

[8] A. Nakajima, S. Nagao, H. Takeda, T. Kurikawa and K. Kaya, *J. Chem. Phys.*, **107(16)**, 6491 (1997).

[9] G.A. Grieves, J.W. Buchanan, J.E. Reddic and M.A. Duncan, "Photodissociation of exohedral transition metal-C60 complexes," *Intl. J. Mass Spectrom.*, **204**, 223 (2001).

[10] A. Streitwieser and U. Müller-Westerhoff, *J. Am. Chem. Soc.*, **90**, 7364 (1968).

[11] (a) T. Kurikawa, Y. Negishi, F. Hayakawa, S. Nagao, K. Miyajima, A. Nakajima and K. Kaya, *J. Am. Chem. Soc.*, **120** 11766 (1998); (b) K. Miyajima, T. Kurikawa, M. Hashimoto, A. Nakajima and K. Kaya, *Chem. Phys. Lett.*, **306**, 256 (1999).

[12] (a) A. Streitweiser, U. Muller-Westerhoff, G. Sonnichsen, F. Mares, D.G. Morell, K.O. Hodgson and C.A. Harmon, *J. Am. Chem. Soc.*, **95**, 8644 (1973); (b) K. O. Hodgeson and K.N. Raymond, *Inorg. Chem.*, **11**, 3030 (1972).

[13] (a) L.J. Nugent, P.G. Laubereau, G.K. Werner, K.L. Vander Sluis, *J. Organomet. Chem.*, **27**, 365 (1971); (b) K.O. Hogson, F. Mares, D.F. Starks, A. Streitwieser, Jr. *J. Am. Chem. Soc.* **95**, 8650 (1973); (c) K.N. Raymond, C.W. Eigenbrot: *Acc. Chem. Res.* **13**, 276 (1980); (d) R.A. Andersen, J.M. Bonsella, C.J. Burns, J.C. Green, D. Hohl, N. Rosch: *J. Chem. Soc., Chem. Commun.* **405** (1986).

[14] (a) P.M. Maitlis, *In Adv. Organomet. Chem.*; F.G.A. Stone, R.W., Ed.; Academic Press: New York, 1966; Vol. 4; pp 95; (b) Efraty, *A. Chem. Rev.*, **77**, 691 (1977).

Chapter 7

Infrared Photodissociation Spectroscopy of Nickel Ion-Carbon Dioxide Solvation Complexes

A great deal of recent interest has focussed on the use of transition metals in heterogenous catalysis[1,2] for the conversion of CO_2 to methane and higher hydrocarbons for use as a synthesis gas as well as for reducing greenhouse gas emissions. Nickel has shown the most promise towards industrializing this process due to its high catalytic activity[3] and complete resistance to deactivation, and because it is relatively inexpensive and readily available.

Recent work in our group has extended spectroscopic measurements to the infrared region,[8−15] where more details about clustering dynamics, coordination layers and possible intracluster reactions can be obtained. The present chapter describes the investigation of $Ni^+(CO_2)_n$ complexes with these new infrared spectroscopy measurements.

Metal ion-CO_2 complexes have been studied previously by our group and others.[5,8,9,12 15,18,19] Electronic photodissociation spectroscopy of $Mg^+(CO_2)$ and $Ca^+(CO_2)$ complexes have established that these complexes have linear structures, as expected for the electrostatic charge-quadrupole binding interaction. Brucat and coworkers have found the same binding configuration for transition metal-CO_2 complexes, including $Ni^+(CO_2)$. High level theory has confirmed that these linear structures are expected. In recent work, we studied a number of $M^+(CO_2)_n$ complexes (M=Fe, Mg, Al) with resonance-enhanced infrared photodissociation

spectroscopy in the region of the asymmetric stretch vibration. Vibrational bands in the small clusters were observed to be shifted to the blue from the free-molecule vibration, while in-phase and out-of-phase motions of the asymmetric stretch could be measured for multiligand complexes. Larger complexes with CO_2 molecules not coordinated directly to the metal exhibited a vibrational band near that of the free-CO_2 molecule. Coordination numbers in these systems were documented and small cluster structures could be addressed with the help of theory. In the present work, we apply this same methodology to a new transition metal system to see the effect of electron configuration on coordination and cluster growth dynamics.

7.1 Experimental

$Ni^+(CO_2)_n$ complexes are produced by laser vaporization of a nickel rod sample in a pulsed-nozzle laser vaporization cluster source. The expansion gas is pure carbon dioxide. Vaporization is accomplished with the third harmonic of a Nd:YAG laser (355 nm). The molecular beam machine for these experiments has been described previously. Clusters are mass analyzed and size selected with a specially designed reflectron time-of-flight mass spectrometer.

The infrared laser system for these experiments is an optical parametric oscillator-amplifier system (Laser Vision). It consists of a grating tuned oscillator section with two KTP crystals pumped at 532 nm with an injection-seeded Nd:YAG laser (Continuum 9010). The amplifier section consists of four KTA crystals. It takes the idler output from the oscillator section and combines it with 1.06 micron radiation from the YAG pump. Difference frequency generation here produces the desired IR output in the 2000-4500 cm^{-1} region.

Laser excitation takes place in the turning region of the reflectron field, as described in earlier work. The selected parent ion cluster is excited with either

focused (25 cm lens) or unfocused IR radiation, depending on the laser power needed to initiate photodissociation. The fragment ion signals produced are monitored as a function of the wavelength to obtain an IR photodissociation spectrum. Mass spectrometer signals are collected with a digital oscilloscope (LeCroy WaveRunner 341) and transferred to a PC via an IEEE interface.

7.2 Results and Discussion

A mass spectrum of clusters of $Ni^+(CO_2)_n$ produced in a pure CO_2 expansion is shown in the upper trace of Figure 7.1. The conditions were adjusted for this spectrum by optimizing production of larger clusters and involved turning the energy of the vaporization laser down to the threshold of cluster production (< 20 mJ/pulse) as well as increasing the gas pulse intensity and duration. These settings produce what we believe to be the coldest expansion conditions, as evidenced by the broader distribution of cluster sizes. The mass spectrum shows little sign of the formation of metal carbides or oxides that may be produced by reactions in the plasma. The cluster intensities are largest for the n=1-4 peaks and then steadily taper off after n=5.

The source conditions can be adjusted to somewhat spoil the optimum cooling capacity of the expansion by increasing the energy deposited by the vaporization laser and by decreasing the amount of gas in the expanding pulse. When these conditions are chosen, the typical result is shown in the lower trace in Figure 7.1. In general, these so called "hotter" conditions tend to emphasize "magic numbers" in cluster generation, as was observed in the discovery of C_{60}.[7] This mass spectrum shows a steady increase in cluster signal leading up to the n=4 peak, and then a more pronounced drop in intensity from n=5 on. Velegrakis and coworkers studied Ni^+Ar_n clusters and found a magic number for n=4.

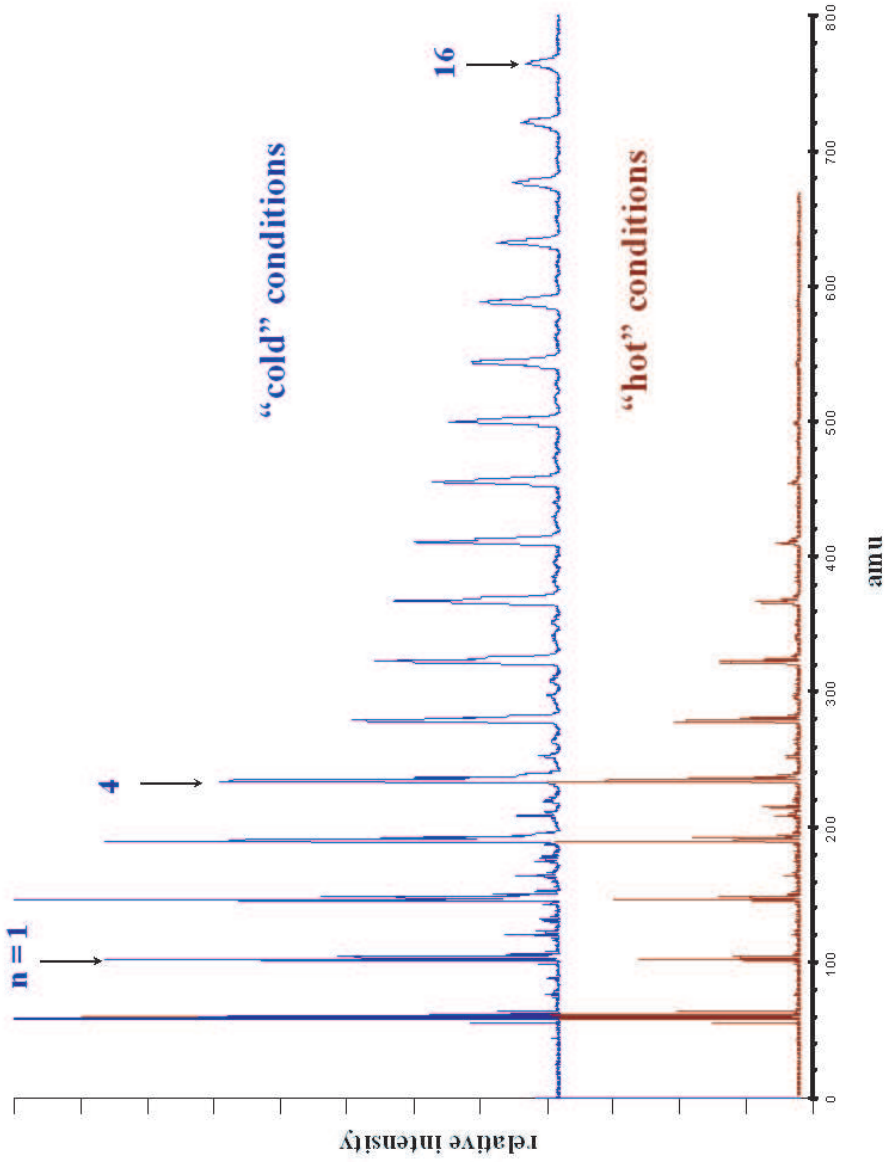

Figure 7.1:
(Upper trace) Mass spectrum obtained by laser vaporization of nickel in pure carbon dioxide expansion. The conditions utilized for this trace tend to create colder expansions. (Lower trace) Mass spectrum under conditions where the cooling capacity of the expansion are somewhat spoiled. These conditions generally emphasize differences in "magic number" cluster intensities.

The photodissociation mass spectra of $Ni^+(CO_2)_{n=6-8}$ are shown in Figure 7.2. These spectra are obtained by first mass selecting the parent ion, then intersecting the ion packet with the infrared laser that is tuned near the free CO_2 asymmetric stretch frequency of 2349 cm^{-1}. Each spectrum shows fragmentation by loss of whole CO_2 molecules. Previous power dependence studies on $Fe^+(CO_2)_n$ clusters indicate that this process is one of sequential fragmentation of the daughter ions.[8] In each case the series of cluster fragments terminates at $Ni^+(CO_2)_4$ cluster. When the n=4 cluster is selected, the photodissociation yield is very small and requires the use of a concave spherical mirror on the opposite side of the reflectron to both double pass and focus the IR light. The same is also true for the n=3. No dissociation was observed for the n=1 or 2 clusters under any conditions. The low fragmentation yields for these complexes is a result of the relative energetics of the system. The binding energy of Ni^+CO_2 has been determined from electronic photodissociation spectroscopy[9] to be 8750 cm^{-1}. By comparison, the energy of the photons being absorbed is only around 2350 cm^{-1}. Thus a multiphoton process is required to achieve the energy needed for bond breaking in the small clusters. As the cluster size increases, two things happen to improve the efficiency of photodissociation. The first is that the density of vibrational states increases with the number of atoms in the system. An increased density of states improves the probability of multiphoton absorption as well as the rate of IVR that carries the energy from a primarily ligand-centered mode into the dissociative coordinate metal-ligand stretch. The second thing that happens is that in general, ligand binding energies decrease with the addition of more ligands.[10] The presence of weaker bonds reduces the number of photons that must be absorbed to achieve dissociation.

The infrared spectra for $Ni^+(CO_2)_n$, n=3,4,5 are shown in Figure 7.3. These spectra were recorded by monitoring the integrated intensity of the loss of CO_2 fragmentation channel. No spectra were obtained for the n=1 or 2 complexes due

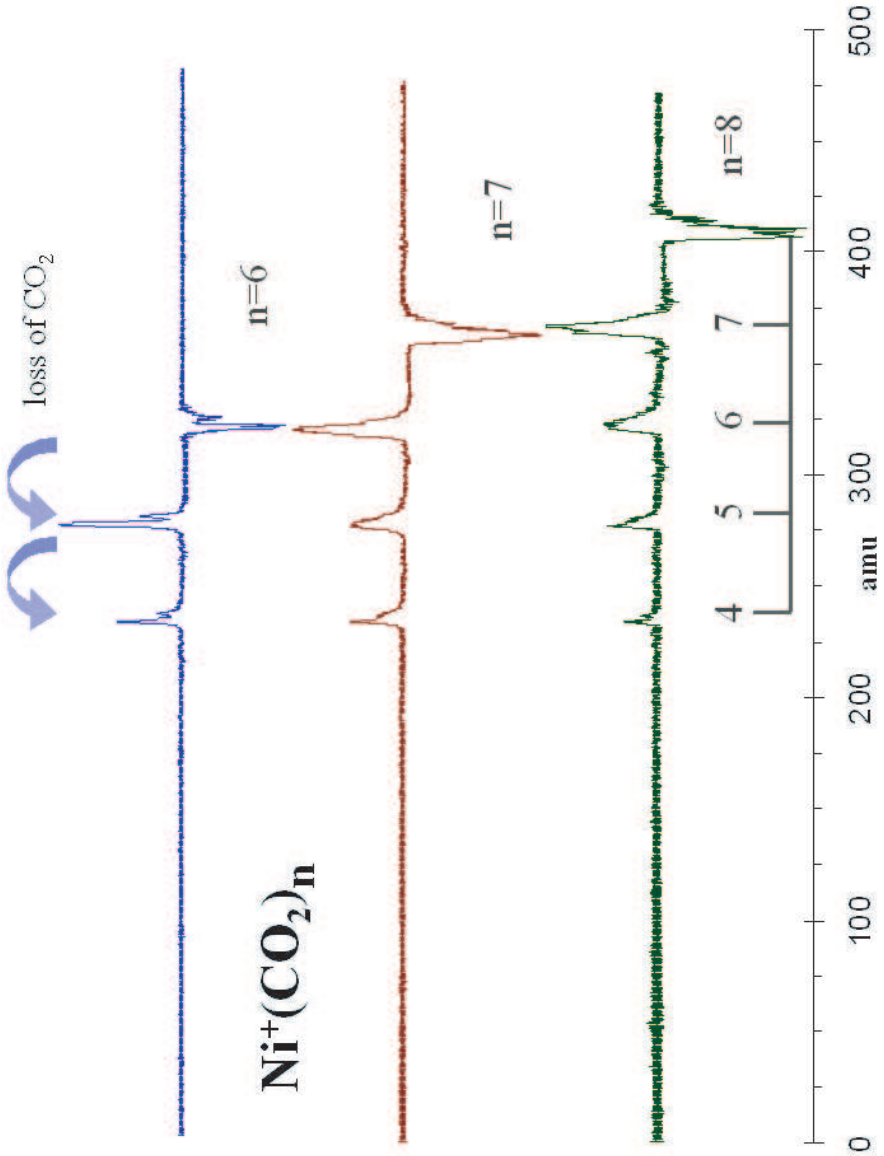

Figure 7.2:
Photodissociation mass spectra for a representative selection of nickel ion carbon dioxide clusters. The clusters fragment by loss of whole CO_2 molecules. In each case the series of photofragments terminates at $Ni^+(CO_2)_4$.

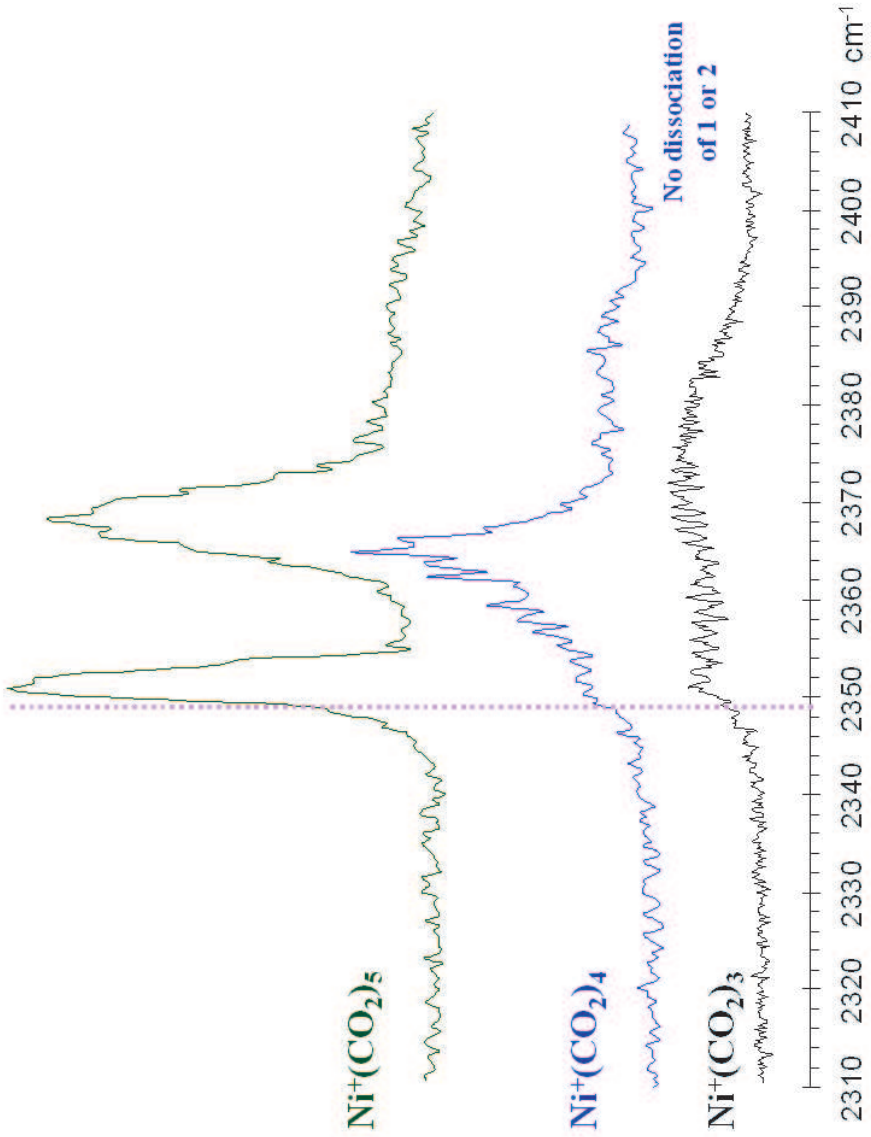

Figure 7.3:
Infrared vibrational spectra for the series of $Ni^+(CO_2)_n$ clusters for n=3,4,5. No dissociation was observed for n=1 or 2.

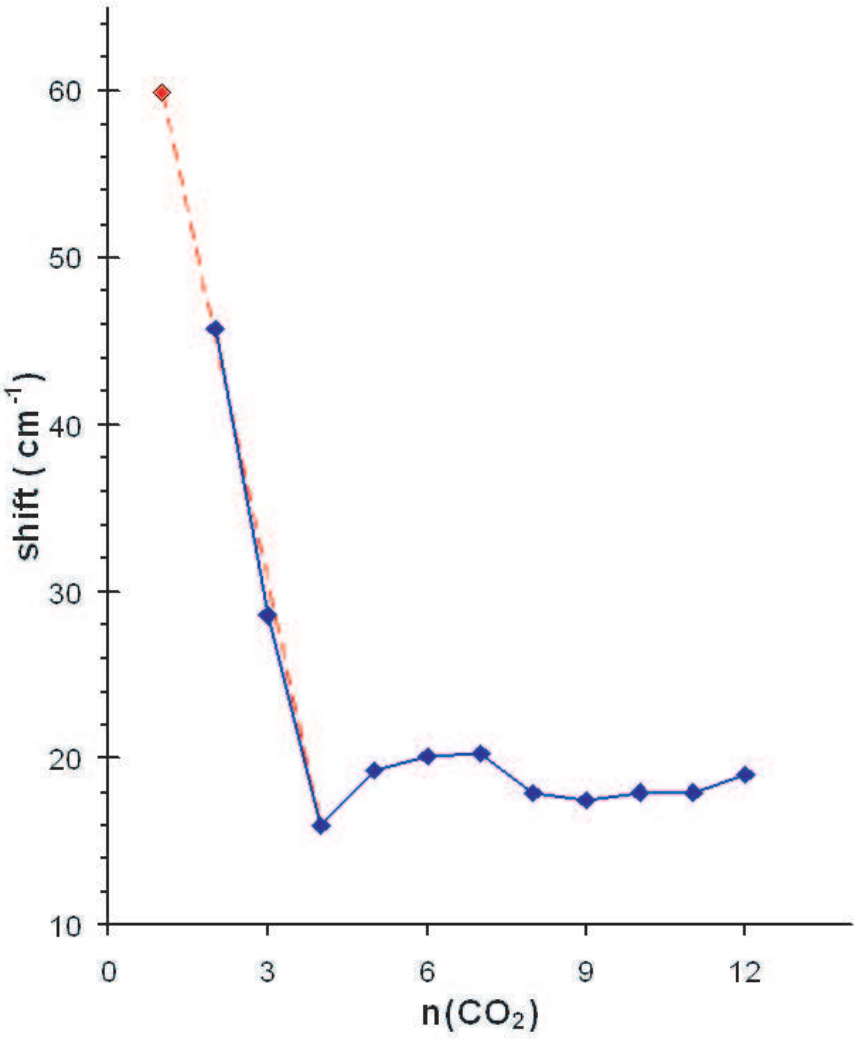

Figure 7.4:
Plot of the shift (in cm^{-1}) of the "core" vibrational band away from the free CO_2 asymmetric stretch frequency for each cluster size n. The data point for n=1 was extrapolated linearly from the values of n=2-4.

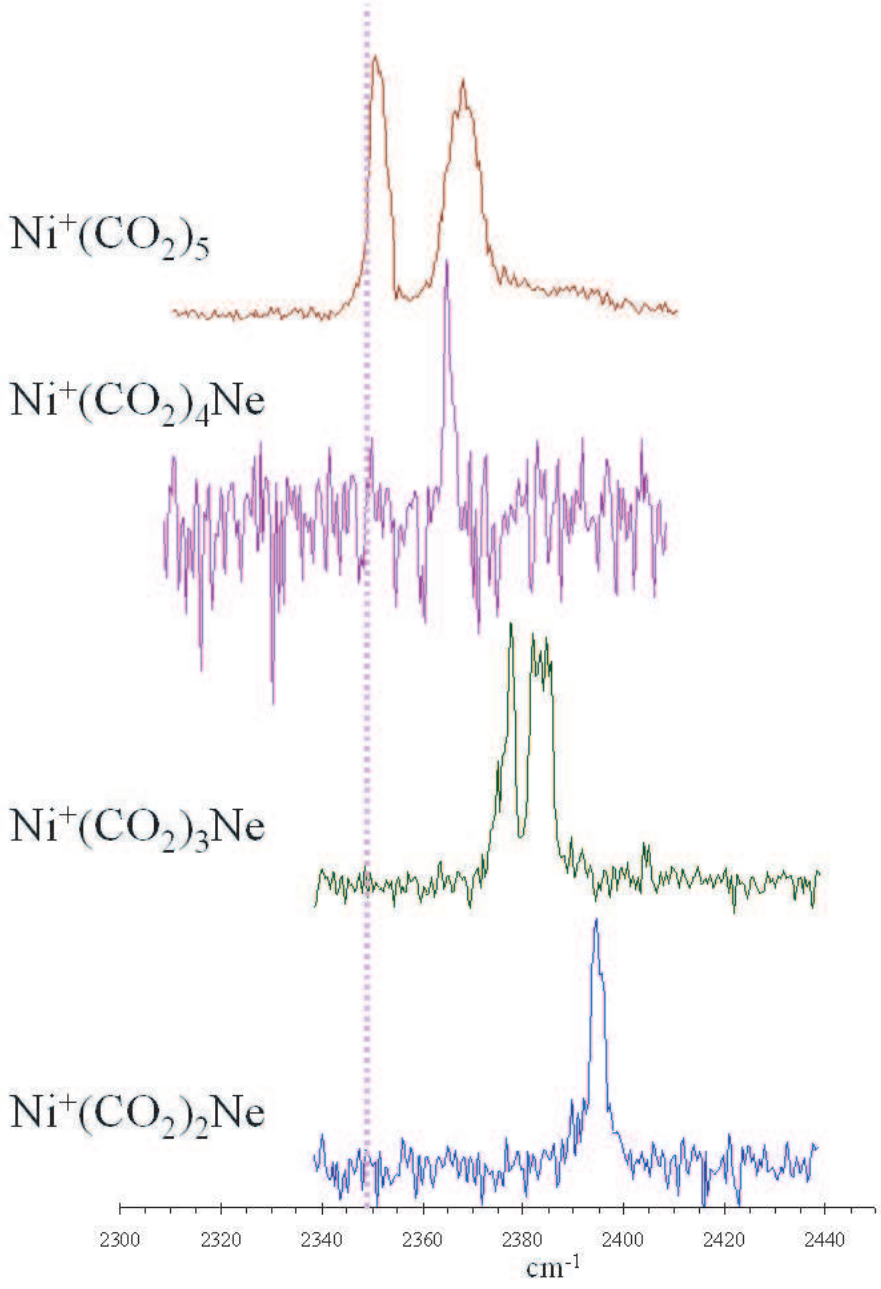

Figure 7.5:
Infrared spectra obtained for the neon tagged $Ni^+(CO_2)_nNe$ clusters for n=2,3,4. The spectrum of the untagged n=5 cluster is also shown for comparison.

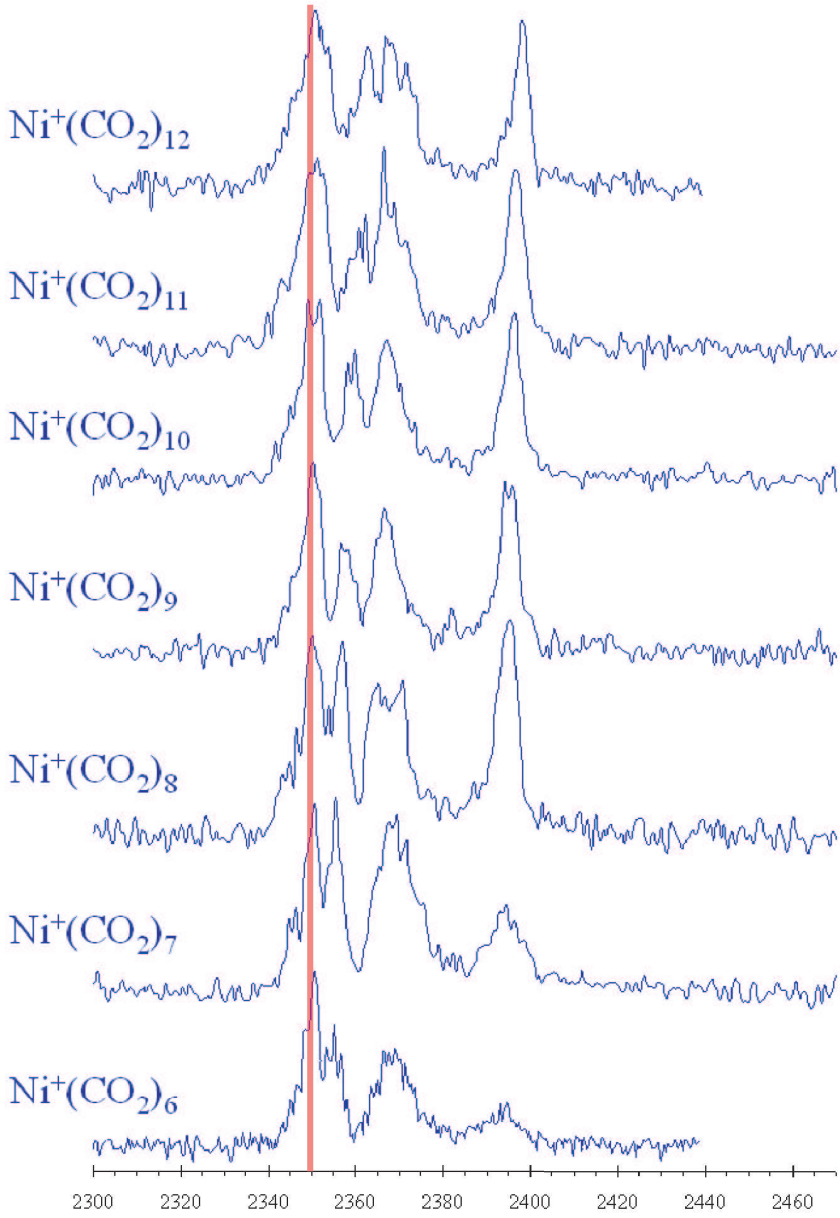

Figure 7.6:
Infrared photodissociation spectra for the series range $Ni^+(CO_2)_{6-12}$. These spectra each exhibit a strong feature very close to that of the free CO_2 asymmetric stretch region at 2349 cm^{-1} indicated by the vertical line. They each also display features blue shifted from this.

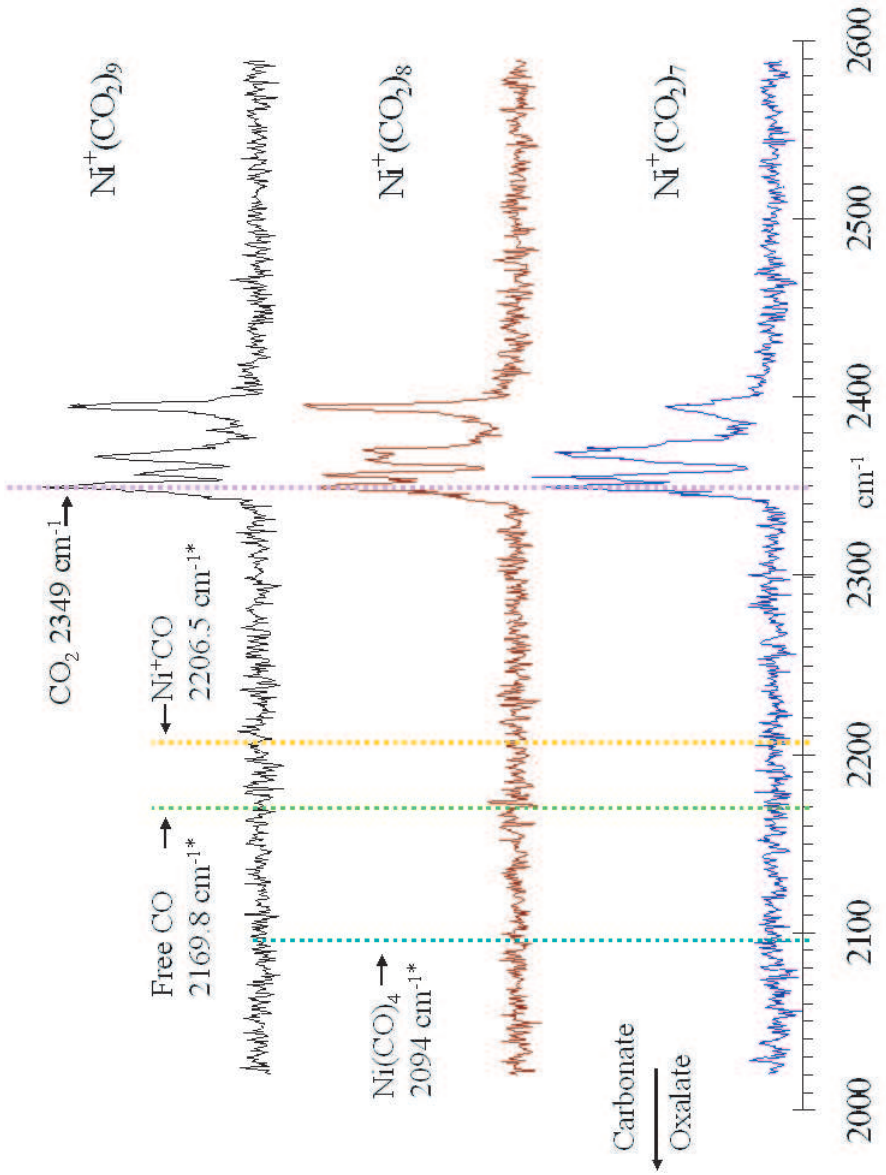

Figure 7.7:
Infrared spectra extending down to the limit of our laser system at 2000 cm^{-1}. Noted are several transition frequencies for selected nickel carbonyl complexes and carbon monoxide.

to lack of signal, as noted above. The n=3 complex shows a broad, featureless peak near the asymmetric stretch of free CO_2 at 2349 cm^{-1}.[11] $Ni^+(CO_2)_4$ exhibits a single sharp feature that is stronger than the n=3 spectrum, but still has a weak signal compared to the noise. This peak falls at 2365 cm^{-1} which is shifted by 16 cm^{-1} higher in energy than that of the ν_3 band of free CO_2.

The blue shift in the vibrational bands is indicative of the type of bonding in the complex. Inorganic coordination compounds of neutral metal atoms with CO_2 that are stable enough to be isolated are generally found with the CO_2 in a bent configuration[13] including nickel.[14] This leads to a strong redshift in the vibrational frequency of the mode associated with the asymmetric stretch of CO_2 down to the 1500-1800 cm^{-1} region.[21] The blue shift observed here would be expected only if the interaction is primarily electrostatic in nature. The bonding in an electrostatic complex would be a result of the interaction of the negative quadrupole moment of CO_2 and the charge on the metal resulting in an end-on linear configuration. The stretching motion of the ligand molecule would then be obstructed by the presence of the heavier metal ion. This added obstruction to the turning point of the vibrational motion creates a steeper repulsive potential and results in a shift to higher vibrational frequency. This effect has been observed and predicted by *ab initio* theory performed on our previous studies of metal ion-carbon dioxide complexes.[8–15]

The spectrum for the n=5 complex in Figure 7.3 is noticeably stronger than that of the smaller clusters, as was noted above for the fixed frequency photodissociation mass spectra. This spectrum also bears a distinction from the others shown in that it has two sharp features. The first falls nearly on top of the free CO_2 frequency at 2352 cm^{-1}, while the second is near the peak of the n=4 spectrum at 2370 cm^{-1}. Qualitatively this suggests that there are two distinct environments which the CO_2 ligands experience. The ligands that are in direct contact with the metal ion exhibit a blue shift as discussed above, and we will refer to these as "core" ligands. We might

expect that the ligand molecules that are not in the core must be attached much more weakly to the outside of the core complex and therefore might experience a much smaller shift in frequency, we will refer to these as "surface". For instance, the vibrational spectrum of pure CO_2 clusters have been measured and the frequency shift was found to be only 1-2 cm^{-1} above that of the free CO_2 asymmetric stretch.[24] CO_2 clusters may adopt either slipped parallel or "T" shaped structures, but in both of these configurations the ν_3 vibration occurs near the free CO_2 frequency. Thus, CO_2 molecules that are not attached directly to the metal should have a resonance essentially at the free CO_2 ν_3 frequency within our experimental error. In addition to this, when CO_2 molecules attach to one another rather than to the metal ion itself their binding energy should more closely resemble that of the pure CO_2 dimer[25] at 500 cm^{-1}. This energy is much lower than the energy of the infrared photon being absorbed and therefore the dissociation yield improves dramatically. The increased dissociation yield and the new vibrational band are consistent with the presence of a weakly bound CO_2 molecule attached to the surface of the n=4 cluster core.

The shifts in frequency with respect to asymmetric stretch of free CO_2 for the core bands in each of the clusters are plotted in Figure 7.4. The shift for the n=1 complex was not determined in our experiment, but to a first approximation its value can be estimated via linear extrapolation of the n=2 through 4 shifts. Using this estimate, the shift for $Ni^+(CO_2)$ is about 60 cm^{-1}. This is the largest shift observed in any of our $M^+(CO_2)$ studies to date. The measured shifts for the n=1 CO_2 cluster with Al^+, Mg^+ and Fe^+ are 17, 32 and 39 cm^{-1} respectively.[15,12,8] This is consistent with the theoretical prediction that nickel is expected to have the greatest binding energy of any of the first row transition metal cations and magnesium and aluminum ions as well.[5,6] The shifts decrease with increasing cluster size until n=4. The larger clusters ($n > 8$) show a general trend back toward higher values. This can also be explained by the "caging" effect model. Just as the intermediate cluster layers

experience a shift to higher frequency due to the presence of outer layers, so too do the innermost core layers. The attraction of the ligands to the metal ion draws them in and effectively creates a pressure on the core. The squeezing of the ligands in the first coordination shell then experience a shift to higher frequency by the same mechanism discussed above.

The difficulty in fragmenting the smaller clusters can be overcome by use of a technique of tagging the clusters with a rare gas atom.[16,17] The binding energy of a rare gas atom to a nickel ion is very weak compared to that of CO_2. The binding energy of Ni^+Ar is 12.68 kcal/mol,[22] whereas that of Ni^+Ne has been determined to be 2.37 kcal/mol[23] (830 cm^{-1}), which are both much lower than that of Ni^+CO_2 at 8750 cm^{-1}.[9] The rare gas atom improves the measured spectrum because the weak bond ensures that the cluster is more limited in the amount of residual thermal energy. A smaller amount of internal energy in the cluster narrows the widths of the peaks. Since the binding energy to the rare gas atom is smaller than the photon energy, it requires less power to fragment the cluster, leading to improved signal intensity and less broadened lines. Neon was chosen as the tag in this study because it has a much weaker binding energy that argon, and also because the mass of argon at 40 amu falls close to that of CO_2 at 44 amu which adds congestion to the mass spectra. The presence of the rare gas atom is expected to be a weak perturbation on the complex due to its small binding energy. Therefore it is assumed that the infrared spectrum of the tagged complex essentially represents a better version of the untagged complex. Infrared photodissociation spectra of a cluster are recorded by monitoring the loss the neon atom fragmentation channel. The spectra of $Ni^+(CO_2)_nNe$, n=2-4 are shown in Figure 7.5 along with the untagged $Ni^+(CO_2)_5$ spectrum. The spectrum for $Ni^+(CO_2)_2Ne$ shows a single sharp feature at 2395 cm^{-1} strongly blue shifted from the free CO_2 asymmetric stretch. The n=3 complex shows a closely split pair of peaks that are less blue shifted than the n=2. The spectrum

for n=4 shows a single sharp feature at 2365 cm^{-1} whose linewidth is significantly narrower (2.5 cm^{-1}) than the one obtained for the untagged $Ni^+(CO_2)_4$ complex of about 9 cm^{-1}. The spectrum for n=4 exhibits a large amount of noise compared to the signal because we could not produce a large amount of parent ion signal for this complex. The n=5 complex was found not to cluster with neon, preventing us from measuring the tagged spectrum for this complex. The poor clustering of these sizes with neon is also consistent with there being no available sites on the metal ion for the neon to attach. The degree of blue shift for metal ion-CO_2 complexes in previous studies has been found to increase with increasing binding energy in the complex.[15] The trend of decreasing shift with increasing cluster size here for the smaller clusters is consistent with the general observation that the binding energy per ligand drops as more ligands are added.[10]

Several observations thus far indicate that the first coordination sphere about the nickel ion is saturated at four carbon dioxide molecules. We can hypothesize what the structure of this cluster is, but the aid of theory is needed to definitively determine it when compared to the spectroscopy reported here. Group theoretical analysis shows that a complexe with either a square planar or tetrahedral geometry would have one infrared allowed vibrational transition. A complex with lower symmetry would exhibit more than one allowed transition. Therefore the n=4 complex must be either D_{4h} or T_d symmetry. Nickel is found to form stable four-coordinate complexes with ligands such as CN and CO.[26] These ligands prefer a tetrahedral geometry about the nickel atom because they are able to interact with the metal d orbitals via σ donation and π backbonding. On the other hand, Ni^+Ar_4 has been determined to adopt a square planar geometry.[27] In this case, the bonding is purely electrostatic and the electrons in the nickel ion d orbitals arrange in a manner that minimizes electron density in the plane of the complex, thereby reducing inter-electron repulsion with the argon atoms. Nickel cation has a d^9 electron configuration and a complex would

place the electron vacancy in the plane of the ligands. If the carbon dioxide ligands in $Ni^+(CO_2)_4$ are participating in π interactions with the metal ion d orbitals it would be expected to weaken the bonding in the ligand and cause a red shift in its vibration. Since only shifts to the blue are observed, it seems likely that this complex is purely electrostatic in nature and therefore a square planar geometry is expected.

The infrared spectra for the larger series of clusters ranging from $Ni^+(CO_2)_6$ through $Ni^+(CO_2)_{12}$ are shown in Figure 7.6. These spectra share several features in common. The so-called core and surface bands remain, but a weaker intermediate band begins to emerge in the n=6 spectrum as a shoulder in the surface band. This band progressively splits away from the surface mode and shifts toward higher frequency until it begins to merge with the core band in the spectrum of n=12. Table 7.1 lists the band positions for each of the $Ni^+(CO_2)_n$ clusters observed. The nature of these bands can also be understood in terms of the previous results on pure CO_2 clusters. In larger pure CO_2 clusters a blue-shifted band was also observed[24] and was assigned to those CO_2 molecules that are confined to the internal regions of the cluster. The additional shift is a result of a "caging" effect in which the CO_2 molecules experience a hindrance at both turning points of the vibrational motion. This same effect is also possible in the metal ion clusters. However, this band is present in clusters as small as $Ni^+(CO_2)_6$. A cluster this small is unlikely to have a complete second or third solvation sphere. The appearance of this third band type a this cluster size may be a result of ligand molecules clustering preferentially to one side of the complex. Some of the spectra appear to have this intermediate band split in to multiple peaks, though the resolution is not high enough to say with certainty. This could be an indication that there are multiple intermediate layers with their own environments, but it is more likely that these are a result of structural isomers.

The strong band at around 2400 cm^{-1} in the larger clusters has never been observed before in any of our previous $M^+(CO_2)$ studies. The last feature that

Table 7.1: Band positions for each of the assigned band types for $Ni^+(CO_2)_n$ clusters. Note that "surface" bands appear first at n=5, "intermediate" bands at n=6 and "reaction" bands at n=7.

Cluster Size (n)	**Surface**	**Intermediate**	**Core**	**Reaction**
2	-	-	2395	-
3	-	-	2378, 2383	-
4	-	-	2365	-
5	2351	-	2368	-
6	2351	2355	2369	-
7	2351	2355	2369	2394
8	2350	2357	2367	2395
9	2350	2358	2366	2396
10	2349	2358	2367	2397
11	2351	2361	2367	2397
12	2351	2363	2368	2398

appears occurs at around 2395 cm^{-1} for the spectra of each of the clusters. This peak is shifted by over 150 cm^{-1} from the free CO_2 asymmetric stretch band. This band is absent in the spectrum for $Ni^+(CO_2)_5$ and appears weakly in $Ni^+(CO_2)_6$ then at $Ni^+(CO_2)_8$ becomes the strongest band in the spectrum. While it was expected to find the shift of CO_2 to be large for nickel ion, *the shift for this peak is nearly 4 times that of* $Fe^+(CO_2)$. This extreme shift makes it unlikely that this peak represents a CO_2 molecule attached to a singly charged metal ion via electrostatic binding.

Since covalent bonding of a metal with carbon dioxide should produce a red-shift in its vibrational frequency, and electrostatic binding produces a blueshift that increases with binding energy, the simplest explanation for this resonance is that it belongs to a CO_2 molecule attached to a *multiply charged* nickel ion. A multiply charged nickel ion could come about as a result of an intracluster reaction. Nearly all of the Group VIII metals prefer a charge state greater than +1, and nickel is found

most frequently in the +2 or +3 oxidation state. Nickel has been used as a supported heterogenous catalyst for reducing CO_2 to methane and the mechanism proceeds via dissociative adsorption of CO_2.[1,2,3] Bauschlicher and coworkers[5] predicted that the light first row transition metal ions Sc, Ti and V would be more thermodynamically stable as the inserted metal oxide-carbonyl $MO^+(CO)$ than as the electrostatic $M^+(CO_2)$ complex. His calculations however predicted that for nickel ion, the insertion product would be 67 kcal/mol higher in energy than the electrostatic complex. We do not, however, observe the far shifted peak until there are at least six CO_2 molecules present. Solvent-induced reactions that set in after a particular cluster size have been observed via infrared spectroscopy in the past for non-metal ion clusters.[30] So called "cluster assisted" reactions have been observed on metal ion complexes in the past and have been drawn on to explain mass spectral data.[29] We recently reported the first observation of intracluster reaction by infrared spectroscopy in a metal ion complex for $Ni^+(C_2H_2)_n$ clusters.[28]

A number of possible chemical transformations can be suggested involving nickel ion and carbon dioxide. As long as the cluster as a whole maintains a +1 charge and does not dissociate by loss of atoms then each proposed reaction product will not be distinguishable in our time-of-flight mass spectrometer from the corresponding $Ni^+(CO_2)_n$ complex. The first and simplest is the insertion to produce $MO^+(CO)(CO_2)_{n-1}$ as discussed above. This complex would give the nickel atom a formal charge of +3 and the metal oxide would have a significant dipole moment. Since the reaction takes place only after a number of ligand molecules are present, the reaction may involve more than one ligand. Another possibility is the interaction of two CO_2 molecules with the metal ion to produce $Ni^{+2}(CO)(CO_3)^-(CO_2)_{n-2}$. This cluster would exhibit a strong ionic bond to the carbonate anion as well as a more preferable oxidation state on the metal. Also utilizing two CO_2 molecules, this system could also undergo a reaction to form an oxalate $Ni^{+3}(C_2O_4)^{-2}(CO_2)_{n-2}$.

This last complex has the benefit of two ionic bonding interactions due to the bidentate nature of the oxalate moiety. It also doesn't require the complete cleavage of a carbon-oxygen double bond to form, perhaps lessening any barriers in the formation. Other possibilities exist, but the more CO_2 molecules there are involved, the less likely, it would seem, to occur. There are also a finite number of valence electrons to distribute in redox processes and so this also places limits on the probable products.

Each of the cases suggested so far have ligands that would have distinct vibrational resonances from that of CO_2. A search was performed to look for any distinguishing spectra features that may give an indication that one of the proposed clusters is present. Figure 7.7 shows a few selected examples of scans taken in the direction of known C-O vibrational frequencies. Indicated on the figure are the positions of the vibrational frequencies of neutral and cationic nickel carbonyl complexes measured in matrix,[31] as well as gas phase CO itself. Unfortunately our laser system is limited in frequency range to about 2000 cm^{-1} so our scans stop short of where such ligands as carbonate and oxalate would absorb and a metal oxide ion stretching frequency would be very much lower still. There are no apparent resonances to be found in this frequency range. It is possible that a carbonyl attached to a nickel oxide ion would be redshifted below our range or it could be that the "reaction" peak we measure is itself a carbonyl resonance extremely far blueshifted. This would be an even more extreme shift than that of CO_2 away from its gas phase value. Therefore the most likely explanation remains that this peak is due to a CO_2 ligand shifted as a result of an interaction with an indeterminate nickel complex. Additionally, with a CO_2 ligand vibrationally coupled to a larger electrostatic charge, the dipole derivative for the mode involving this ligand would increase substantially, resulting in a more intense oscillator strength. The "reaction" peak in the spectra is often among the most intense peaks for clusters n=8 and above .

7.3 Conclusions

Nickel-carbon dioxide clusters of the form $Ni^+(CO_2)_n$ for n=1-12 are produced by laser vaporization, and their infrared spectroscopy is studied via mass selected photodissociation. Small clusters are difficult to dissociate, but the dissociation yield improves after n=4. Infrared excitation of larger clusters near the free CO_2 ν_3 frequency results in fragmentation down to the n=4 complex. This is consistent with a most stable coordination sphere of four carbon dioxide molecules analogous to the electrostatic $Ni^+(Ar)_4$[27] complex. The use of neon tagging was employed to obtain the spectrum for the n=2-4 complexes. The spectra for the small clusters was shifted to the blue of free CO_2 indicating and end-on bonding configuration consistent with an electrostatic complex. The spectrum for the $Ni^+(CO_2)_4$ complex exhibited a single peak, which indicates either a square planar or tetrahedral geometry. Clusters for n=5 and above exhibit a strong band nearly on top of where free CO_2 absorbs. This is indicative of CO_2 molecules weakly attached to the outside surface of a closed shell core. Further addition of CO_2 causes the appearance of a shoulder structure on this band. This shoulder feature gradually shifts further to the blue with increasing cluster size and is a result of layering of additional shells of ligands.

The clusters larger than $Ni^+(CO_2)_5$ all exhibit a strongly blueshifted peak unlike anything that has been observed previously in metal-carbon dioxide systems.[8,68,15,17] We attribute this peak to a resonance of a CO_2 ligand that is bound strongly to a NiO^+ core. This metal oxide core would occur as a result of an intracluster reaction where the nickel ion inserts into a CO_2 ligand in clusters with six or more ligands.

7.4 References

[1] E. Fukita, B. Brunschwig, D. Cabelli, M.W. Renner, L.R. Furenlid, T. Ogata, Y. Wada and S. Yanagida, "Studies in Surface Science and Catalysis," Volume

114 (Advances in Chemical Conversions for Mitigating Carbon Dioxide) In T. Inui, M. Anpo, K. Izui, S. Yanagida and T. Yamaguchi eds., Elsevier Science B. V., Netherlands. 1998.

[2] C.A. Wright, M. Thorn, McGill, A. Sutterer, S.M. Hinze, R.B. Prince and J.K. Gong, "Studies in Surface Science and Catalysis," Volume 114 (Advances in Chemical Conversions for Mitigating Carbon Dioxide) In T. Inui, M. Anpo, K. Izui, S. Yanagida and T. Yamaguchi eds., Elsevier Science B. V., Netherlands. 1998.

[3] S. Wang and G.Q. Lu, *Energy and Fuels*, **10**, 896 (1996).

[4] D.H. Gibson, *Chem. Rev.*, **96**, 2063 (1996).

[5] M. Sodupe, V. Branchadell, M. Rosi and C.W. Bauschlicher, *J. Phys. Chem. A*, 101, 7854 (1997).

[6] D. Stockigt, *Chem. Phys. Lett.*, **250**, 387 (1996).

[7] H.W. Kroto, A.W. Allaf and S.P. Balm, *Chem. Rev.*, **91**, 1213 (1991).

[8] (a) G. Gregoire, J. Velasquez and M.A. Duncan, *Chem. Phys. Lett.*, **349**, 451 (2001); (b) G. Gregoire and M.A. Duncan, *J. Chem. Phys.*, **117**, 2120 (2002).

[9] R.L. Asher, D. bellert, T. Buthelezi, G. Weerasekera and P.J. Brucat, *Chem. Phys. Lett.*, **228**, 390 (1994).

[10] *Organometallic Ion Chemistry*, ed. B.Freiser, Kluwer Academic Publishers, Dordrecht, The Netherlands 1996.

[11] T. Shimanouchi, *Molecular Vibrational Frequencies*, 69ed.; Chemistry WebBook, NIST Standard Reference Database (http://webbook.nist.gov) 2001.

[12] G. Gregoire, N.R. Brinkmann, D. van Heijnsbergen, H.F. Schaefer and M.A. Duncan *J. Phys. Chem. A.*, **107(2)**, 218 (2003).

[13] J. Mascetti and M. Tranquille, *J. Phys. Chem.*, **92**, 2177 (1988).

[14] A.M. Mebel and D.-Y. Hwang, *J. Phys. Chem. A*, **104**, 11622 (2000).

[15] R.S. Walters, G.A. Grieves, N.R. Brinkmann, H.F. Schaefer and M.A. Duncan, *J. Phys. Chem. A, submitted.*

[16] (a) P. Ayotte, G.H. Weddle, J. Kim and M.A. Johnson, *Chem. Phys.*, **98**, 239 (1998); (b) P. Ayotte, G.H. Weddle, J. Kim and M.A. Johnson, *J. Am. Chem. Soc.*, **120**, 123361 (1998).

[17] M.A. Duncan, *Int. Rev. Phys. Chem. in press.*

[18] (a) K.F. Willey, C.S. Yeh, D.L. Robbins and M.A. Duncan, *Chem. Phys. Lett.*, **192**, 179 (1992); (b) C.S. Yeh, K.F. Willey, D.L. Robbins, J.S. Pilgrim and M.A. Duncan, *J. Chem. Phys.*, **98**, 1867 (1993); (c) C.S. Yeh, K.F. Willey, D.L. Robbins and M.A.Duncan, *J. Phys. Chem.*, **96**, 7833 (1992).

[19] C.T. Scurlock, S.H. Pullins and M.A. Duncan, *J. Chem. Phys.*, **105**, 3579 (1996).

[20] *Infrared and Raman Spectra of Inorganic and Coordination Compounds; Part A* 5th ed., K. Nakamoto, Wiley-Interscience, New York 1997.

[21] *Infrared and Raman Spectra of Inorganic and Coordination Compounds; Part B* 5th ed., K. Nakamoto, Wiley-Interscience, New York 1997.

[22] D.E. Lessen and P.J. Brucat, *Chem. Phys. Lett.*, **152**, 473 (1988).

[23] P.R. Kemper, M.-T. Hsu and M.T. Bowers, *J. Phys. Chem.*, **95**, 10600 (1991).

[24] (a) T.E. Gough, R.E. Miller and G. Scoles, *J. Phys. Chem.*, **85**, 4041 (1981); (b) K.W. Jucks, Z.S. Huang, D. Dayton, R.E. Miller and W. Lafferty, *J. Chem. Phys.*, **86**, 4341 (1987); (c) K.W. Zucks, Z.S. Huang, R.E. Miller, G.T. Fraser, A.S. Pine and W.J. Lafferty, *J. Chem. Phys.*, **88**, 2185 (1988) (d) G.T. Fraser, A.S. Pine, W.J. Lafferty and R.E. Miller, *J. Chem. Phys.*, **87**, 1502 (1987) (e)M.J. Wieda, J.M. Sperhac and D. Nesbitt, *J. Chem. Phys.*, **103**, 7685 (1995) (f) M.J. Weida and D. Nesbitt, *J. Chem. Phys.*, **105**, 10210 (1996); (g) J.S. Muenter, *J. Chem. Phys.*, **94**, 2781 (1991); (h) M.A. Walsh, T.H. England, T.R. Dyke and B.J. Howard, *Chem. Phys. Lett.*, **120**, 313 (1985); (i) R. Disselkamp and G.E. Ewing, *J. Chem. Phys.*, **99**, 2439 (1993).

[25] R. Bukowski, J. Sadlej, B. Jeziorski, P. Jankowski, K. Szalewicz, S.A. Kucharski, H.L. Williams and B.M. Rice, *J. Chem. Phys.*, **110**, 3785 (1999).

[26] G.L. Miessler and D.A. Tarr, *Inorganic Chemistry* 2nd Ed., Prentice Hall, New Jersey 1998.

[27] M. Velegrakis in *Advances in Metal and Semiconductor Clusters*, Vol. 5, ed. M.A. Duncan, Elsevier Press, New York, 2001.

[28] R.S. Walters, T.D. Jaeger and M.A. Duncan, *J. Phys. Chem. A*, **106**, 10482 (2002).

[29] F. Misaizu, M. Sanekata, K. Tsukamoto, K. Fuke, S.K. Iwata, *J. Phys. Chem.*, **96**, 8259 (1992).

[30] J.H. Choi, K.T. Kuwata, B.M. Haas, Y. Cao, M.A. Johnson and M. Okumura, *J. Chem. Phys.*, **100**, 7153 (1994).

[31] B. Liang and L. Andrews, *J. Phys. Chem. A*, **104**, 3905 (2000).

Chapter 8

Conclusions

Metal ion-ligand complexes investigated in the gas phase via mass spectrometry, fixed frequency photodissociation and infrared resonance enhanced photodissociation spectroscopy have allowed us to observe a number of interesting properties in the chemistry of ion-molecule interactions. These properties include the relative energetics of binding and ionization and the influence of solvation on multiply charged systems, new and interesting structural motifs in small and extended organometallic systems, and quantitative information about cluster coordination and solvation assisted intracluster chemistry.

The doubly charged metal ion-ligand systems discussed in Chapter 4 demonstrate that, contrary to conventional opinion, the laser vaporization cluster source can be used to produce a wide variety of higher oxidation state metal complexes. Even complexes that are metastable to charge transfer can be made and studied effectively by mass spectrometry and photodissociation. The laser vaporization source provides a convenient alternative to other sources that produce multiply charged ions in the gas phase. Future work in this area may include either electronic or vibrational photodissociation spectroscopy. The pulsed source produces ions in intense packets suitable for further study with pulsed laser spectroscopy. Spectroscopy would provide quantitative information about the fundamental ion-molecule interactions in these important systems. The demonstration of the applicability of the well tested and widely used method of laser vaporization for the study of multiply charged cluster ions may also broaden the field to more researchers and to additional tools to probe them with.

The studies presented here in Chapter 6 of the f-block $Ln_n^+(COT)_m$ clusters probe the nature of the structure and bonding in organometallic systems that are not feasible to produce in solution by wet chemical means. Fixed frequency photodissociation provides an indirect, but independent means of inferring the structure of these novel multi-decker sandwich complexes that is complementary to the methods

used by other groups also interested in these systems. More direct insight can be garnered by study of these complexes with IR-REPD spectroscopy. An important aspect of the question of structure in these clusters is the aromaticity and planarity of the COT ligand. The degree of aromaticity should be an indirect measurement of the degree of oxidation of the metal ion. Infrared spectroscopy in the C-H stretch region where our OPO operates should be able to distinguish between aromatic and non-aromatic hydrocarbons. Additionally, the intriguing $M^+(C_5H_5)$ and $M^+(C_4H_4)$ clusters could also be studied to determine their nature and answer the question of what oxidation state these metals actually are adopting.

New results for $Ni^+(CO_2)_n$ clusters presented in this work show evidence for a solvent induced intracluster reaction where the metal ion inserts into the carbon dioxide molecule. This reaction may have important implications for the use of nickel as a means to reduce carbon dioxide to a more useful form and for reclaiming the greenhouse gas from emissions. Multi-ligand clustering for this system was observed and seen to behave in a manner consistent with the trend of other $M^+(CO_2)_n$ systems studied so far. Layering of successive solvation shells was observed and the number of the first coordination sphere determined. The unique "reaction" peak is unlike anything yet seen in these systems. By utilizing the combination of IR + UV multiphoton photodissociation, future research may be able to positively identify NiO^+ in the core of the clusters. Studies should also be undertaken using the light transition metals Ti and V, since these are more likely to insert at smaller cluster sizes.